THE UNIVERSITY OF ALBERTA

DEFORMATION CHARACTERISTICS OF PRETENSIONED CONCRETE

BEAMS SUBJECTED TO BENDING AND SHEAR

by

THEODORE BELKE

A THESIS

SUBMITTED TO THE FACULTY OF GRADUATE STUDIES

IN PARTIAL FULFILMENT OF THE REQUIREMENTS FOR THE DEGREE OF

MASTER OF SCIENCE

DEPARTMENT OF CIVIL ENGINEERING

EDMONTON, ALBERTA

MAY 1965

UNIVERSITY OF ALBERTA

FACULTY OF GRADUATE STUDIES


The undersigned certify that they have read, and
recommend to the Faculty of Graduate Studies for acceptance,
a thesis entitled "DEFORMATION CHARACTERISTICS OF PRETEN-
SIONED CONCRETE BEAMS SUBJECTED TO BENDING AND SHEAR" sub-
mitted by THEODORE BELKE in partial fulfilment of the
requirements for the degree of MASTER OF SCIENCE .

ABSTRACT

The object of this investigation was to study the
deformation characteristics of bonded, prestressed concrete
beams subjected to bending and shear. The effects of several
variables on the moment-curvature relationship, load-deflec-
tion relationship and the distribution of curvature were
studied.

In all, fifteen beams having a 6 x 14 5/8-in.
cross-section and a 10-in. effective depth were tested.
Twelve beams were loaded with a single concentrated load at
midspan and the remaining three beams were loaded with two
loads symmetrical about midspan.

From the test data obtained, load-deflection re-
lationships, moment-curvature relationships, distributions
of curvature and distributions of strain in the extreme
compression fiber were derived. In addition, the derived
moment-curvature relationships were compared with theoretical
moment-curvature relationships and measured load-deflection
relationships were compared with load-deflection relationships

computed from the measured distributions of curvature.

Correlation between the measured and theoretical moment-curvature relationships was good, except for the second and third stages of behavior. Computed deflections were found to be lower than the measured values for beams with a shear-span-to-depth ratio of 3.3 .

The tests indicated that the moment-curvature and load-deflection relationships were dependent on the characteristics of the beam cross-section. Span length and type of load condition also affected the load-deflection relationship.

## ACKNOWLEDGEMENTS

## TABLE OF CONTENTS

viii

# LIST OF TABLES

# LIST OF FIGURES

# CHAPTER I

## INTRODUCTION

### 1.1 Introductory Remarks

The work reported here is part of a series of investigations into the deformation characteristics of pretensioned prestressed concrete beams. The first series of tests conducted in 1964, (1)* dealt mainly with beams loaded in flexure. A constant moment region was extensively analysed and the beam behavior was related to data obtained from this region. Emphasis in this study is given to the deformation characteristics of beams subjected to combined flexure and shear.

To date considerable testing has been done on prestressed concrete members in order to obtain a general flexural analysis. Approximate methods for the determination of flexural strength of prestressed concrete beams were

---

* The numbers in parenthesis refer to the entries in the list of references.

1

advanced in 1962, (2). Work in this area has now progressed

to the point where strength may be predicted with a satisfactory

degree of accuracy. Only a limited amount of work has been

done on the aspect of deformations, particularly as related

to curvature. Investigators have long realized that the

curvature of a section and the associated moment, throughout

various stages of loading, is representative of beam behavior.

Even though the moment-curvature relationship is a useful

means of explaining behavior, this is not its only or most

valuable application. The moment-curvature relationship is

useful in limit design where knowledge of the deformation

capacity of a section is required. Also, if the moment-curva-

ture relationship and the distribution of curvature across the

beam can be derived, deflections at various stages of loading

can be predicted. In this form moment-curvature is most

important and can be applied to design.

## 1.2   Object

This investigation was initiated to study the effects

of several variables on the moment-curvature relationship and

the distribution of curvature. A limited number of two-point

loaded beams of low concrete strength were tested to determine

the effect of different amounts of tension reinforcement on the moment-curvature relationship. However, the main object of this investigation was to study deformation characteristics and to obtain moment-curvature diagrams of beams subjected to combined bending and shear under a single load. In addition, the moment-curvature distributions were used to calculate deflections, which were compared with the corresponding measured values. Also, theoretical moment-curvature relationships were derived and compared with those obtained from measurement of deformations on several gage lines on the side of the beam.

The major variables in this study were:

(a)    amount of tension reinforcement

(b)    concrete strength

(c)    type of loading

(d)    shear-span-to-depth ratio

Slight unintentional variation in the level of effective prestress resulted throughout the three series of beams tested.

Strain in the extreme concrete fiber, strains over the depth of the beam, and beam deflections were measured. From this data moment-curvature relationships, load-deflection relationships, distribution of curvature and distribution of

strain in the extreme fiber were obtained. The effects of
the variables on these relationships were studied.

## 1.3   Scope

Three series of beams were tested. The first
series consisted of Beams 11, 12 and 13, the second Beams
1A to 6A and the third Beams 1B to 6B. All beams were of
rectangular cross-section measuring 6 x 14 5/8-in. Beams in
the first series were reinforced with 2, 4 and 6, seven-wire
strand of 5/16-in. nominal diameter. The beams in series A
and B were reinforced in tension with 4, 6 and 8 strands. The
effective depth of all beams was constant at 10-in. The span
lengths for all beams were 11-ft. except series B which were
5.5-ft.

Beams 11 to 13 represented a low concrete strength
and had the amount of tension reinforcement as the major
variable. The percentages of reinforcement were: 0.193,
0.385 and 0.578 respectively. Concrete strength was in the
order of 3600 psi. These beams were loaded at two points with
a constant moment region of 5-ft.

Series A consisted of two groups of beams, one of low
concrete strength and the other of high concrete strength. The

percentage of tension reinforcement was varied within each group. The percentages were: 0.385, 0.578 and 0.770. The concrete strengths were approximately 3600 psi and 6800 psi. These beams were tested under a single point load at midspan. The shear-span-to-depth ratio in this series is 6.6.

Beams 1B to 6B were the same in all respects to those in series A, except the span length which was 5.5-ft. with a shear-span-to-depth ratio of 3.3.

In this thesis deformation characteristics and the related relationships as determined from tests performed on fifteen beams are reported. As well, cracking moments and ultimate moments as determined from the tests are compared with values obtained from a section analysis. No attempt was made to derive empirical parameters or make extensive correlation with the first investigation on deformations.

CHAPTER II

REVIEW OF PREVIOUS WORK

## 2.1    Introduction

Investigators working in the field of prestressed

concrete have, in the past, been primarily concerned with the

strength of members.  Tests with the most usual cases of

loading have been conducted and reported in the technical

literature.  In some investigations where strength was the

main factor deformation characteristics, to a limited degree,

have been discussed as well.

The series of tests, reported here, were carried

out on bonded prestressed concrete beams.  Of primary concern

were the deformation characteristics as related to moment-

curvature and load-deflection relationships of beams subjected

to bending and shear.  Except for tests performed at the

University of Illinois (2), (3), there is a lack of informa-

tion on this type of load condition for prestressed concrete

beams.  Extensive work on reinforced concrete, however, has

been done for the bending and shear condition.  Generally,

6

these investigations were done to gain knowledge of rotation

capacities of members or deformation characteristics of

structural connections for purposes of limit design.

## 2.2 Research on Flexural Strength

One of the earliest comprehensive studies of flexural

behavior and subsequent development of a rational analysis

was reported in 1954 (4). The tests consisted of 26

rectangular bonded, post-tensioned beams loaded at the third-

points of a 9-ft span. The tests covered a wide range of

variables, and provided the basis for empirical evaluation

of certain parameters that appeared in the analysis. An

analysis for computing ultimate moment and steel stress at

failure was developed. Approximate expressions were given for

computing ultimate steel stress for the cases where the stress-

strain curve for steel reinforcement may be approximated by

two straight lines.

In 1953-54 tests (5) were performed on pretensioned,

post-tensioned bonded, post-tensioned unbonded and post-tensioned

unbonded beams with reinforcing bars. This investigation,

conducted by the Portland Cement Association, used analytical

and experimental studies for flexural strength. In all, 19 beams

with three percentages of reinforcement were tested under a

third point load condition. Strengths of pretensioned, post-

tensioned bonded and pretensioned unbonded beams of similar

cross-section were compared. The effects on ultimate strength

of imbedded deformed bars, replacing one strand in unbonded

beams were studied.

The most extensive investigation of strength and

flexural behavior of prestressed concrete beams was conducted

at the University of Illinois commencing in 1951. Tests on

82 rectangular prestressed concrete beams were presented and

discussed in 1962 (2). These tests involved bonded, unbonded

and partially bonded beams. The results of the tests given in

reference (4) were included in this study. The major variables

were: amount of reinforcement, concrete strength, effective

prestress and load condition.

A flexural strength analysis applicable to bonded,

partially bonded and unbonded beams was developed, which could

be applied to various stages of loading. Procedures for

determining flexural deformations using the relationship

between moment and average curvature were presented. For

the beams of the investigation this procedure was used to

compute midspan deflections which were compared to the measured

deflections.

## 2.3    Research on Deformations

Analytical procedures developed in reference (2) were used in 1964 (6), to derive moment-curvature relationships for beams having different amounts and levels of prestress. A modified Hognestad stress block was used and a limiting strain of 0.0035 was chosen. The derived moment-curvature relationship was used to analyse the uniform load condition and predict general behavior. After studying the curves presented, it was stated that the moment-curvature and load-deflection relationships for any beam could be controlled by partial prestressing. In this way, it was hoped, a section could be designed to obtain both optimum service load and ultimate load conditions.

Tests (7), to study moment redistribution were carried out at Turin in 1957. Three prestressed beams continuous over three spans were tested to failure by applying two point loads near the midspan. Using equations of equilibrium theoretical moment-curvature relationships which could be idealized with three sloping straight lines were derived. It was concluded that before practical design methods for this

problem could be established, experimental checking of assumptions concerning calculated rotations was required. Also, the method of plotting moment-curvature diagrams used at that time would have to be improved.

Deformation characteristics of 10 beams with varying amounts of tension reinforcement and varying concrete strength were studied at the University of Alberta (1). Both two point loaded and single point loaded beams were tested. In all cases the agreement between the theoretical and measured moment-curvature relationship was good.

## 2.4    Beams Subjected to Bending and Shear

In general tests on beams subjected to bending and shear have been conducted by various investigators for two reasons. The objects have been to obtain information either on shear and flexural strength of members or deformation capacities. Work done on deformation capacities, for purposes of limit design, has been restricted to non-tensioned reinforced concrete beams. Investigations of shear and flexural strength have been done on both prestressed and reinforced concrete.

A series of tests, (8), were conducted in 1963, on reinforced concrete beams to determined the amount of concentrated

plastic rotation possible at a beam-column connection. Measured

moment-curvature relationships were obtained for the critical

section to explain behavior. Similarly tests (9) conducted at

Illinois were used to develop analytical procedures for

estimating moments and deflections at yield, first crushing

and ultimate load. Again, the area investigated was the connec-

tion between a column and a beam.

Tests of 87 simply-supported prestressed beams con-

ducted at the University of Illinois are reported (3). Obser-

vations from these tests led to a new explanation of the

strength of prestressed concrete beams failing in shear.

Results from tests of beams with web reinforcement, draped

reinforcement and beams under moving loads were presented and

discussed. Observed patterns of behavior were classified and

discussed with reference to the development of inclined crack-

ing and the mode of failure. Design recommendations were also

presented based on expressions developed to predict cracking

and failure loads.

# CHAPTER III

## MATERIALS, FABRICATION AND TEST PROCEDURES

### 3.1   Materials

#### 3.1.1   Cement

Type III Portland Cement was used for all beams tested.   This cement was purchased from a local manufacturer in one lot and stored under proper conditions.

#### 3.1.2   Aggregate

All aggregate used was obtained from local sources.   The coarse aggregate was crushed with a maximum size of 3/4-in.   When delivered to the laboratory the coarse aggregate and sand were in a saturated condition and dried progressively with time in storage.   At the time of mixing the moisture content was found to vary from 3 to 8%.   The size analyses of the aggregates are given in Table 3.1 . Fineness Modulus of the sand was found to be 2.79.   The other physical properties of the aggregates are given in Table 3.2.

TABLE 3.1

SIEVE ANALYSIS OF AGGREGATES

| | Coarse Aggregate | | | Fine Aggregate | |
|---|---|---|---|---|---|
| Sieve | % Retained | Cumulative % Retained | Sieve | % Retained | Cumulative % Retained |
| 1 | 0 | 0 | #4 | 1.6 | 1.6 |
| 3/4 | 10.5 | 10.5 | #8 | 13.8 | 15.4 |
| 3/8 | 66.5 | 77.0 | #16 | 15.1 | 30.5 |
| #4 | 21.8 | 98.8 | #30 | 20.9 | 51.4 |
| pan | 1.2 | 100.0 | #50 | 32.7 | 84.1 |
| | | | #100 | 12.2 | 96.3 |
| | | | Pan | 1.6 | - |
| | | | Silt | 2.0 | - |
| TOTAL | 100.0 | 286.3 | | 99.9 | 279.3 |

TABLE 3.2

PHYSICAL PROPERTIES OF AGGREGATES

| Material | Absorption % | Specific Gravity | | |
|---|---|---|---|---|
| | | Bulk | Apparent | Saturated Surface Dry |
| Sand | 1.36 | 2.55 | 2.63 | 2.58 |
| Crushed Rock | 1.85 | 2.51 | 2.61 | 2.53 |

### 3.1.3    Concrete Mixes

Concrete mixes were designed according to the method recommended by ACI 613-54 Standard of the American Concrete Institute, (10).  Prior to the actual casting of specimens trial batches were prepared and air cured under laboratory conditions.  Modifications to the mix design were then made as required on the basis of 3-day compressive strength tests.

Due to the day to day variation of moisture content of the aggregate, the amount of mixing water used was adjusted from beam to beam on the basis of visual observation and slump tests.  The concrete properties for each specimen  cast are given in Table 3.3.  Compressive strengths $f_c'$ were obtained from standard 6 by 12-in. control cylinders tested on the same day as the beam.  Tensile strengths were obtained from splitting tests done on 6 by 12-in. cylinders.  The modulus of rupture, $f_r$, is the result of tests on $4\frac{1}{2}$ x $3\frac{1}{2}$ x 16-in. control beams loaded at the third points of a 12-in. span.

### 3.1.4    Reinforcement

Seven-wire high strength strand of 5/16-in.

## TABLE 3.3

### PROPERTIES OF CONCRETE MIXES

| Beam No. | Cement: Sand: Gravel by Weight | Water/ Cement by Weight | Slump in. | Compressive Strength p.s.i. 1 | 2 | Tensile Strength p.s.i. 1 | 2 | Modulus of Rupture p.s.i. 1 | 2 | Age at Test days | Compressive Strength 3-d | 7-d |
|---|---|---|---|---|---|---|---|---|---|---|---|---|
| 11 | 1:3.3:4.0 | 0.67 | 3 | 4070 | 3980 | 363 | 379 | 570 | 860 | 28 | 2560 | 2980 |
| 12 | 1:3.4:4.1 | 0.71 | $3\frac{1}{2}$ | 3670 | 3560 | 348 | - | 606 | 600 | 28 | 2110 | 2930 |
| 13 | 1:3.4:4.1 | 0.74 | 4 | 3260 | 3510 | 378 | 366 | 563 | 577 | 29 | 2110 | 2840 |
| 1A | 1:3.4:4.1 | 0.63 | 3 | 4250 | 4370 | 310 | 331 | 610 | 644 | 27 | 3050 | 4120 |
| 2A | 1:3.5:4.1 | 0.56 | 4 | 3610 | 3300 | 288 | 235 | 500 | 460 | 27 | 1960 | 2960 |
| 3A | 1:3.5:4.1 | 0.64 | 3 | 3480 | 3610 | 287 | 372 | 654 | 556 | 28 | -- | 2920 |
| 4A | 1:1.6:2.4 | 0.45 | 4 | 5270 | 6670 | 491 | 417 | 556 | 697 | 25 | 5960 | 6450 |
| 5A | 1:1.6:2.4 | 0.42 | 3 | 6880 | 6800 | 500 | 508 | 632 | 740 | 24 | 5820 | 5840 |
| 6A | 1:1.6:2.4 | 0.44 | $3\frac{1}{2}$ | 6850 | 6920 | 540 | - | 566 | 610 | 22 | 5300 | 6540 |
| 1B | 1:3.5:4.1 | 0.64 | $2\frac{1}{2}$ | 3480 | 3600 | 301 | 364 | 556 | 545 | 29 | 2180 | 3110 |
| 2B | 1:3.5:4.1 | 0.66 | $1\frac{1}{2}$ | 4180 | 4320 | 310 | 340 | 675 | 665 | 31 | 3040 | 3300 |
| 3B | 1:3.5:4.1 | 0.71 | $1\frac{1}{2}$ | 3500 | 3590 | 341 | 385 | 655 | 655 | 34 | 2140 | 3420 |
| 4B | 1:1.4:2.2 | 0.48 | 5 | 6100 | 6520 | 420 | 474 | 632 | 600 | 30 | 4980 | 6050 |
| 5B | 1:1.4:2.2 | 0.44 | $2\frac{1}{2}$ | 6270 | 6650 | 530 | - | 610 | 600 | 27 | 5160 | 6160 |
| 6B | 1:1.4:2.2 | 0.44 | $3\frac{1}{2}$ | 5880 | 6000 | 438 | 526 | 730 | 676 | 34 | 4820 | 6040 |

nominal diameter was used for tension reinforcement for
all beams. This strand is designated as "Seven-wire
Uncoated Stress-Relieved" and meets ASTM A-416 grading.
Two separate lots of this reinforcing were purchased. The
stress-strain relationships as determined by the manufacturer
are shown in Figure 3.1 and Figure 3.2

Transverse reinforcement for shear was provided
by No. 2 plain or No. 3 deformed bent bars.

## 3.2   Fabrication

### 3.2.1   Forms

All beams were cast in a collapsible
12' - 16" long form. It was constructed from three steel
channel sections. Each side consisted of a 12-in. channel
section bolted at two foot intervals to an 18-in. channel
section base. End plates, also steel channel sections, were
drilled with an appropriate number of holes to accommodate
the tension reinforcing. These, when clamped into position,
completed the assembly. This construction provided a fair
degree of flexibility and relatively easy assembly. In
order to obtain a depth of section greater than 12-in.,
the form was modified by the addition of two 3 x 4-in.
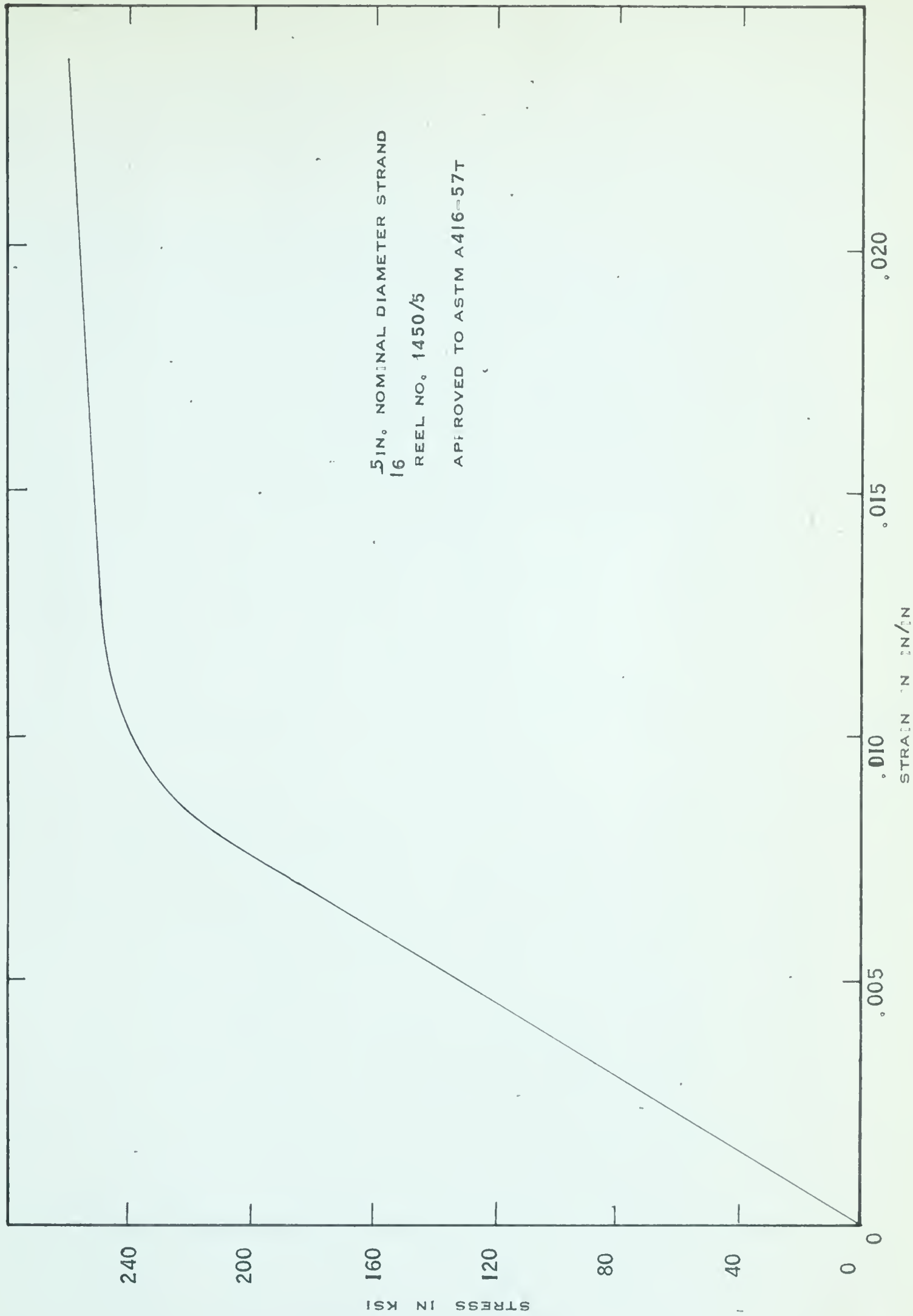
FIGURE 3.1 STRESS-STRAIN RELATIONSHIP FOR REINFORCEMENT

$\frac{5}{16}$ IN. NOMINAL DIAMETER STRAND

REEL NO. 1450/5

APPROVED TO ASTM A416-57T

STRAIN IN IN/IN

STRESS IN KSI

STRESS-STRAIN RELATIONSHIP FOR REINFORCEMENT

The plotted curve is labeled as follows:

$\frac{5}{16}$ IN. NOMINAL DIAMETER STRAND

REEL NO. 1235/9

APPROVED TO ASTM A416-57T

Axis labels: STRESS IN KSI (vertical), with gridlines at 240, 200, 160, 120, 80, 40, 0; STRAIN IN IN/IN (horizontal) with gridlines at 0, .005, .010, .015, .020.
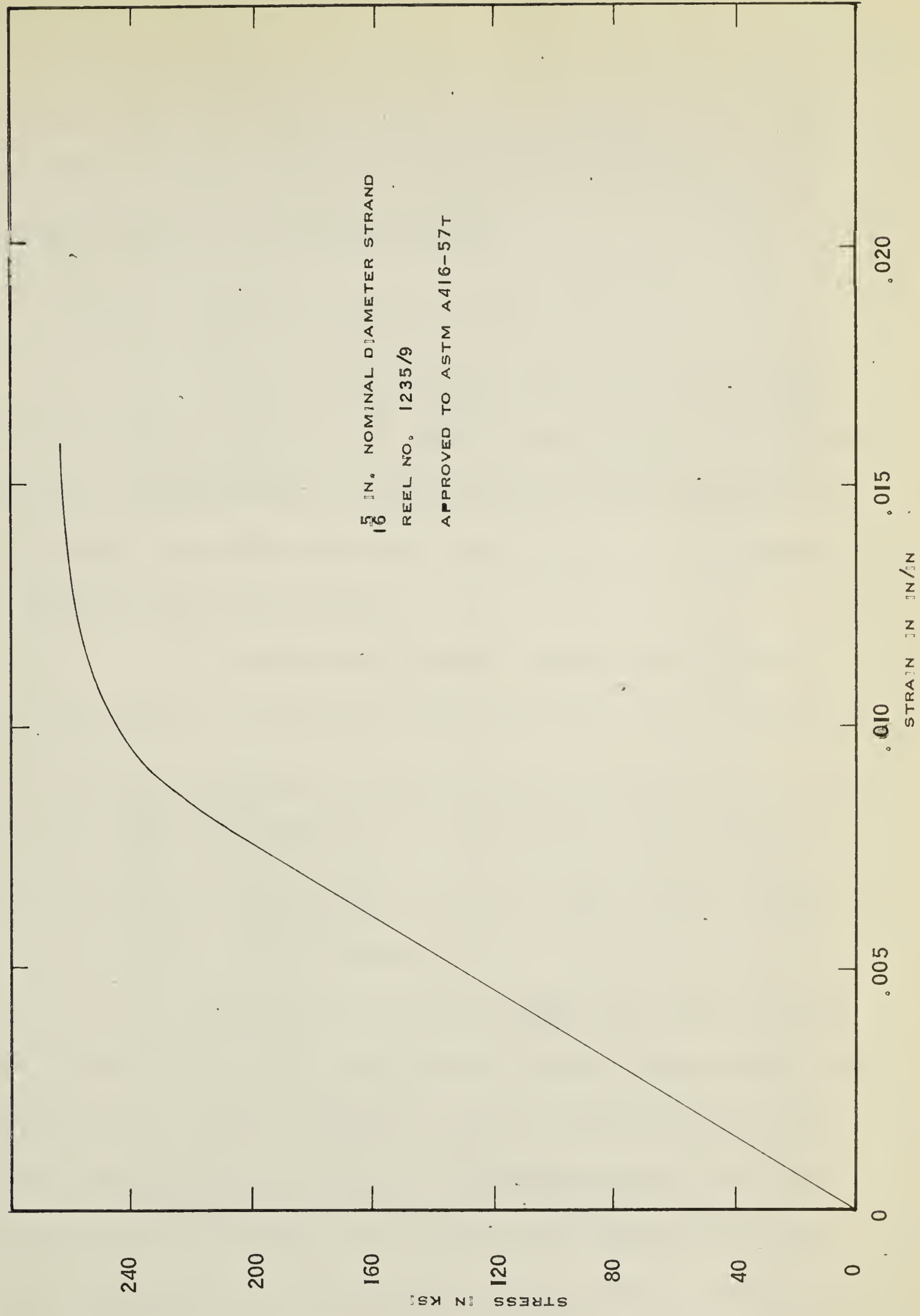
FIGURE 3.2 STRESS-STRAIN RELATIONSHIP FOR REINFORCEMENT

nominal size wood members between the sides and the base.
By adding a spacer block at mid-length, two beams for
Series B were cast simultaneously.

### 3.2.2 Prestressing Procedure

After assembling the form and positioning it
in the prestressing bed the reinforcing cables were threaded
through the end plates. The separation and arrangement of
the cables was maintained and controlled by a configuration
of holes in the end plates.

A thirty-ton Simplex center-hole hydraulic
ram operated by a Blackhawk hand pump was used to tension
the wires individually. The jacking arrangement and equip-
ment is shown in FIGURE 3.3. Reactions of the stressing
operation were provided by concrete blocks which are part
of the laboratory prestressing bed.

Wedge grip end anchorages were used to grip
the strand. The grips consisted of three wedge shaped jaws,
housed in a tapered cylinder, held in position by a coil
spring and threaded end cap. Gripping results from the
wedging action between the jaws and the tapered housing
when a tension force is applied to the cable. FIGURES 3.3
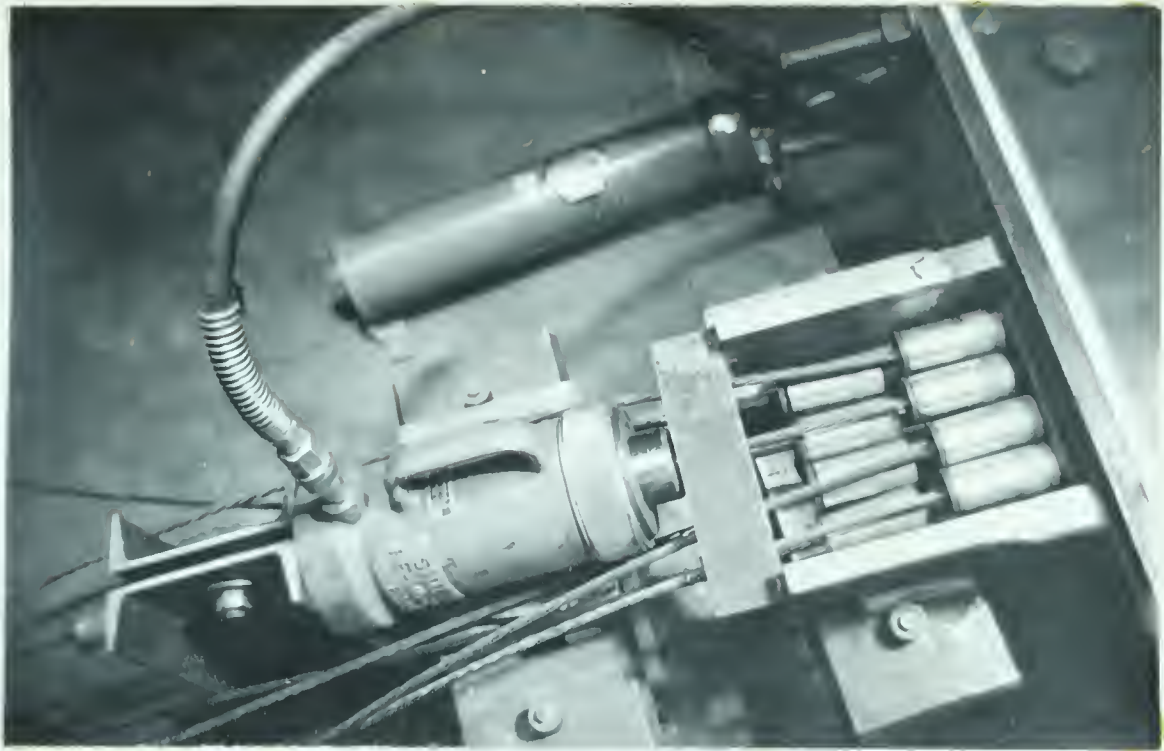
FIGURE 3.3   HYDRAULIC RAM AND GRIP ASSEMBLY
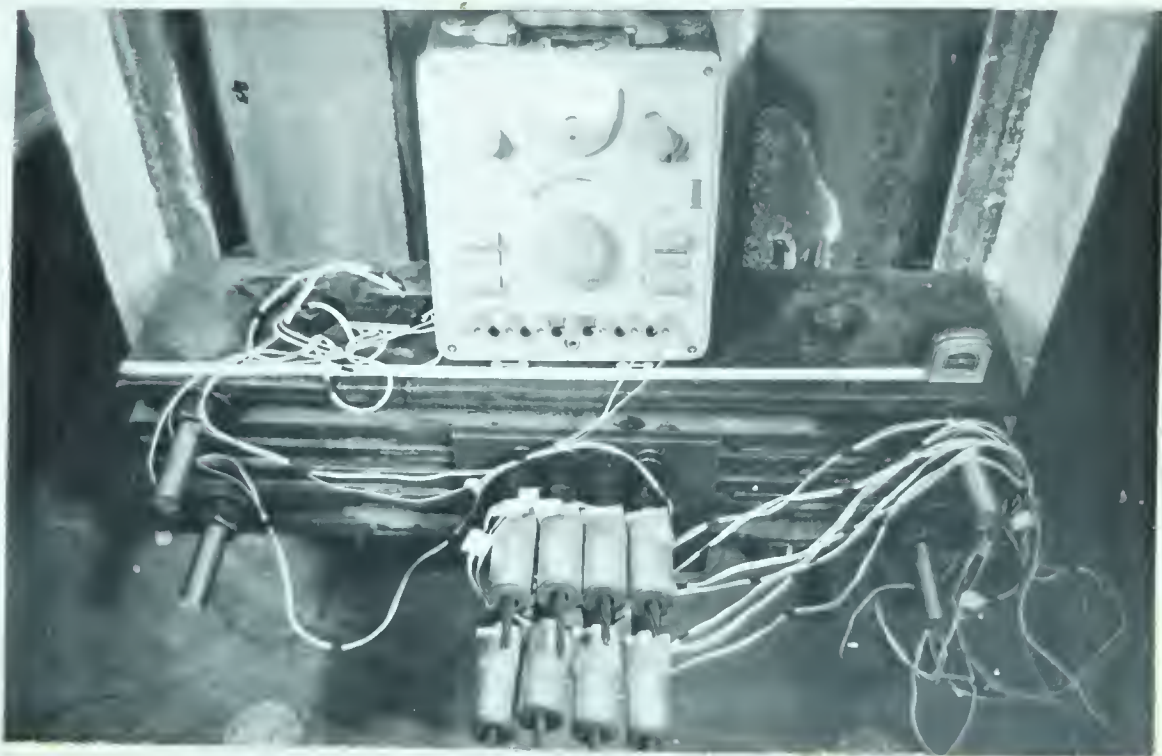


FIGURE 3.4   DYNAMOMETERS AND STRAIN INDICATOR

and 3.4 show the end anchorages with the grips in position.

The level of prestress in each cable was measured by specially constructed aluminum dynamometers placed between the wedge grip and the bearing plate at the opposite end to which the tension was applied. Strain in the dynamometers were measured with two A7 SR-4 electrical resistance strain gages wired in series. Calibration curves were used to relate the strains to the force applied. Prior to the start of the tensioning, the strain required to obtain the desired stress level in the cable, was set on the strain indicator. When this value was reached the grips were set and minor adjustments to account for slip were made by adding thin shims.

Shear reinforcement was placed after all cables had been prestressed. The stirrups were fixed by wiring them directly to the cables. No. 3 reinforcing bars were laid across the top of the form and the stirrups were fastened to these as well to keep them in an upright position as shown in FIGURE 3.5. After the concrete was placed the wires were cut and the top bars were removed.

FIGURE 3.5 FORM WITH STIRRUPS AND TOP BARS
IN PLACE
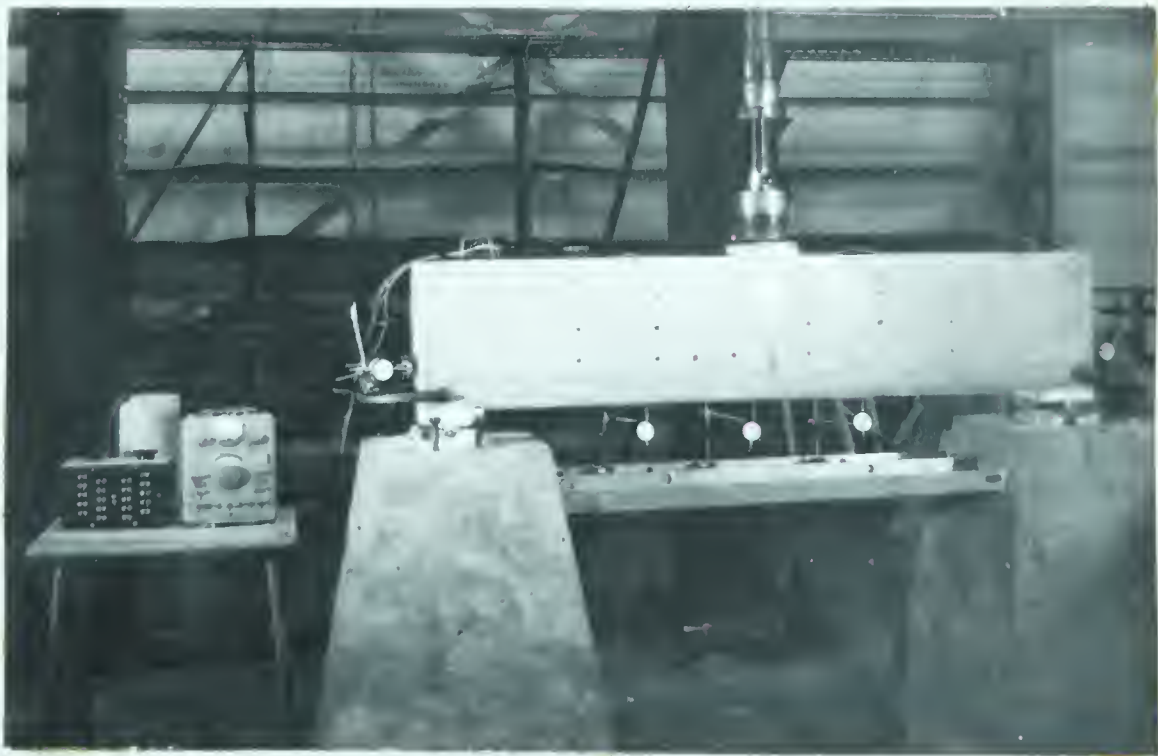


FIGURE 3.6 INSTRUMENTED TEST SPECIMEN

### 3.2.3   Casting and Curing

Concrete was mixed in a 9 cu. ft. capacity non-tilting mixer. For the long beams two batches of approximately 5 cu. ft. each were required. The first batch from each mix was placed in the end regions of the beam and the second in the center. This was done to insure that concrete in the region of failure was from one batch and of uniform quality.

Initially a butter mix of about 1.5 cu. ft. was used to condition the mixer. This mix was of the same proportions as the batches to be used in the beam. Since the moisture content of the aggregates varied from day to day the amount of water to be added was determined largely by visual inspection. The water requirement for the butter mix served as a criterion for mixing the batches used in the beam. Slump tests were made on each batch before placing in the form. Concrete was placed and compacted with the aid of an immersion type high frequency vibrator.

Six control cylinders and two $3\frac{1}{2}$ x $4\frac{1}{2}$ x 16-in. control beams were cast from the last batch which represented the region of failure. Compressive strengths were obtained

from one cylinder tested at three and seven days and two
cylinders tested on the day of the beam test. Also on the
test day two more cylinders were tested in splitting and two
control beams were tested in flexure. These beams were
loaded at the third points of a 12-in. span.

After the concrete had set, the beam and control
specimens were covered with soaked burlap and a polythene
sheet. After 24 hours the forms were stripped and the beam
was again covered. Moist curing continued for an additional
two to three days at which time it was removed from the
prestressing bed. Once removed from the bed the beams were
cured in air at laboratory conditions until the time of
test.

Release of prestress was carried out three to
four days after casting at which time concrete strength was
sufficient to allow transfer of prestress to the beam. In
order to minimize unbonding along the cables, it was
desirable to effect transfer as gently as possible. This
was done by slowly heating the cables with an acetylene
torch. Heating caused an expansion of the cables followed
by loss of tensile strength and subsequent failure of

individual strands. Time required for this part of the operation was five to six minutes. Tensile stresses in the extreme fiber were computed from the elastic strains caused by transfer. In no case did the tensile stress exceed 200 psi.

### 3.2.4    Test Specimens

All beams were of a 6 x 14 5/8-in. cross-section with an effective depth of 10-in. Beams 11 to 13 and 1A to 6A were 12'-4" overall length and beams 1B to 6B were 6'-0". Span length for the long beams was 11'-0" and for the short beams was 5'-6". Details of the test specimens are given in TABLE 3.4.

Beams 10, 11 and 12 constituted one series. The major variable to be investigated was the percentage of tension reinforcements with concrete strength and effective prestress remaining constant. These beams were loaded at two points with a constant moment region of 5-ft.

Beams 1A to 6A were designed for testing with a single point load at mid-span. Variables for this series were concrete strength and amount of reinforcing. For each

TABLE 3.4

DETAILS OF TEST SPECIMENS

| Beam No. | $f_c'$ (psi) | Area of Reinforcement $A_s$ (in$^2$) | $P = \dfrac{A_s}{bd}$ | $\dfrac{p}{f_c}$ $10^7$/psi | Effective Prestress $f_{se}$ (ksi) |
|---|---|---|---|---|---|
| 11 | 4030 | 0.1156 | 0.00193 | 4.78 | 139 |
| 12 | 3620 | 0.2312 | 0.00385 | 11.06 | 139 |
| 13 | 3390 | 0.3468 | 0.00578 | 17.10 | 137 |
| 1A | 4310 | 0.2312 | 0.00385 | 8.90 | 138 |
| 2A | 3450 | 0.3468 | 0.00578 | 16.78 | 138 |
| 3A | 3550 | 0.4624 | 0.00770 | 21.70 | 130 |
| 4A | 5970 | 0.2312 | 0.00385 | 6.44 | 146 |
| 5A | 6840 | 0.3468 | 0.00578 | 8.47 | 142 |
| 6A | 6890 | 0.4624 | 0.00770 | 11.20 | 144 |
| 1B | 3540 | 0.2312 | 0.00385 | 10.85 | 141 |
| 2B | 4250 | 0.3468 | 0.00578 | 13.62 | 136 |
| 3B | 3550 | 0.4624 | 0.00770 | 21.70 | 137 |
| 4B | 6310 | 0.2312 | 0.00385 | 6.10 | 143 |
| 5B | 6460 | 0.3468 | 0.00578 | 8.95 | 143 |
| 6B | 5940 | 0.4624 | 0.00770 | 12.95 | 144 |

concrete strength, low or high, three quantities of tensile reinforcement were tested. Series B was the same as Series A, except that the span length was reduced by half.

Shear reinforcement for all beams was designed to meet ACI 318-63, (11), requirements. The amount of transverse reinforcement was governed by the section proper-ties and thus varied from beam to beam. Beams 10, 11 and 12 were reinforced with stirrups only in the outer shear span. Stirrup spacing was kept constant throughout a particular beam. Details of shear reinforcement are given in TABLE 3.5.

## 3.3   Testing

### 3.3.1   Instrumentation

Distribution of strains in the concrete throughout the depth of the beam were measured with an 8-in. Demec strain gage. Sufficient gage lines to instrument the entire cracked region were provided. The number of gage lines used were as follows:

Beams 11 to 13 : 4

Beams 1A to 6A : 9

Beams 1B to 6B : 5

TABLE 3.5

DETAILS OF SHEAR REINFORCEMENT

| Beam No. | Bar Size | Spacing (in) |
|---|---|---|
| 11 | #3 | 8 |
| 12 | #3 | 6 |
| 13 | #3 | 5 |
| 1A | #2 | 6 |
| 2A | #2 | 6 |
| 3A | #3 | 6 |
| 4A | #2 | 6 |
| 5A | #2 | 5 |
| 6A | #3 | 5 |
| 1B | #3 | 4 |
| 2B | #3 | $2\frac{1}{2}$ |
| 3B | #3 | 2 |
| 4B | #3 | 4 |
| 5B | #3 | $2\frac{1}{2}$ |
| 6B | #3 | 2 |

These were arranged symmetrically about the center line.

The distribution with depth was arranged to obtain maximum

coverage in the compression zone.  Gage lines were set

at the following distances from the top of the beam:

Beams 11 to 13 - 1, 3, 6 and 10 in.

Beams 1A to 6B - 1, 2, 4, 7 and 10 in.

Steel Demec points, $\frac{1}{4}$-in. in diameter, fastened to the

beam with sealing wax, were used to establish the gage

lines.

In addition to deformations over the depth

of the beam limiting strains in the top fiber were

measured.  Both Demec gages and type A3, SR-4 electrical

resistance strain gages were used.  Electrical gages were

mounted on the longitudinal center line of the beam at

the following dinstance from the center line of the span:

Beams 11 to 13 : 3, 9, and 18-in. (summetrical
about midspan)

Beams 1A to 6A : 8, 16, 24 and 32-in. (one side
only)

Beams 1B to 6B : 8 and 16-in. (symmetrical
about midspan)

For Beams 1A to 6B Demec gages on the top face of the beam

were mounted coincident with the gages on the side.  Since

the load was applied at the mid-span the gage in this posi-
tion could not be measured.

The electrical resistance strain gages were
mounted as follows:  the desired location was first ground
smooth with a portable grinder.  A thin coat of Cycle-weld,
for sealing purposes, was then applied and allowed to dry
for two to three days.  Gages were then attached to the
beam using a Budd GA-1 Cement Kit according to the manu-
facturer's recommended procedure.  A Baldwin-Lima-Hamilton
electrical strain indicator was used to measure the
strains.

Beam deflections were obtained from dial
gages.  The dial gages were attached by means of magnetic
bases to a rigid member, spanning between the beam supports.
For the long beams the dials were located at mid-span
and at 15 and 30-in. to each side.  On the short beams
the dials were located at mid-span and 12-in. to each
side, except for Beam 1B which had the dials 15-in. to
each side.  The arrangement of dial gages and Demec points
is seen in FIGURES 3.6 and 3.7.  Dial gages were also
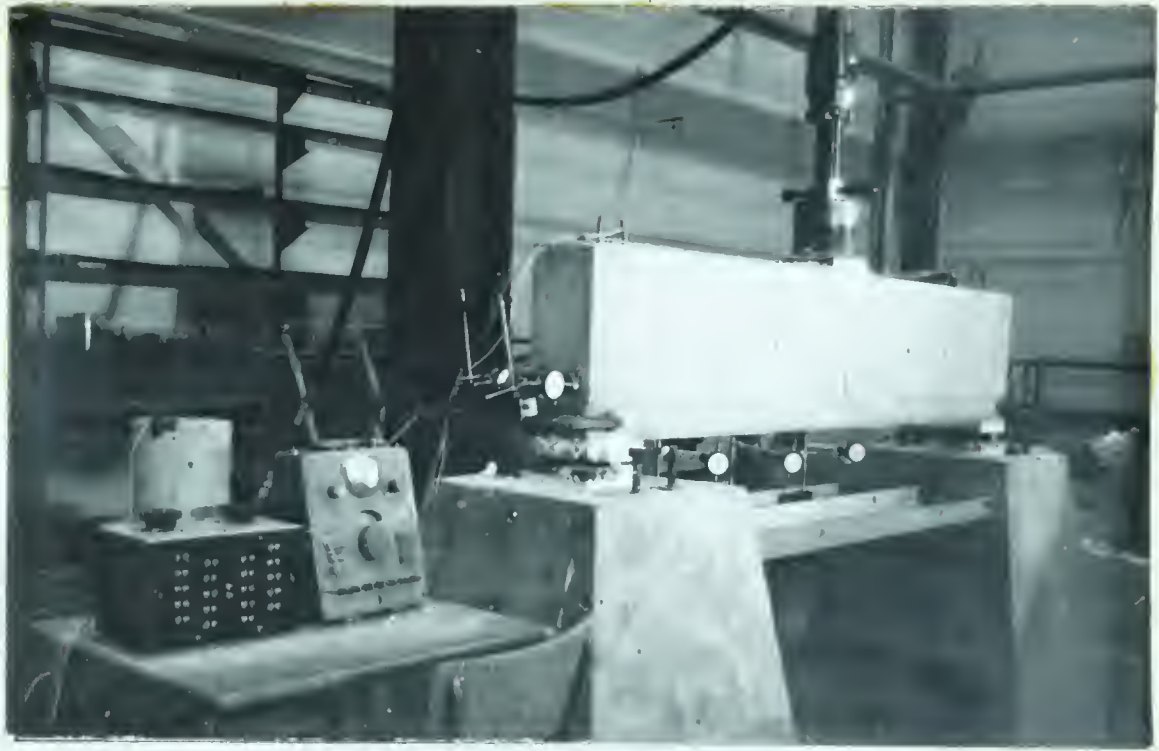attached to the cables to indicate initiation and

FIGURE 3.7 TEST SPECIMEN AND INSTRUMENTATION
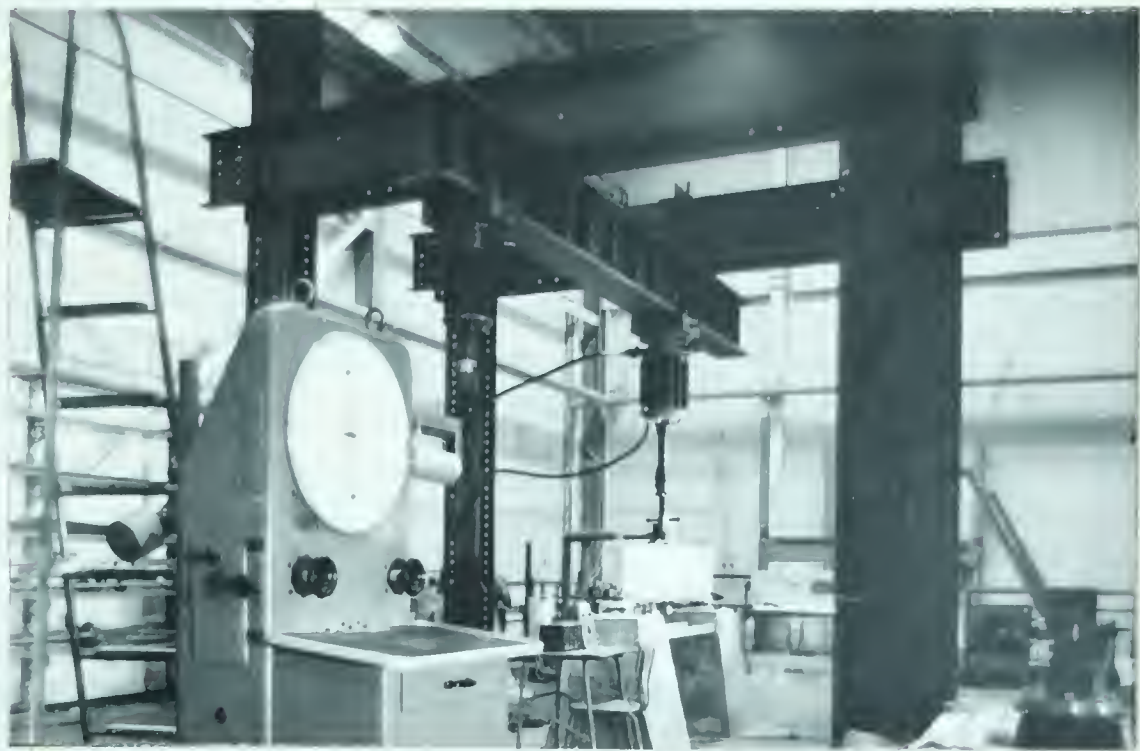


FIGURE 3.8 LOADING APPARATUS

degree of unbonding. On the short beams a surveying level trained on a steel rule attached to the beam was used to read deflections after crushing.

### 3.3.2    Loading Apparatus

The beams were tested in a loading frame employing a single 44 or 110 Kip. Amsler hydraulic jack. The loading frame and associated equipment are shown in FIGURE 3.8. Oil pressure to operate the hydraulic jacks was measured by an Amsler Pendulum Dynamometer. The force applied by the jack was infinitely variable from zero to maximum jack capacity. A load maintaining device ensured that a load, once set, would be maintained without variation even though the specimen was creeping at a high rate.

For the two-point loaded beams, No. 11, 12 and 13, a distributing beam was used. Load was applied to the beams through a ball bearing, between bearing plates, on one end of the distributing beam and a roller between bearing plates on the other end. The load was applied directly through a 6 x 6-in. bearing plate for the single-point loaded beams. Bearing plates were attached to the

beams with Plaster of Paris to provide an even distribution of stress.

### 3.3.3  Testing Procedure

At the start of the test, before any load was applied, initial readings were taken on the strain gages and the deflection dials were set to zero. An average of 10 load increments were applied before failure. Usually three increments of load were applied before initial cracking. After cracking and in the later stages the size of load increment was reduced. A more uniform increase in strain with each load increment was thus maintained. In all cases the load was maintained at a constant value after each increment was applied, while readings were taken.

The procedure for reading and recording of data throughout a test was the same for all beams. The gages were read in the following order:

(a)  dial gages

(b)  demec gages

(c)  electrical resistance strain gages

(d)  level (Series B only)

(e)  dial gages

The crack pattern was marked while the above readings were taken. The beams were loaded until total collapse or, in cases where unbonding resulted, until large deformations were being obtained at a constant load less than that at crushing. Photographs were taken after failure to record the crack patterns and modes of failure.

# CHAPTER IV

## PRESENTATION OF TEST RESULTS

### 4.1    Distribution of Strain Over the Depth of the Beams

The distribution of strain over the depth of the

beam was obtained by measuring the deformation between

gage points with an 8-in. Demec gage.  For Series A and B

deformations were measured at six different levels over the

depth of each beam.  For Beams 11, 12 and 13 measurements

were made at four different levels.  The top three rows of

gage lines in Series A and B were located so that they

would be essentially in the uncracked compression zone at

failure.

Sufficient columns of gage lines were established

to instrument fully the cracked region of the single-point

loaded beams.  During the early stages of loading each gage

line showed a linear distribution of strain.  Once cracking

occurred, the strains on a particular gage line, varied over

the depth.  With cracks between the Demec points, the strains

measured were largely a function of the crack opening rather than deformation of the concrete. In some cases, where cracking did not occur within the gage lines, a decrease in strain with increasing load was observed. The strains measured depended upon extent, spacing and type of cracking. The strain distribution throughout the uncracked compression zone, however, remained linear.

The average strain distributions for the entire instrumented region of the beams were found to be linear. For the two-point loaded beams, the region between the loads was subjected to a constant moment. The average strain distributions for the constant moment region could be used for the determination of curvature. FIGURE 4.1 shows the average strain distribution at successive increments of load for a two-point loaded beam.

For the single-point loaded beams a moment gradient existed along the entire span. The average distribution of strain for the instrumented region was not valid for derivation of relationships. Another means of representing the distribution of strains at various sections of the beam had to be found. During the course of the investigation it
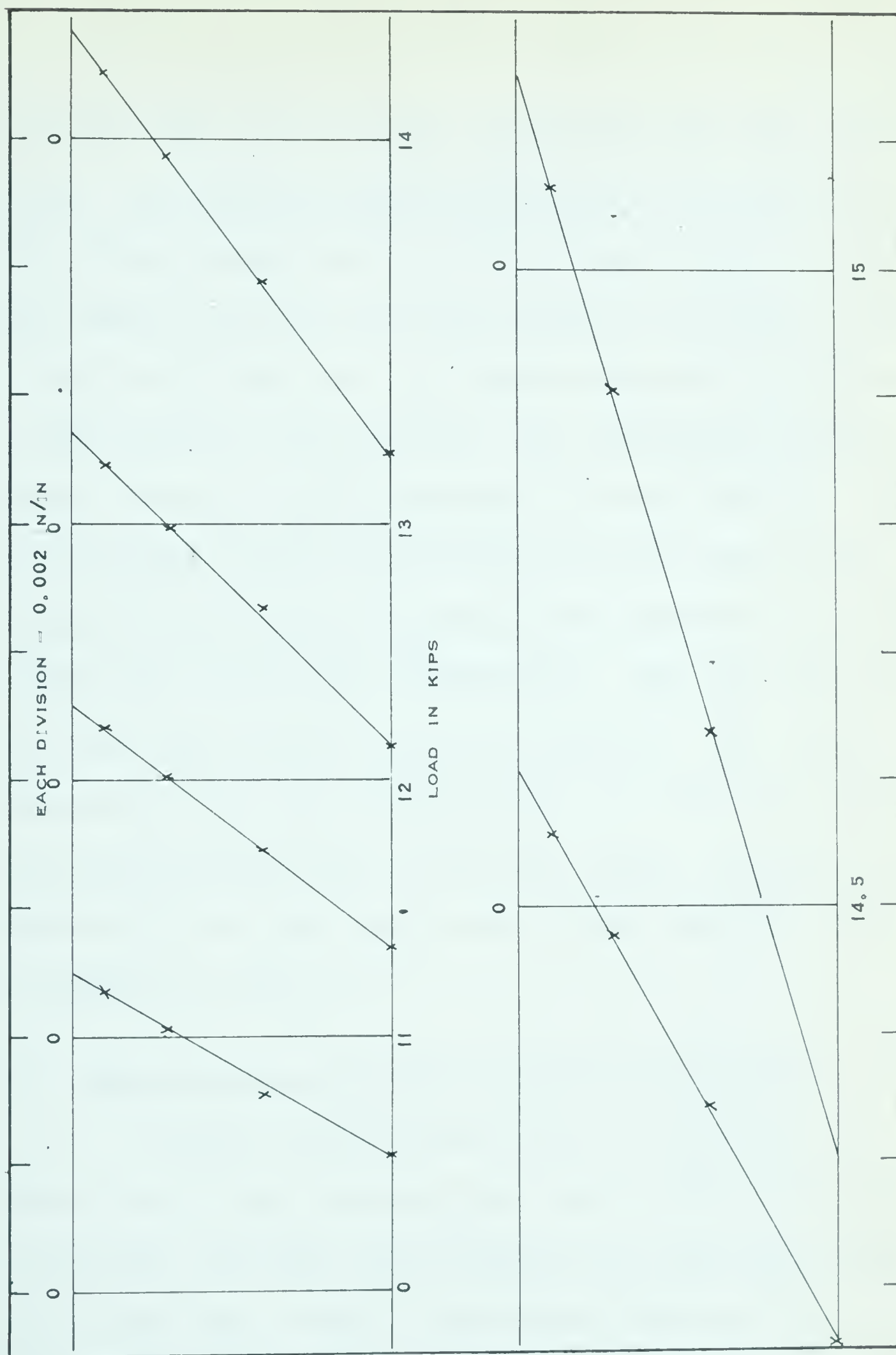
FIGURE 4.1 AVERAGE DISTRIBUTION OF STRAIN OVER DEPTH OF BEAM II

was found that strains in the compression zone were consistently
linear. The tension strains were found to be either too
large, when measured over a well developed crack or too small,
when measured over an uncracked section of concrete. Both
of these conditions were of a local nature and not indicative
of the "average" beam behavior. The compressive strains,
however, were not greatly affected by local cracking. Represen-
tative average strain distributions over the depth were
obtained by extending the linear strain distributions of the
cracked zone through the cracked area. This was done for
each gage line across the span of the beam. The strain
distributions obtained in this manner are "average" distribu-
tions representing 8-in. of the beam length. Typical strain
distributions for the single-point loaded beams are shown
in FIGURES 4.2 and 4.3 .

4.2   Distribution of Strain on the Top of the Beam

Strains in the extreme fiber of the beams in
Series A and B were measured with Type A3, SR-4 electrical
strain gages and Demec gages placed along the longitudinal
axis of the beam. Since a distributing beam was used to
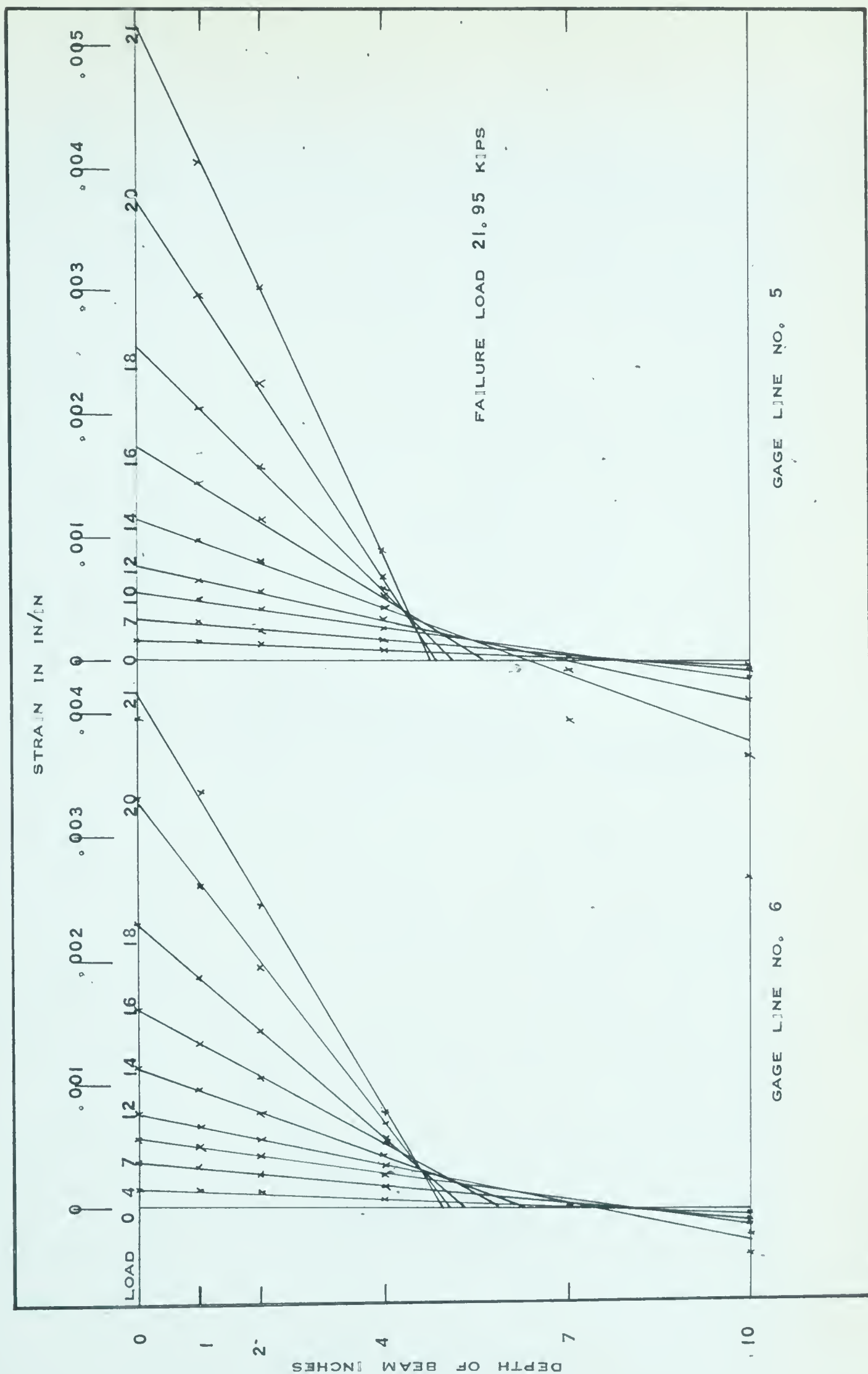apply load at two points on Beams 11, 12 and 13 the Demec

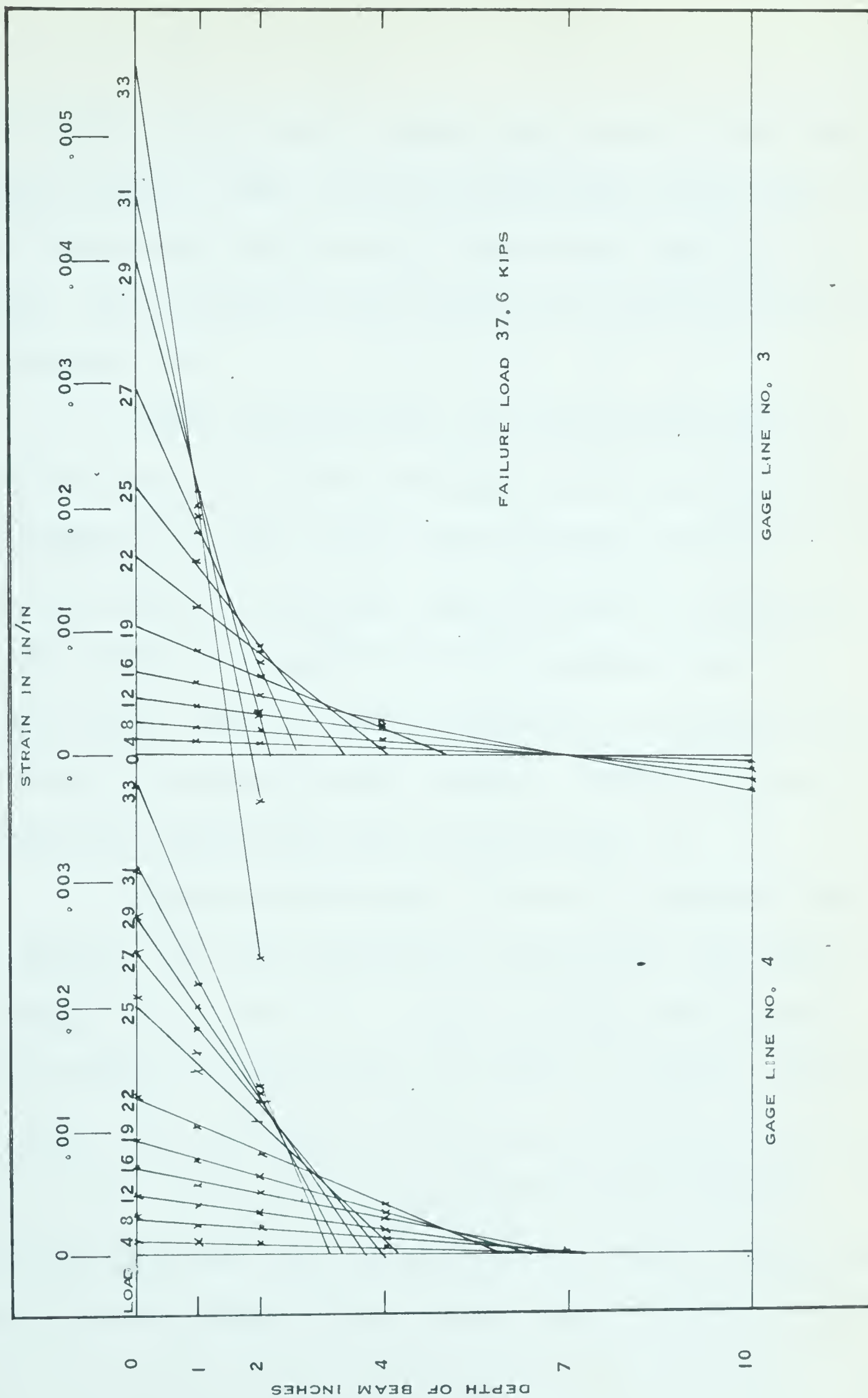FIGURE 4.2 DISTRIBUTION OF STRAIN OVER DEPTH OF BEAM 2A

FIGURE 4.3 DISTRIBUTION OF STRAIN OVER DEPTH OF BEAM 4B

gage could not be used to measure top strains in the constant moment region. Thus, only SR-4 electrical strain gages were used to measure the strains in the extreme fiber of these beams. The location and spacing of the gages was discussed in Section 3.3.1 .

Strain distributions over the flexure span at various stages of loading for Beams 11, 12 and 13 are plotted in FIGURE 4.4 . The largest strains shown correspond to the load just prior to failure. Beam 11 failed by fracturing of the cables at a maximum recorded concrete strain of 0.003 in/in. Beams 12 and 13 failed due to crushing of the concrete at maximum recorded concrete strains in excess of 0.004 in/in. and 0.006 in/in. respectively.

Typical distribution of strain at various stages of loading, for the single-point loaded beams, are shown in FIGURES 4.5, 4.6 and 4.7 . All the single-point loaded beams showed a concentration of strain at midspan. Before cracking, the distribution of strain on the top of the beam was similar to the shape of the bending moment diagram. As cracking progressed the concentration of strain became more severe in the region of the applied load. The strain plotted
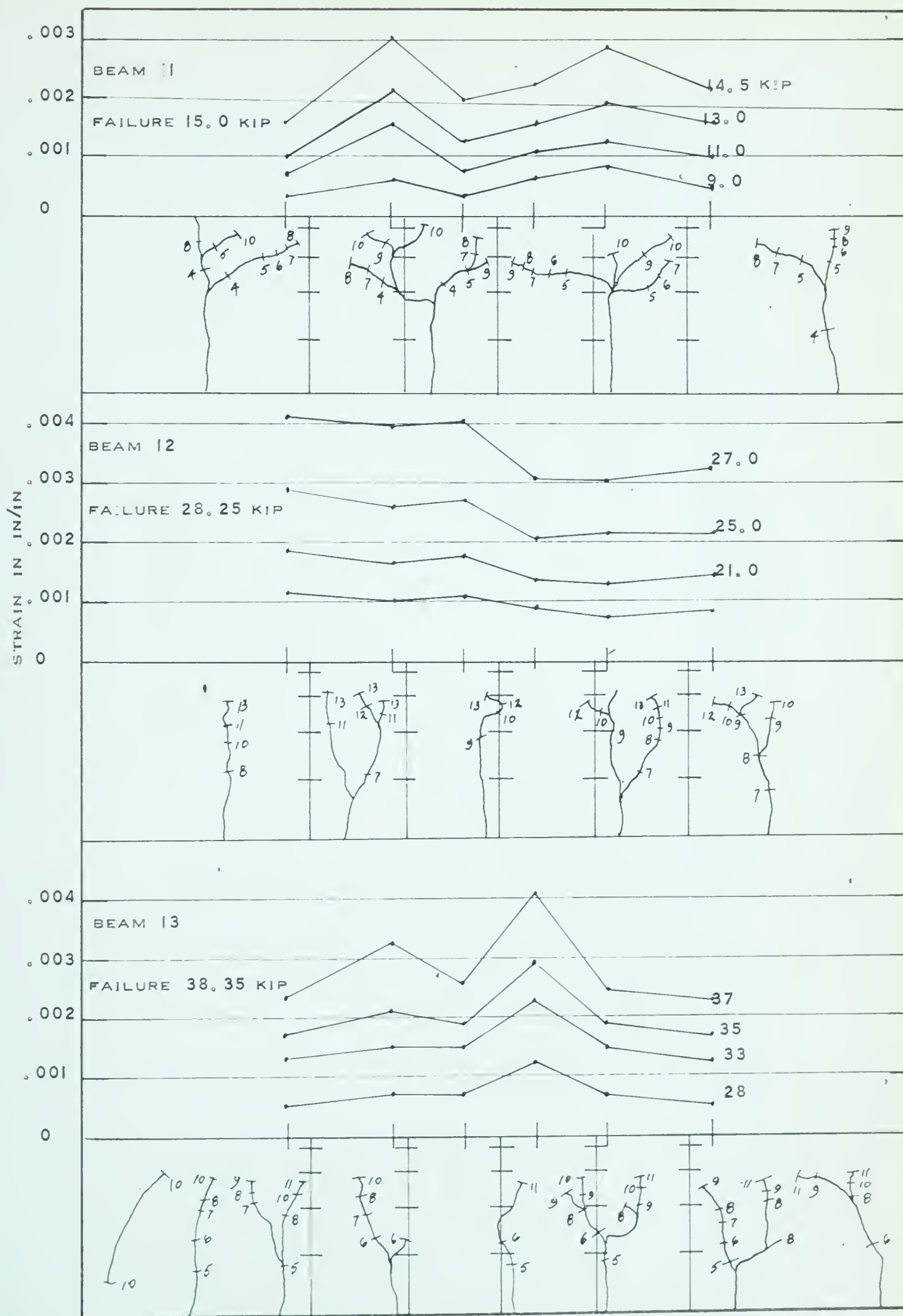
FIGURE 4.4 STRAIN DISTRIBUTION ACROSS THE BEAMS AND
CRACKING PATTERN
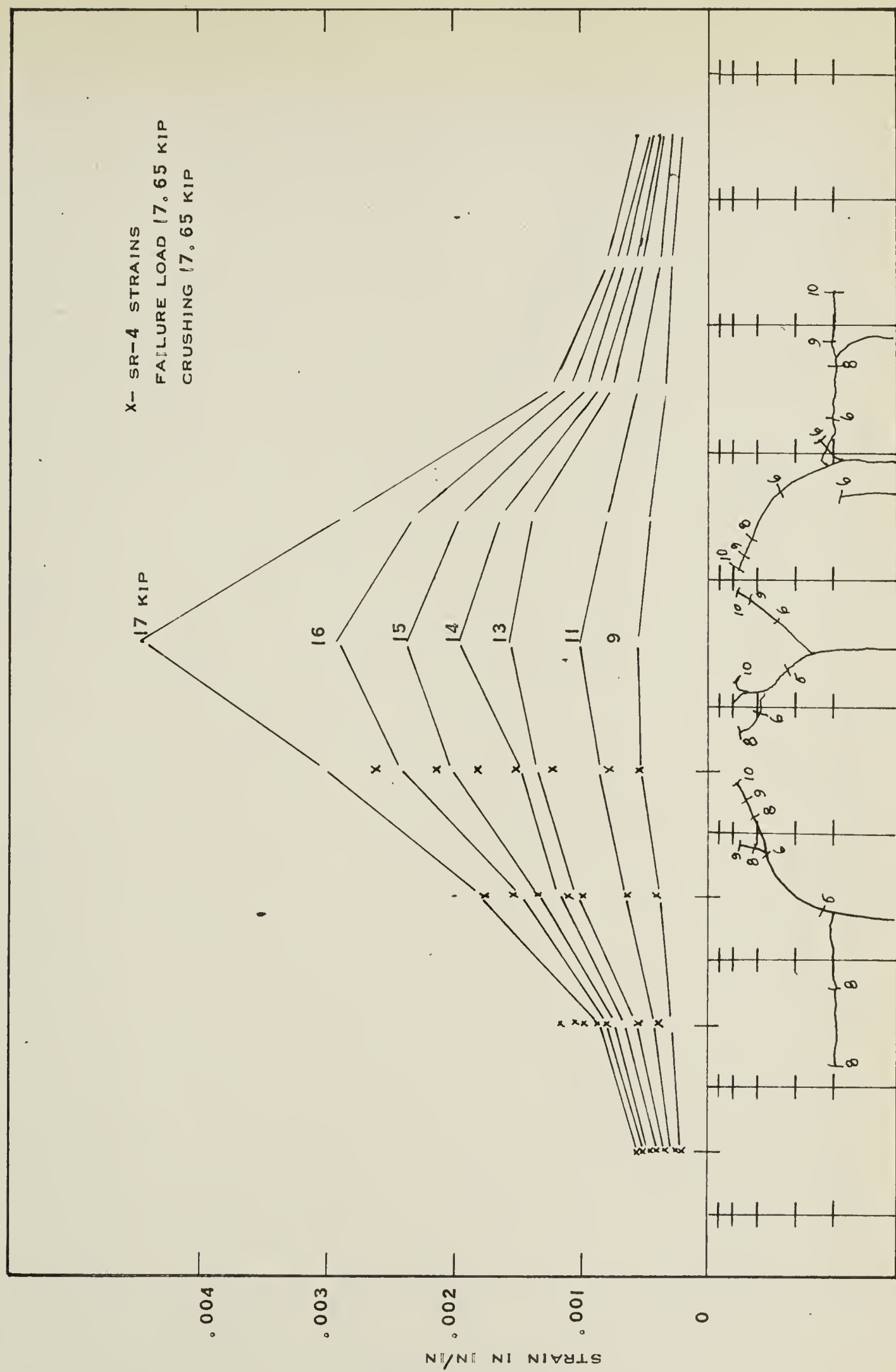
FIGURE 4.5 DISTRIBUTION OF STRAIN IN EXTREME FIBER AS READ BY DEMEC GAGE BEAM IA
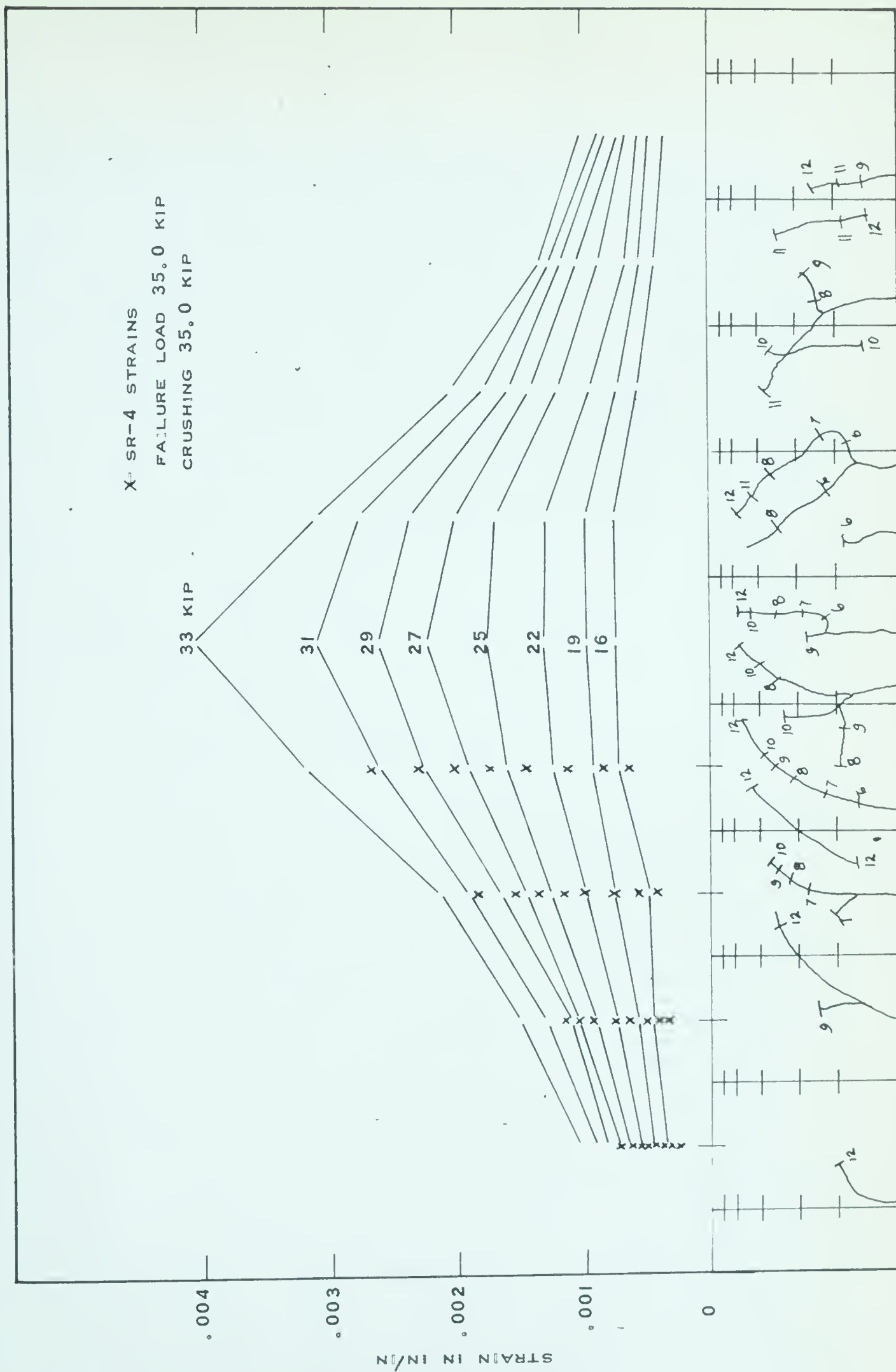
FIGURE 4.6  DISTRIBUTION OF STRAIN IN EXTREME FIBER AS READ BY DEMEC GAGE BEAM 6A
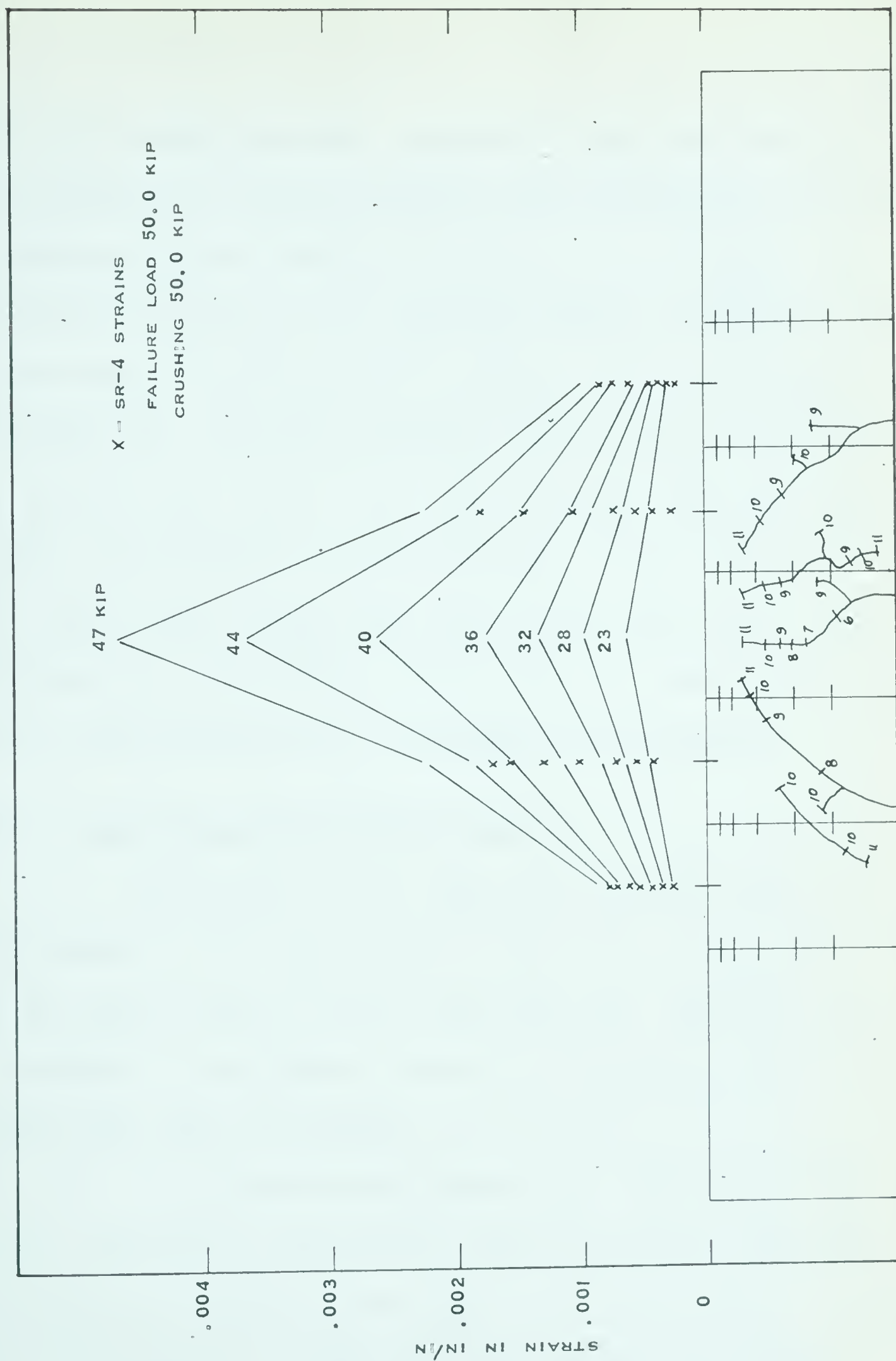
FIGURE 4.7 DISTRIBUTION OF STRAIN IN EXTREME FIBER AS READ BY DEMEC GAGE BEAM 2B

for the midspan position, occupied by the load bearing plate,
was obtained by extrapolation of the distributions of strain
obtained by Demec readings on the side of the beam. Distri-
butions of strain for the remaining beams, obtained at the
last stage of loading before failure, are shown in FIGURES 4.8,
4.9 and 4.10. Strains obtained from the SR-4 strain gages,
as a rule, were lower than those obtained from the Demec
gages. The maximum recorded concrete strains at midspan
for these beams ranged from about 0.002 in/in. for a beam
failing due to unbonding of the cables, to about 0.006 in/in.
for a beam failing due to crushing of the concrete.

## 4.3   Load Deflection Relationships

Deflection of the beams was measured using five
dial gages on the long beams and three dial gages and a level
on the short beams. In all cases one dial gage was located
at midspan. Load midspan deflection curves for all the beams
tested are shown in FIGURES 4.11 to 4.15 .

A load maintaining device was used for all the
tests. Wherever a particular load was reached, this load
was maintained constant throughout the time required to take
all the readings. During the later stages of loading,
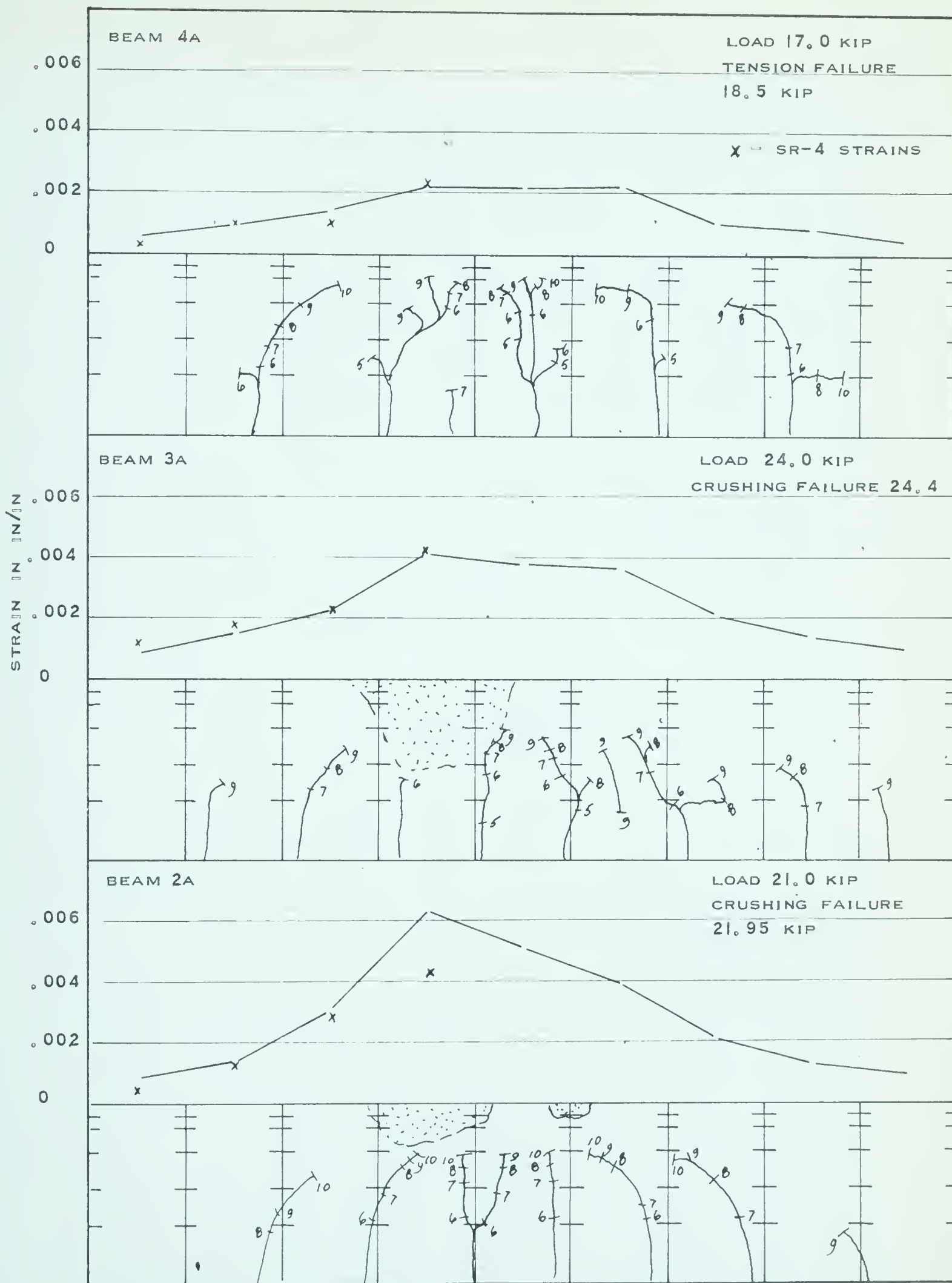
FIGURE 4.8   STRAIN DISTRIBUTION ACROSS THE BEAMS AND
             CRACKING PATTERNS
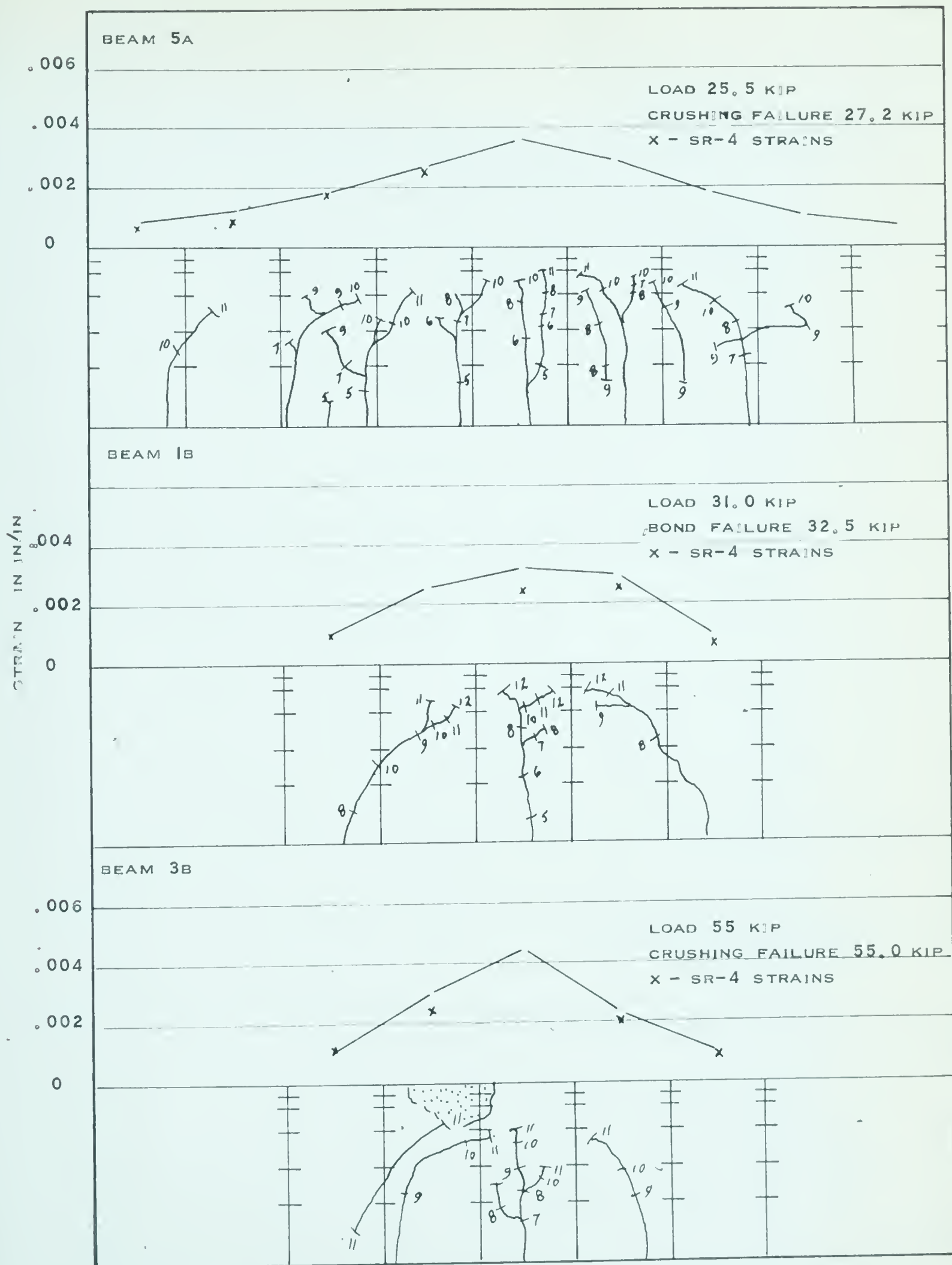
FIGURE 4.9  STRAIN DISTRIBUTION ACROSS THE BEAMS AND
CRACKING PATTERNS
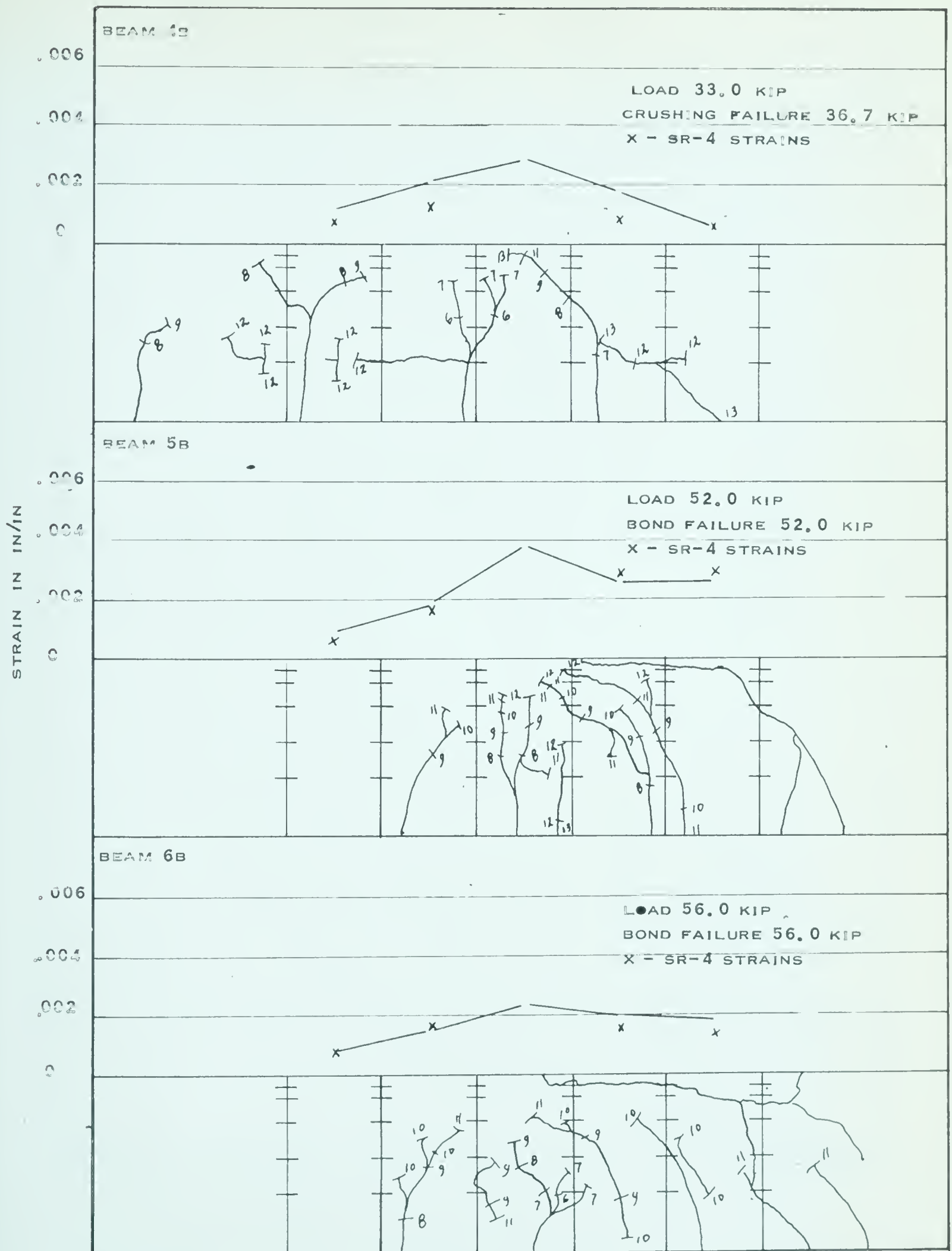
FIGURE 4.10  STRAIN DISTRIBUTION ACROSS THE BEAMS AND
CRACKING PATTERNS
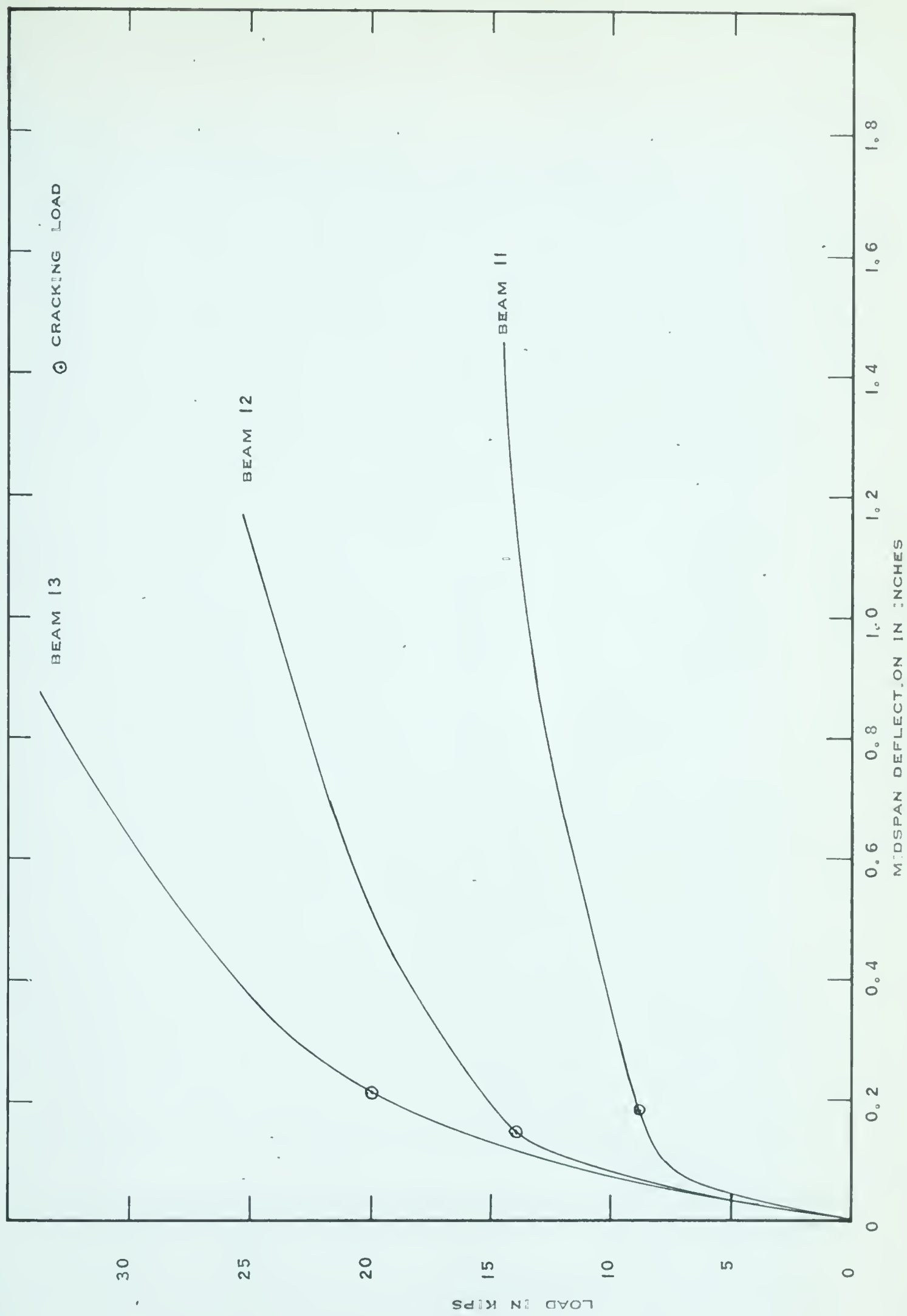
FIGURE 4.11 LOAD - MIDSPAN DEFLECTION CURVES
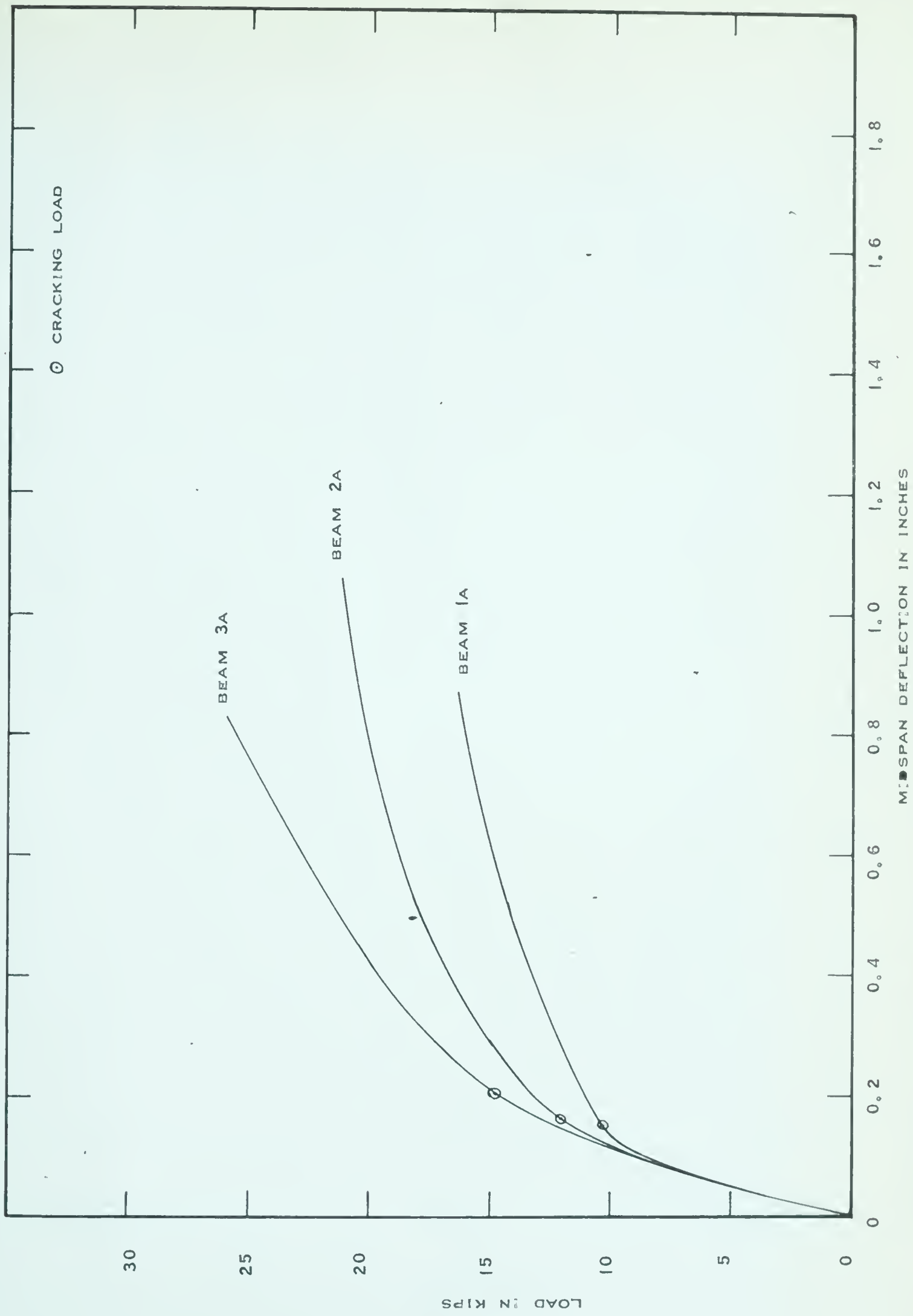
FIGURE 4.12 LOAD - MIDSPAN DEFLECTION CURVES
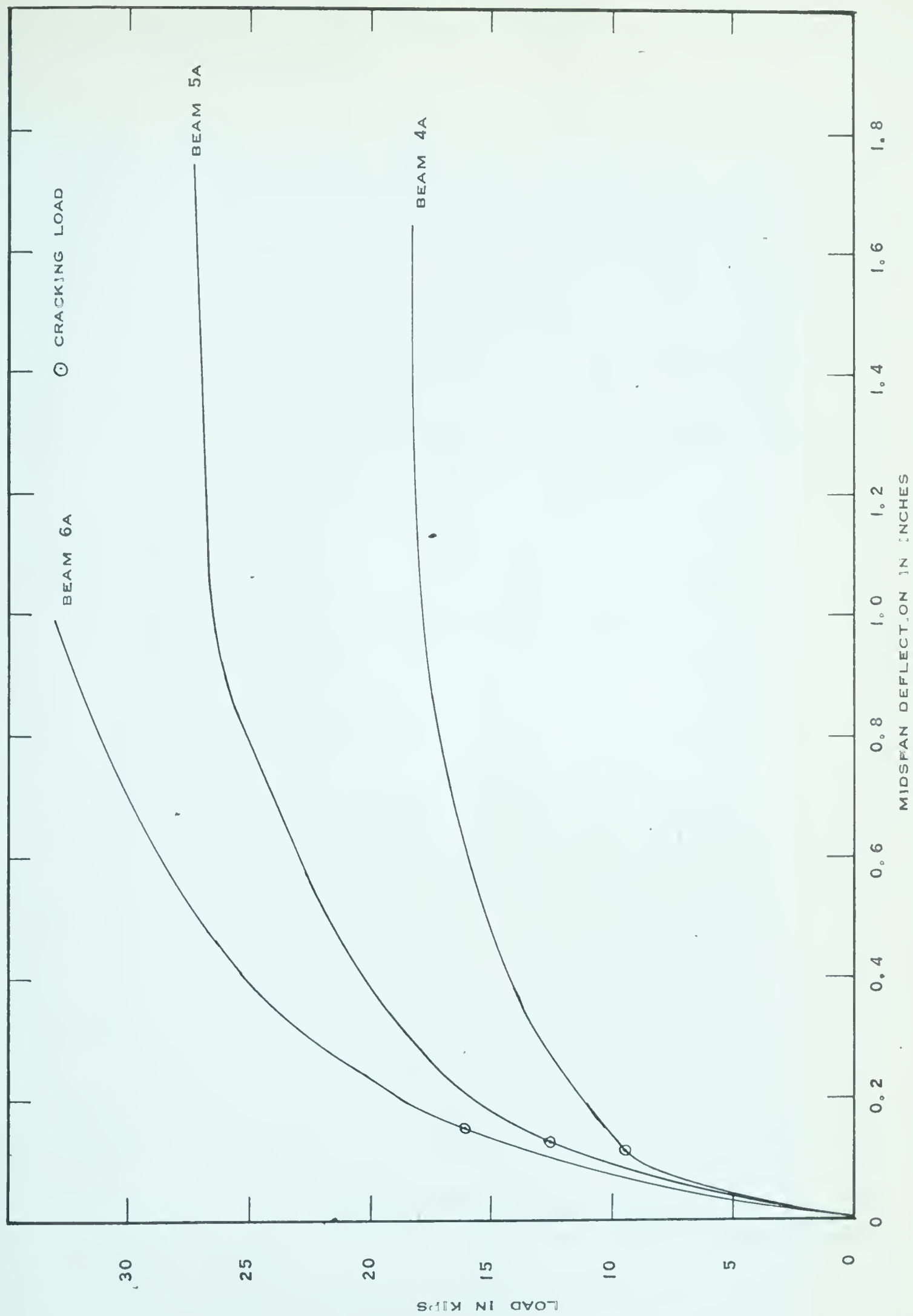
FIGURE 4.13 LOAD - MIDSPAN DEFLECTION CURVES
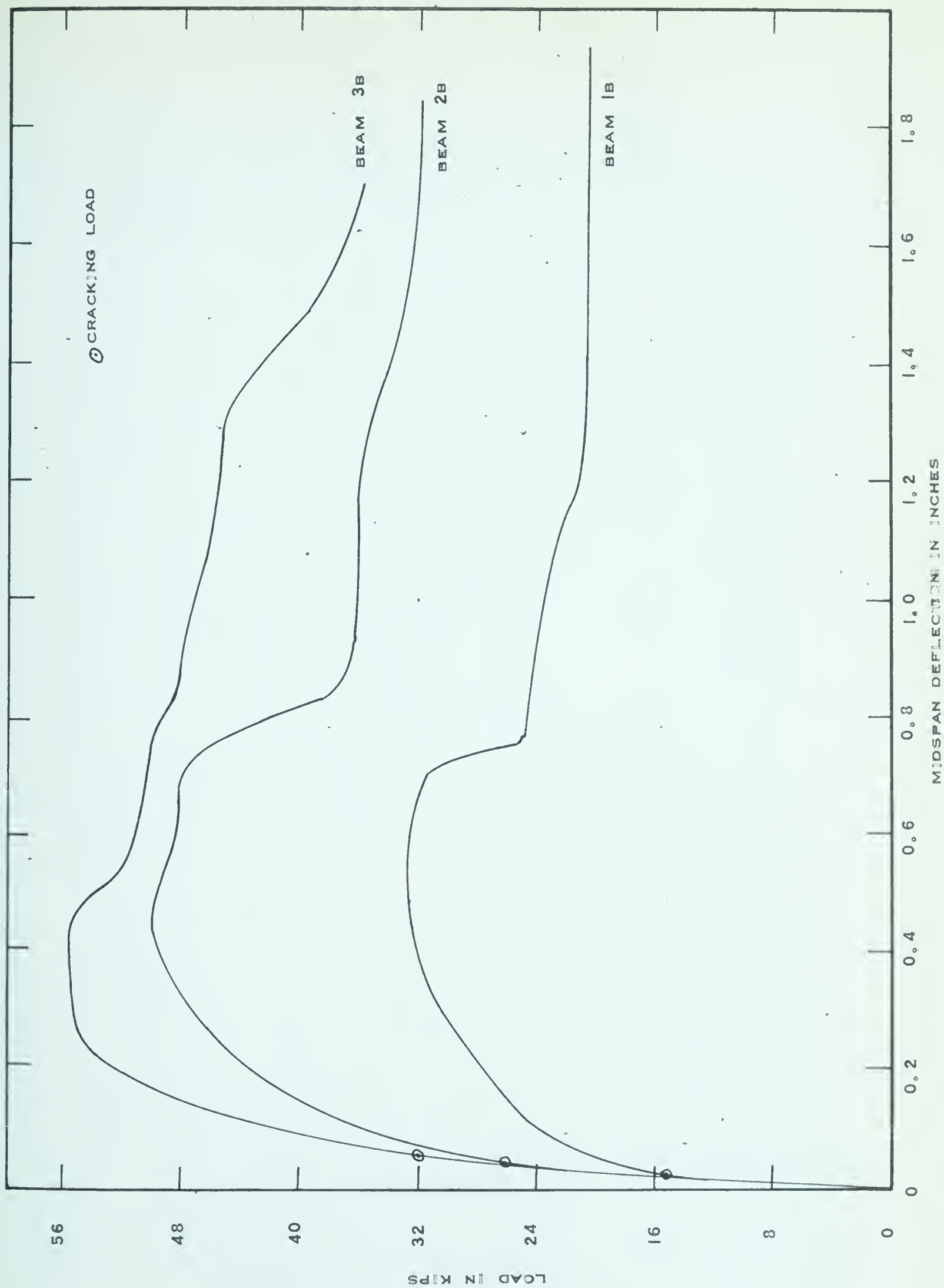
FIGURE 4.14 LOAD – MIDSPAN DEFLECTION CURVES
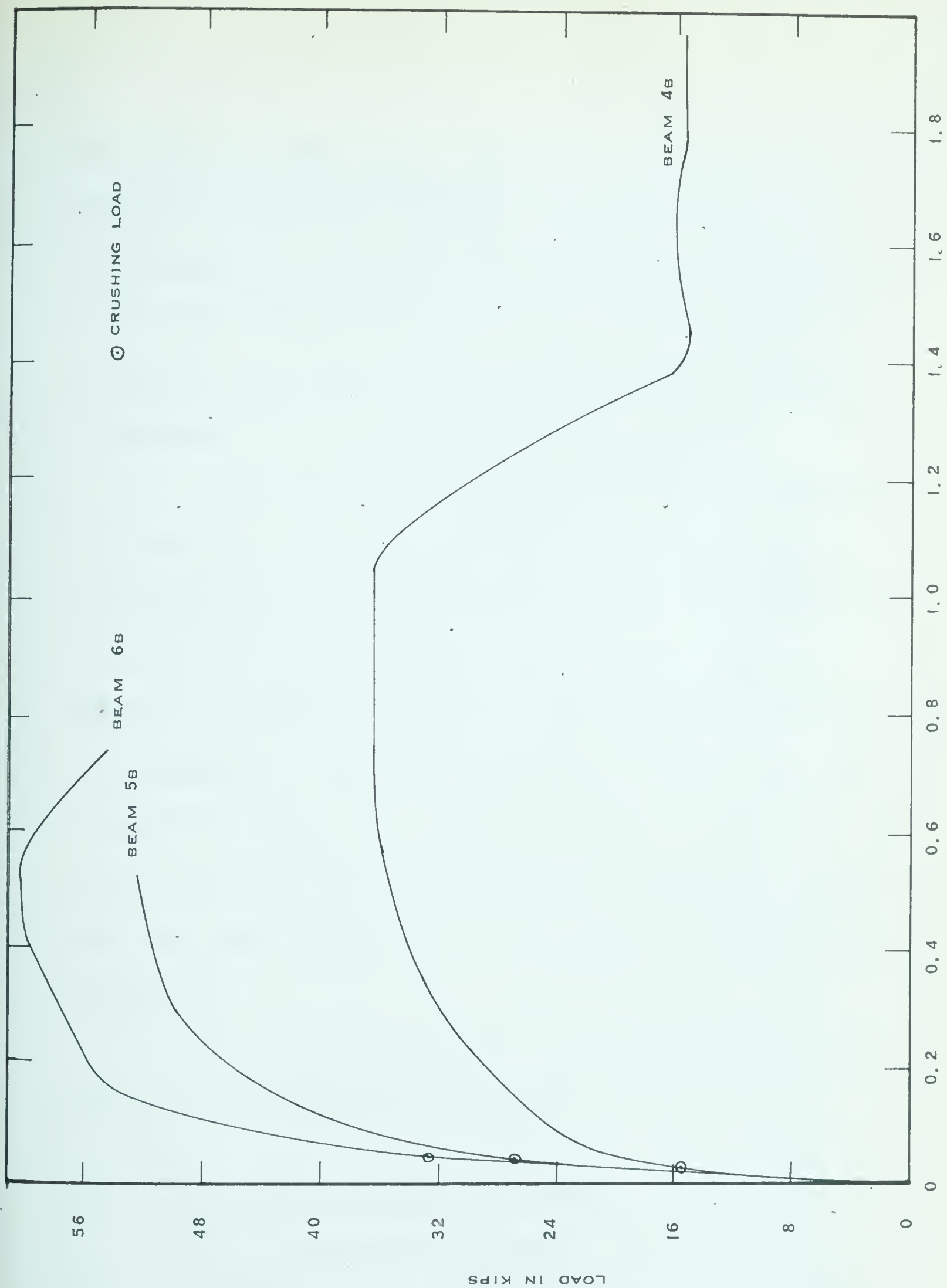
FIGURE 4.15 LOAD - MIDSPAN DEFLECTION CURVES

considerable creep of the beam occurred during the time required to take the readings. Dial gages were read immediately upon reaching the desired load and again just before the load increased. The deflections plotted in FIGURES 4.11 to 4.15 are the initial values obtained immediately after applying the load increment.

The dial gages were removed before the failure load was reached to avoid damaging them when the beam collapsed. Thus, the last value plotted in FIGURES 4.11, 4.12 and 4.13 are for loads just before failure. For Series B, however, a level was used to measure the deflections at midspan after the dial gages were removed. By this means deflections were obtained through and in most cases beyond initial failure of the beams. FIGURES 4.14 and 4.15 show the load-midspan deflection diagrams for the beams in Series B.

All deflections measured were referenced to the initial upward cambered position.

4.4    Behavior of the Test Specimens

    4.4.1    Introductory Remarks

        The response of a member to load is best

illustrated by load-deformation characteristics, which show both the strength and ductility of the member. Since all specimens tested were bonded beams with the same level of prestress, the behavior for each beam was generally the same. This is evident from the similarity of the load-midspan deflection curves shown in FIGURES 4.11 to 4.15 . Three distinct stages are indicated, each marked by a change in slope of the curve. The extent to which each stage developed in a particular beam depended on the characteristics of the beam. The major factors influencing behavior were: the stress-strain relationships of the concrete and the steel, the amount of longitudinal reinforcement and the span length.

Observations made during the tests indicated that each stage of behavior was related to a particular stress condition in either the reinforcement or the concrete of the beam. The first stage represented an elastic condition in both the concrete and the steel. In this stage the load-deflection relationship is characterized by a virtually linear line. The second stage showed an increased rate of deflection with applied load and represented the

behavior after the concrete had cracked. The reinforcement stress was still in the elastic range of the stress-strain curve. The third stage corresponded to an inelastic stress condition in the reinforcement. The load-deflection curve in this stage was a reflection of the reinforcement stress-strain curve and was nearly flat.

### 4.4.2 First Stage of Behavior

In the first stage of behavior the deflections were proportional to the applied loads and the beams were still uncracked. The first stage ended with the formation of a vertical flexural crack in the region of maximum moment.

The extent of this stage depended on the modulus of rupture of the concrete, the magnitude and eccentricity of the prestressing force and the type of loading. The load-midspan deflection curves show that the cracking load was higher for the more heavily reinforced beams. This was due to the higher prestressing force which produced higher compressive stresses in the bottom fiber. Before cracking occurred, this compressive stress had to be overcome and the limiting tensile stress reached. Similarly the cracking load

was found to be higher for beams with high strength concrete.

The initial slope of the load-deflection curve was a function of the beam stiffness. As a rule, the stiffness of the uncracked sections increased with higher concrete strength, higher prestressing force and shorter span length.

4.4.3    Second Stage of Behavior

The second stage of behavior commenced with initial cracking and continued until the inelastic range of the reinforcement was reached. The first vertical cracks appeared in the region of maximum moment and with additional load more flexural cracks appeared away from midspan. With a center-point load the cracks extended vertically to the level of the prestressed steel and then inclined toward the load. With the two-point loaded beams the cracks in the constant moment region remained vertical except for "forking" in the later stages of load. FIGURE 4.16 and 4.17 show crack patterns on single-point and two-point loaded beams, up to failure. It can be seen that the cracks developed very rapidly at first, but as loading progressed existing cracks rose slowly and "forked". The spacing and number of cracks formed depended on the amount of reinforcement. Crack
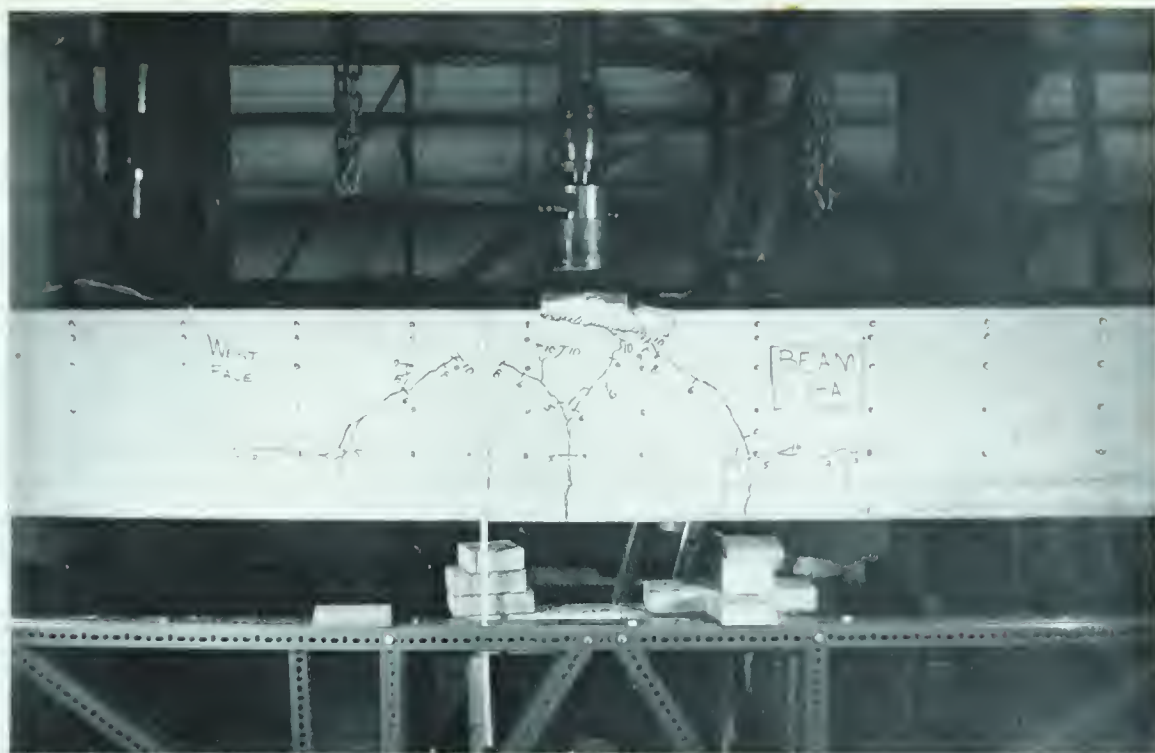
FIGURE 4.16 SINGLE POINT LOADED BEAM AT FAILURE



FIGURE 4.17 TWO POINT LOADED BEAM AT FAILURE

patterns of all the beams tested are shown in FIGURES 4.4 to 4.10 .

For beams having a low percentage of reinforcement, flexural cracking produced an abrupt change in the slope of the load-deflection curves. When the percentage of reinforcement was low, the transfer of tensile force from the concrete when cracking occurred caused an appreciable increase in the reinforcment stress and strain. The load-deflection relationship did not change abruptly after flexural cracking for beams having a high percentage of reinforcment and the point of flexural cracking was difficult to determine.

During the second stage of behavior the rate of increase in deflection with respect to load increased continually as the load increased. This was due to a decrease in stiffness of the beam caused by formation of additional flexural cracks and a continued rise of the neutral axis as the cracks extended higher into the beam.

The slope of this part of the load-deflection curve was dependent upon the percentage of reinforcement. Highly reinforced beams were much stiffer and deformed less for an increment of load. Similarly, the short beams of

Series B were stiffer than similar beams of Series A. The
short beams exhibited a considerable increase in the rate of
increase of deflection with respect to load, throughout the
second stage. The extent to which this stage developed also
depended on the percentage of reinforcement. Beams 3A, 6A,
3B and 6B failed by crushing of the concrete before the third
stage of behavior was reached.

4.4.4   Third Stage of Behavior

The third stage of a beam failing in flexure
commenced with inelastic straining of the tension reinforce-
ment and concrete. It was marked by a rapid increase in
beam deflection. An increase in moment caused large steel
strains with a small change in steel stress or length of
internal moment arm. At this stage of loading the cracks
were fully developed and inclined cracks had appeared in
the shear span of the two-point loaded beams.

The extent to which this stage developed
depended on the percentage of reinforcement and the concrete
strength. When the amount of reinforcement was large
crushing in the concrete occurred before inelastic strains
were reached in the steel. The load-deflection curves for

Beams 1A, 4A, 1B and 4B, which had low percentages of reinforcement, show a well developed third stage of behavior. The load-deflection curve for Beam 4A, which failed in tension, is typical for an under-reinforced beam.

The behavior of the beams in Series B was essentially the same as that of the long beams. Any difference in the load-deflection curves was due to shorter span length which increased the stiffness of the beams. The deflection for an increment of load was considerably less than for similar long beams. Both the second and third stage of behavior for these beams was limited and not as well developed as for the long beams.

## 4.5   Modes of Failure

### 4.5.1   General Remarks

The strength of a member depended on the capacity of the concrete to take compression and shear forces and the tensile strength of the tension and web reinforcement. Failure of any one of the integral components resulted in failure of the test specimen. The modes of failure of the beams tested were classified as:   tension failure, compression failure, shear failure or bond failure.

These classifications refer to the predominant conditions which determined initial failure of the member.

### 4.5.2    Tension Failure

Tension failure occurred when tension in the longitudinal reinforcement reached the yield stress before the concrete in the compression zone had crushed.  The occurrence of this type of failure depended on the percentage of reinforcement and the concrete strength.  Tension failures were sudden and resulted in total collapse of the member.

A two-point loaded beam and a single-point loaded beam, which failed in tension, are shown in FIGURES 4.18 and 4.19 respectively.  The number of cracks were small and widely spaced.  Since the ratio of steel to concrete was small for these beams, large tensile strains occurred.  The load-deflection curves in FIGURES 4.11 and 4.13 show the large deformations and ductile behavior associated with tension failure.

Tension failure of the longitudinal reinforcement caused final collapse of Beams 5A and 6A, even though initial failure was due to crushing of the concrete.  These failures were classified as compression failures and are

FIGURE 4.18 TWO - POINT LOADED BEAM, TENSION FAILURE
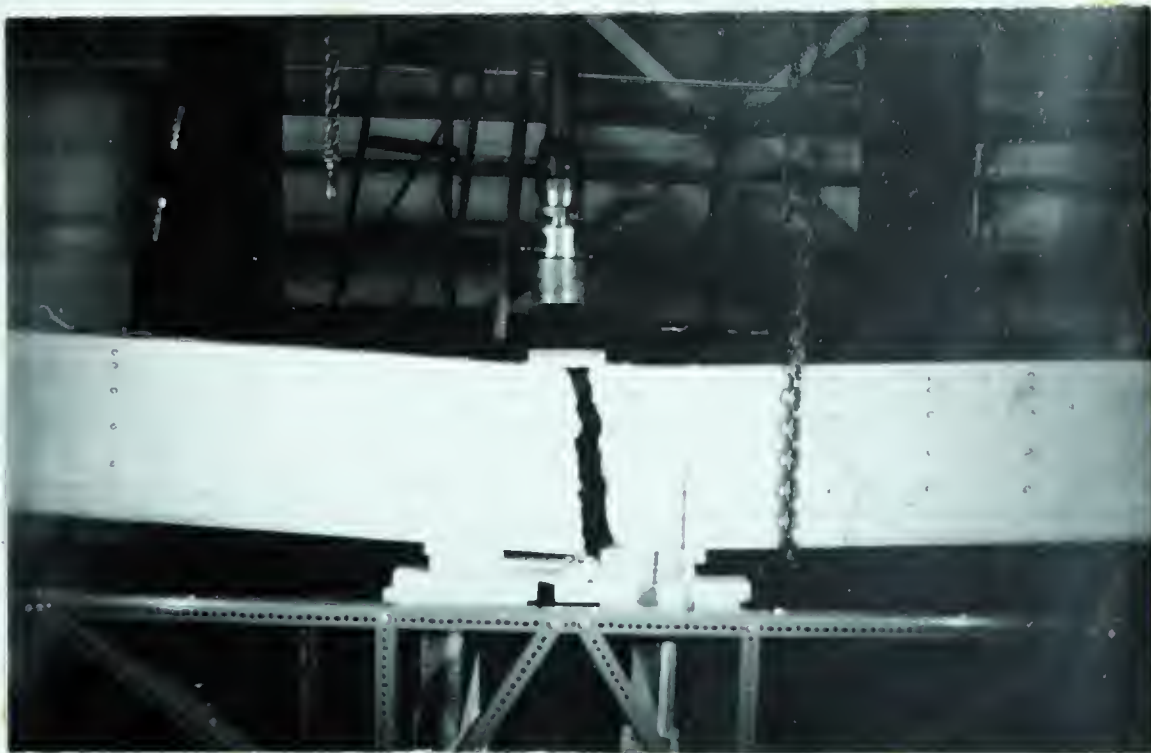


FIGURE 4.19 SINGLE - POINT LOADED BEAM, TENSION
FAILURE

discussed in the following section.

### 4.5.3    Compression Failure

The compressive force was carried entirely by the concrete above the neutral axis.  When the percentage of longitudinal reinforcement was high crushing of the concrete occurred before the yield stress of the steel was reached.  This condition was classified as a compression failure.  This type of failure is shown in FIGURES 4.20 and 4.21 .

Compression failures in the two-point loaded beams were explosive.  No indication of crushing was observed before failure.  This type of failure occurred because the entire centre portion of the beam is subjected to a constant bending moment.  With no moment gradient in this region, redistribution of stress upon initial crushing is restricted. The single-point loaded beams were subjected to a variable moment along the whole span and redistribution of moment was possible.  These beams carried considerable additional load after initial crushing of the concrete.  Crushing in these beams was gentle and progressed slowly downward from the extreme fiber as the load increased.  This progressive dis-
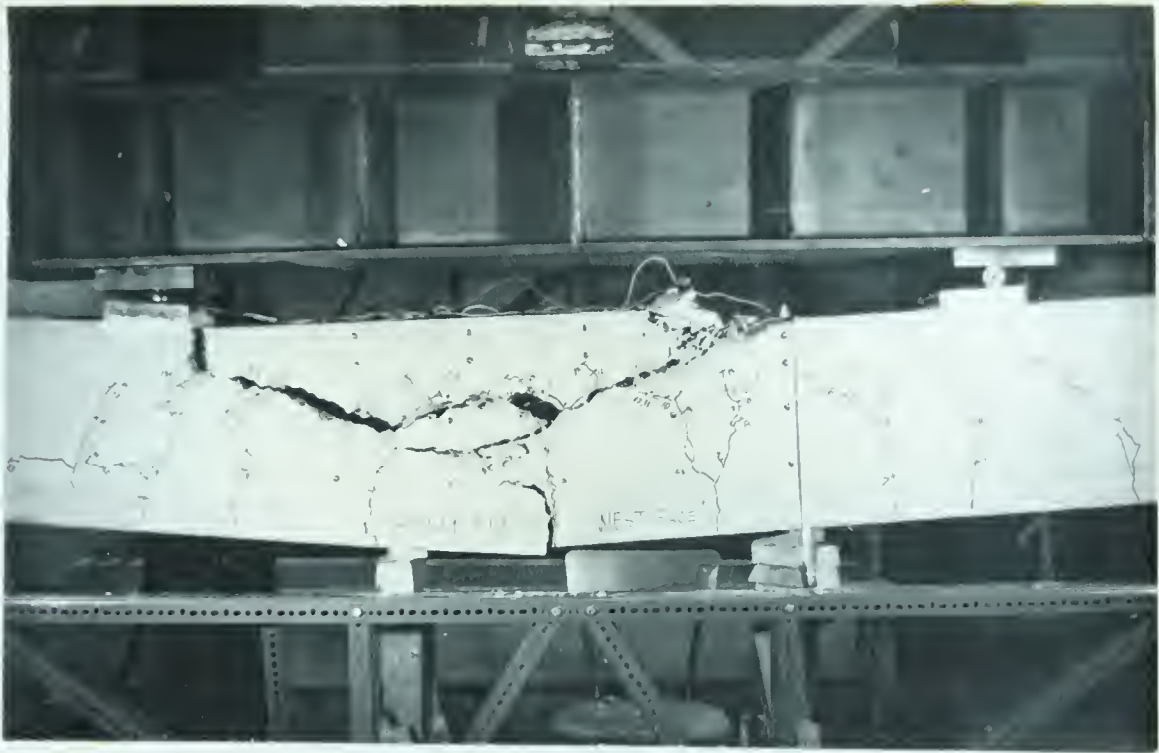
FIGURE 4.20 TWO - POINT LOADED BEAM, CRUSHING
FAILURE
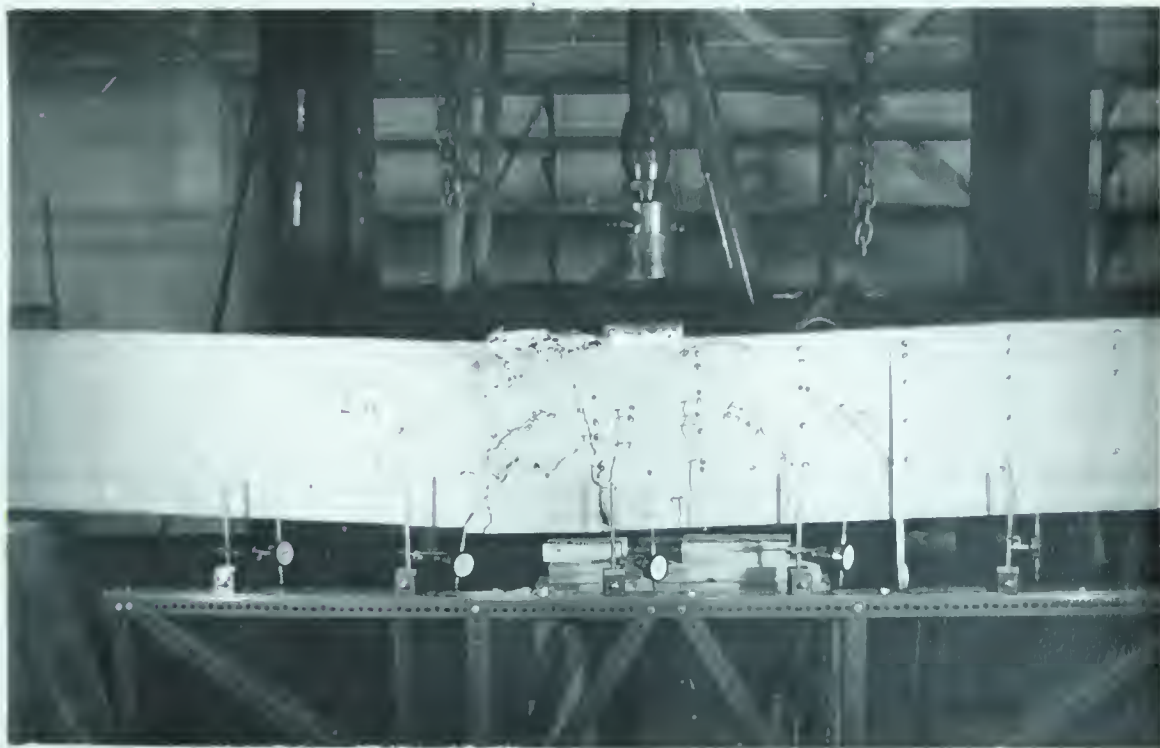


FIGURE 4.21 SINGLE - POINT LOADED BEAM, CRUSHING
FAILURE
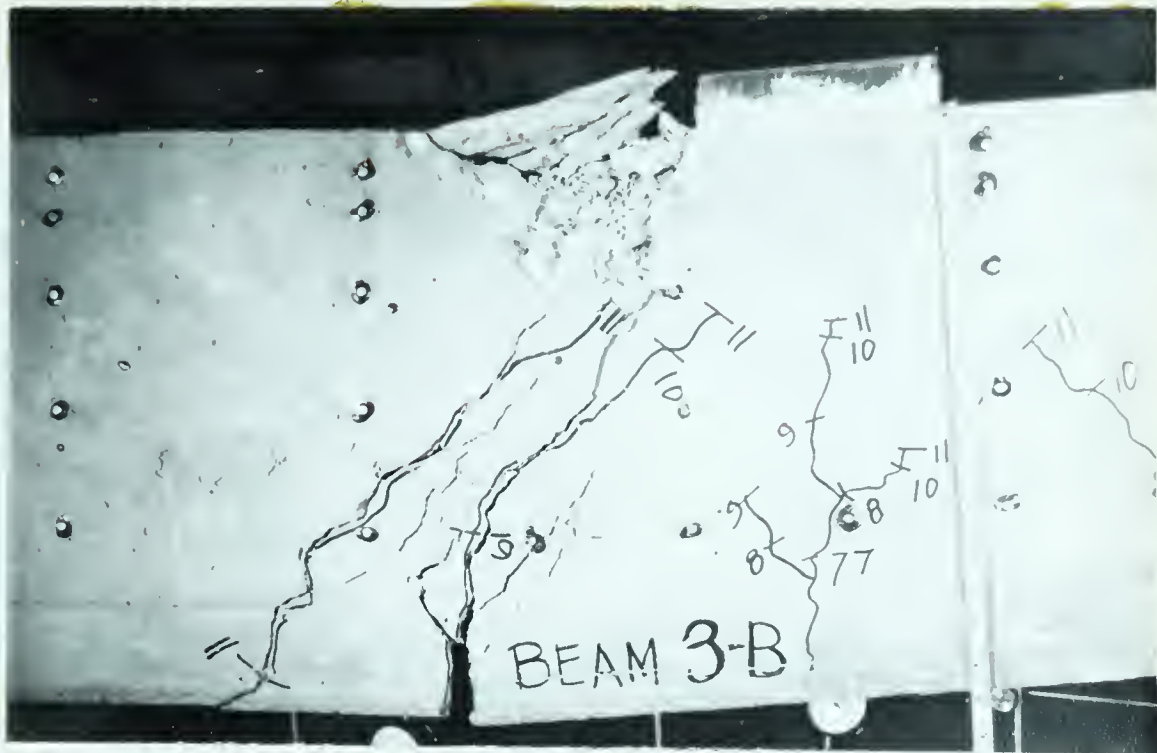
FIGURE 4.22 FAILURE ZONE SHORT SINGLE-POINT
LOADED BEAM
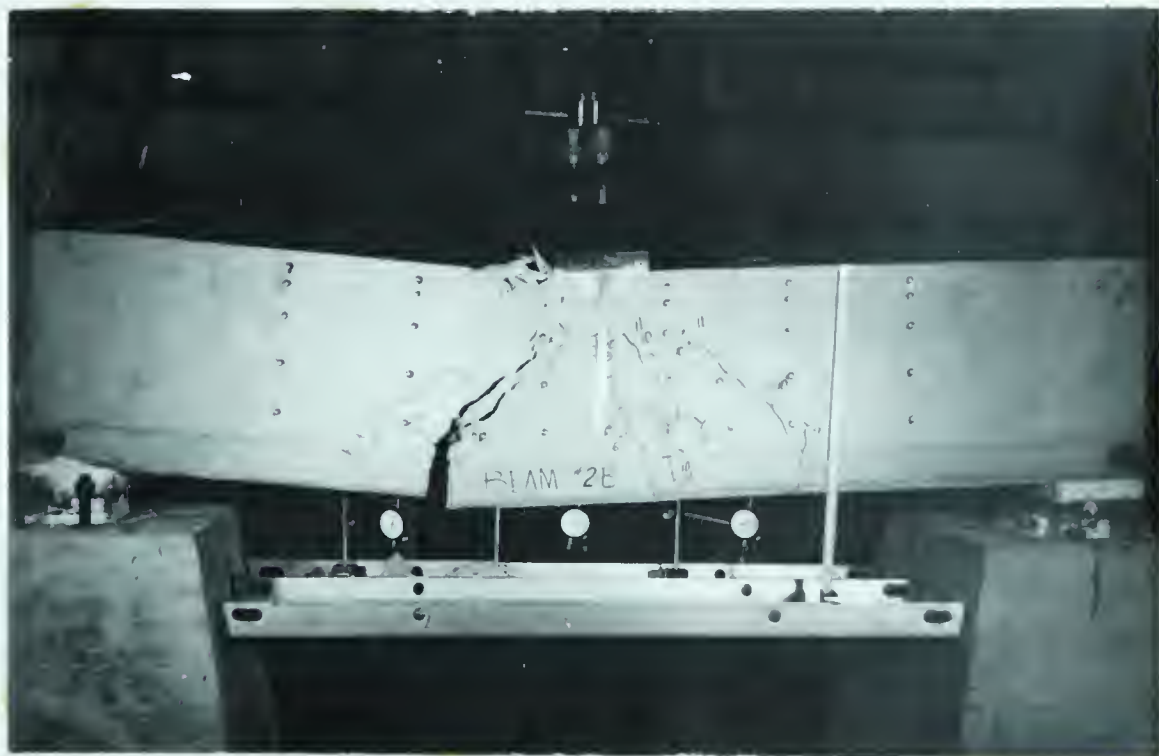


FIGURE 4.23 SHORT SINGLE-POINT LOADED BEAM
CRUSHING FAILURE

ruption of the compression zone caused the neutral axis to move downward as well, and reduced the internal moment arm. In order to resist the applied load with the reduced internal moment arm, the compressive and tensile forces increased substantially. This action continued until complete disruption of the concrete or failure of the cables occurred. Closely spaced stirrups probably increased the resistance of the concrete in the compression zone causing failure of the longitudinal reinforcement. The longitudinal reinforcement in Beams 5A and 6A failed after crushing in the concrete was observed.

### 4.5.4 Shear Failure

Even though the beam components at a critical section are strong enough to carry compression and tension forces, the member can fail if the shear force necessary to develop the moment capacity cannot be carried. Shear failure is characterized by a "faulting" movement along an inclined crack. This movement of adjacent sections was generally observed after crushing started. Since crushing initiated the failure, the full moment capacity of the section had been reached and the failure mode should not

be classified as shear failure.

The amount of shear carried by the concrete decreased with a decrease in area of the compression zone. Extensive unbonding in Beams 1B, 5B and 6B resulted in the formation of large diagonal cracks. These cracks reduced the area of the compression zone causing a failure as shown in FIGURES 4.24 and 4.25 . This type of failure is discussed in the following section.

### 4.5.5    Bond Failure

Unbonding of the cables was observed in all the beams in Series B during later stages of loading. Loss of bond resulted in large deformations, either due to the formation of diagonal cracks or accelerated crushing in the compression zone. The ultimate capacity of all the beams was affected to some degree by the loss of bond.

Beams 2B, 3B and 4B exhibited signs of crushing before and during the time unbonding occurred. However, unlike Series A, no additional load was carried by these beams after initial crushing. This was because the cables were on the verge of pulling out and could not carry additional tension force to compensate for the reduction in
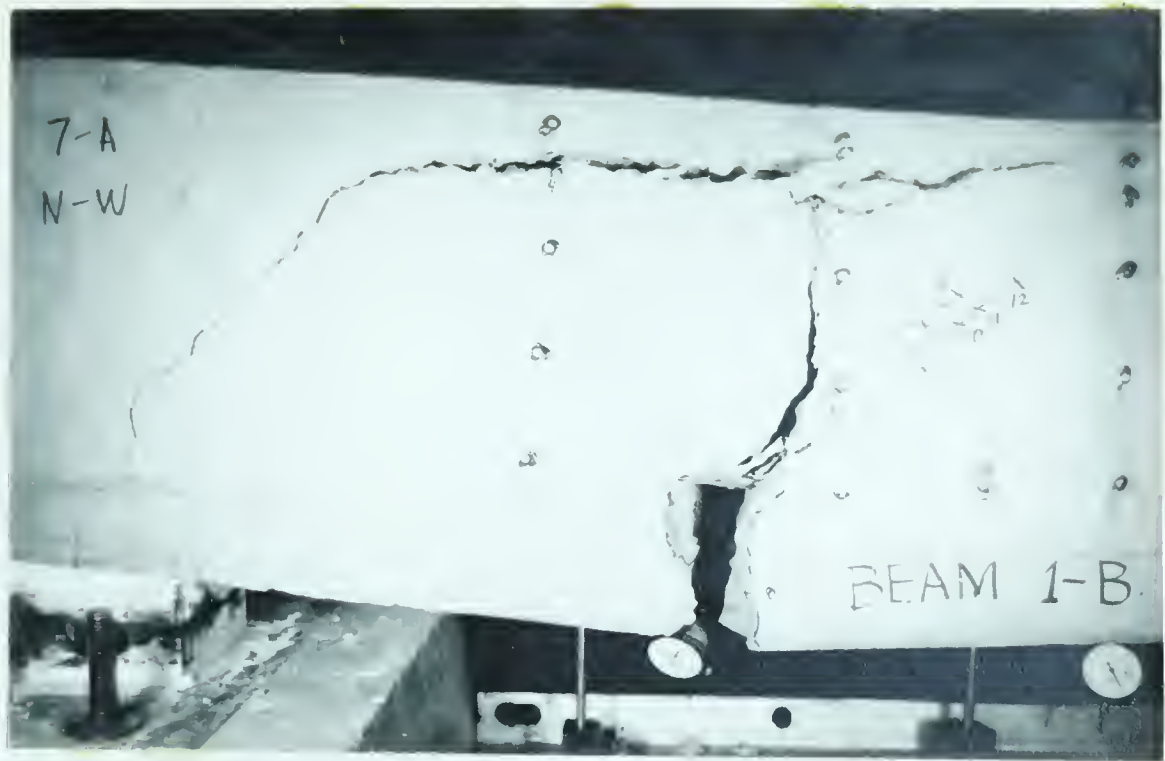
FIGURE 4.24 DIAGONAL TENSION CRACK IN A SHORT
BEAM
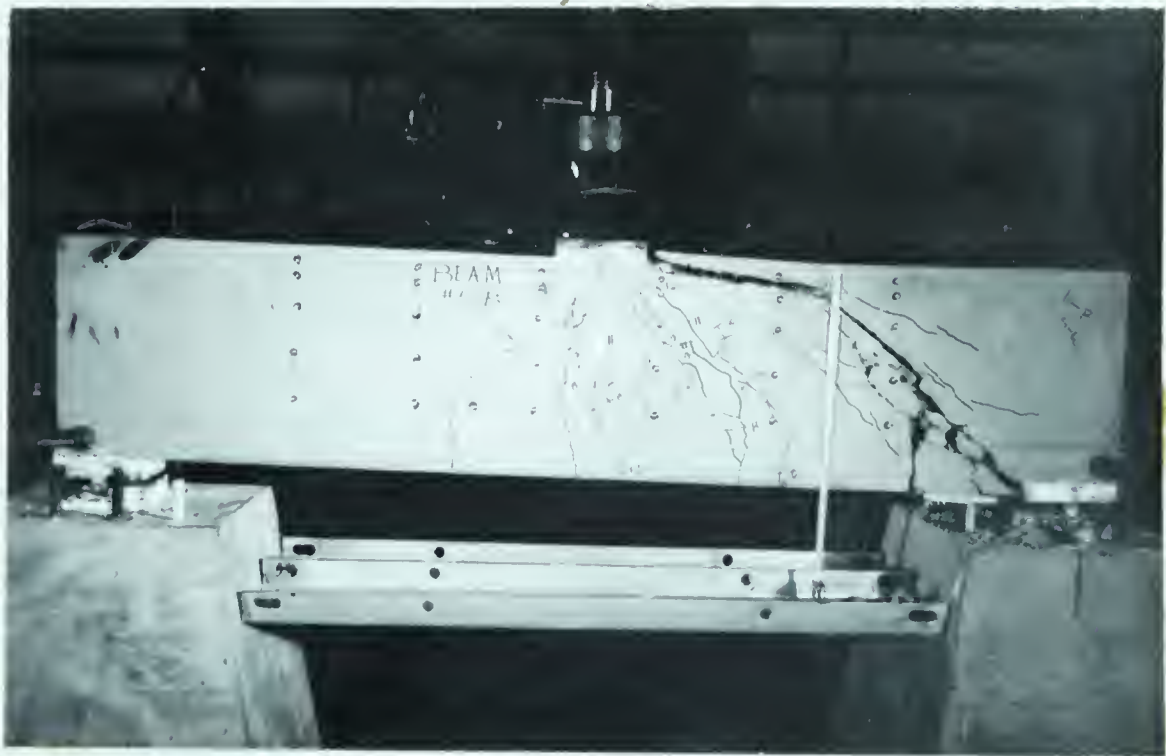


FIGURE 4.25 BOND FAILURE WITH DIAGONAL TENSION
CRACK IN A SHORT BEAM

internal moment arm due to crushing.  Once crushing started, collapse due to unbonding followed immediately.

In Beams 1B, 5B and 6B unbonding of the cables occurred before the full moment capacity of the beams was developed.  Unbonding started in the prestress transfer zone at the end of the beam and progressed toward the center.  The end portion of the beam then became an untensioned beam which was inadequately reinforced.  Diagonal cracks, shown in FIGURES 4.24 and 4.25, starting at the support developed rapidly and disrupted the compression zone.  Failure of the member occurred as a result of shear in the reduced section.

When the load was removed the flexure cracks which had formed in the midspan region closed while the diagonal crack remained open.  This indicated that the cable was still bonded from the diagonal crack to the center of the beam.

CHAPTER V

ANALYSIS AND DERIVATION OF RELATIONSHIPS

## 5.1    Introduction

The beam theory as outlined in Appendix A requires a homogeneous, elastic section throughout all stages of loading. In a prestressed concrete member these conditions are satisfied only in the early stages of loading. In a cracked prestressed concrete beam the characteristics of the cross-section vary from point to point. Since the relationship between moment and curvature is a function of the cross-sectional characteristics, it will vary as well. The distribution of curvature will no longer be the same as the distribution of moment, as is the case for a homogeneous elastic beam.

When a beam is cracked concentrations of compression strain will be found above the cracks. The strain in the extreme fiber varies with the crack location, being maximum over the crack and minimum between the cracks. The

73

depth of the neutral axis will also be variable; maximum

between cracks and minimum at the crack.  Curvature is

defined as the ratio of the strain in the extreme fiber to

the depth of the neutral axis.  Minimum depth of the neutral

axis and large strains will give large curvature over a

crack, while maximum depth of neutral axis and small strains

will give small curvatures between cracks.  The distribution

of curvature along the span will be influenced by the crack

pattern that develops as well as the distribution of moment.

In terms of beam behavior the relationship between moment

and curvature at a particular section is not representative

of conditions in general.  A moment versus average curvature

relationship must be obtained to approximate the behavior of

the beam as a whole.  This is accomplished, in part, by

measurement of the strains over a gage line of sufficient

length to include cracked and uncracked sections.

## 5.2    Computations of Moment-Curvatures from Side Strains

Curvature was determined from the compressive

strain in the extreme concrete fiber and the depth to the

neutral axis.  Strains in the extreme fiber of the single-

point loaded beams and side strains, on all the beams tested

were measured over an 8-in. gage length. The strains obtained

in this manner were averages and did not represent a particular

section. Curvatures computed from these average strain

distributions were average curvatures representing an 8-in.

portion of the beam.

For Beams 11, 12 and 13, which were loaded at

two points symmetrical about midspan, the central region was

subjected to constant moment. The curvature along this

length was assumed to be constant as well. The strains

obtained from the four columns of gage lines in this region

were averaged. The strain distribution over the depth of

the beam, obtained in this manner, was very nearly linear.

An average curvature, representing the whole region between

the loads, was obtained by dividing the average strain in

the extreme fiber by the depth of the neutral axis. The

same procedure was used for each load increment. The

relationship between the average curvatures and the moments

for the first series of beams are shown in FIGURE 5.1 .

For the single-point loaded beams, a moment

gradient existed along the entire span. Consequently, the

curvature along the span was not constant but varied from

zero at the support to maximum at the point of loading.
Averaging of strains from adjacent gage lines to obtain a
linear strain distribution over the full depth of the beam
was not valid. The strain distributions across the compres-
sion zone, however, were found to be consistently linear.
Strain distributions across the compression zone were used
to compute average curvatures for each gage line. For each
increment of load an average curvature was computed at all
the gage lines along the length of the beam. The relation-
ship between the average curvatures for the gage line at
midspan and the moments at midspan are shown in FIGURES 5.2
to 5.5 .

Distributions of strain over the depth of the
beam, for all beams in Series A and B, were obtained for
the entire portion of the beam length affected by cracking.
Average curvatures representing 8-in. of beam length were
obtained from these strain distributions. These curvatures
when plotted along the beam, as shown in FIGURES 5.6 to 5.9,
represented the distribution of average curvature for this
region. The ends of the beam which remained uncracked
behaved elastically and the distribution of curvature was
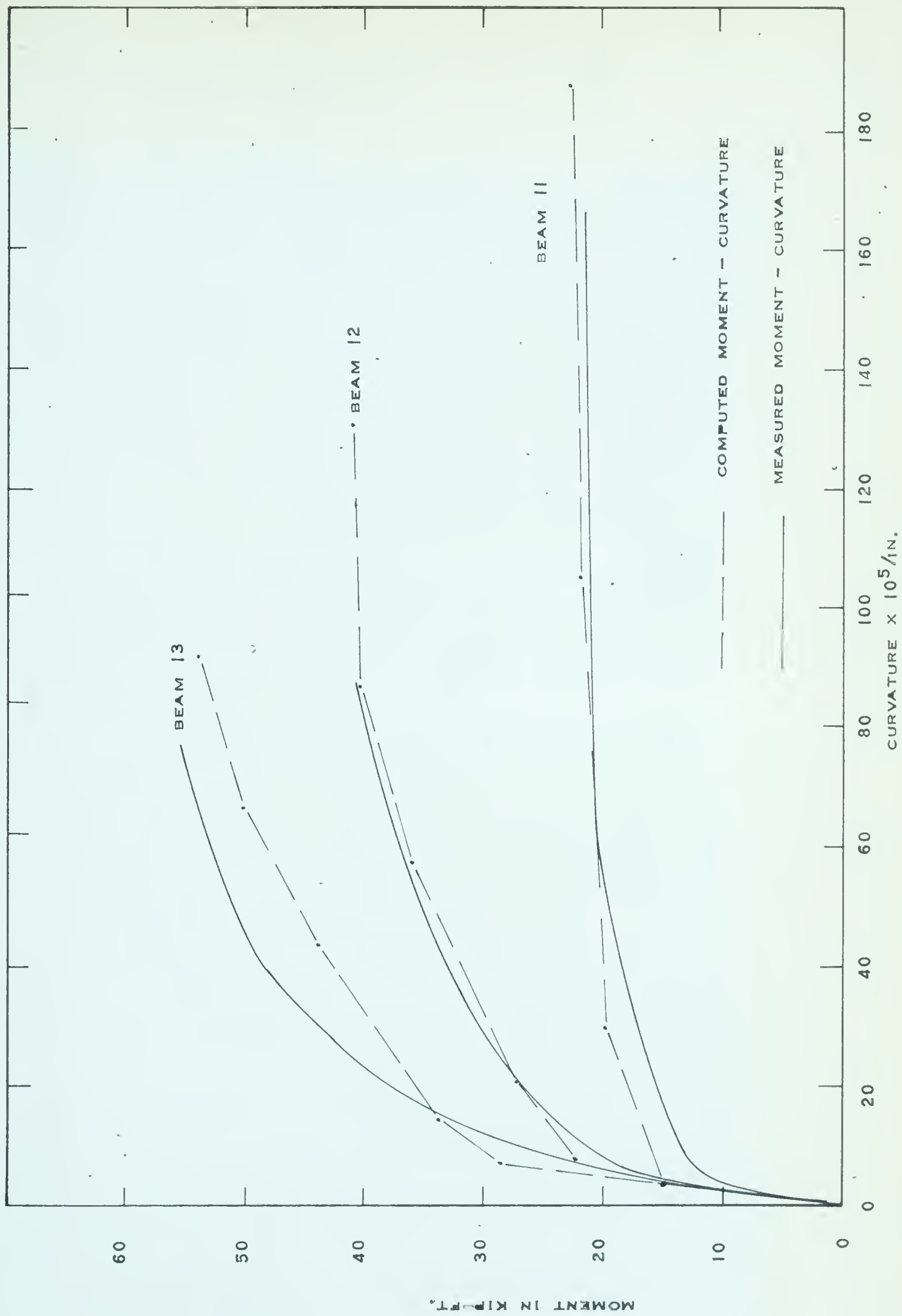
FIGURE 5.1  MEASURED AND COMPUTED MOMENT - CURVATURE RELATIONSHIPS
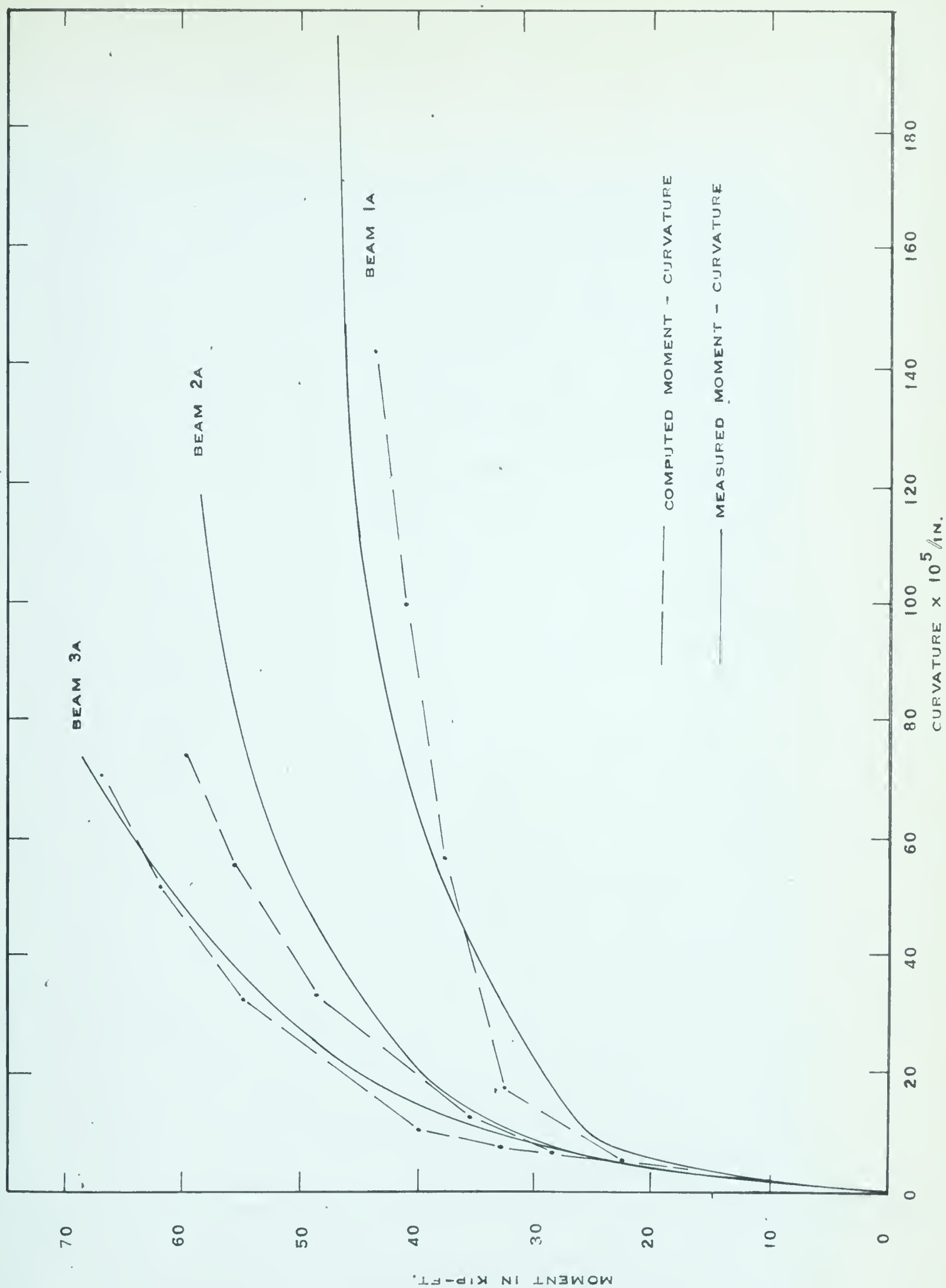
FIGURE 5.2 MEASURED AND COMPUTED MOMENT - CURVATURE RELATIONSHIPS
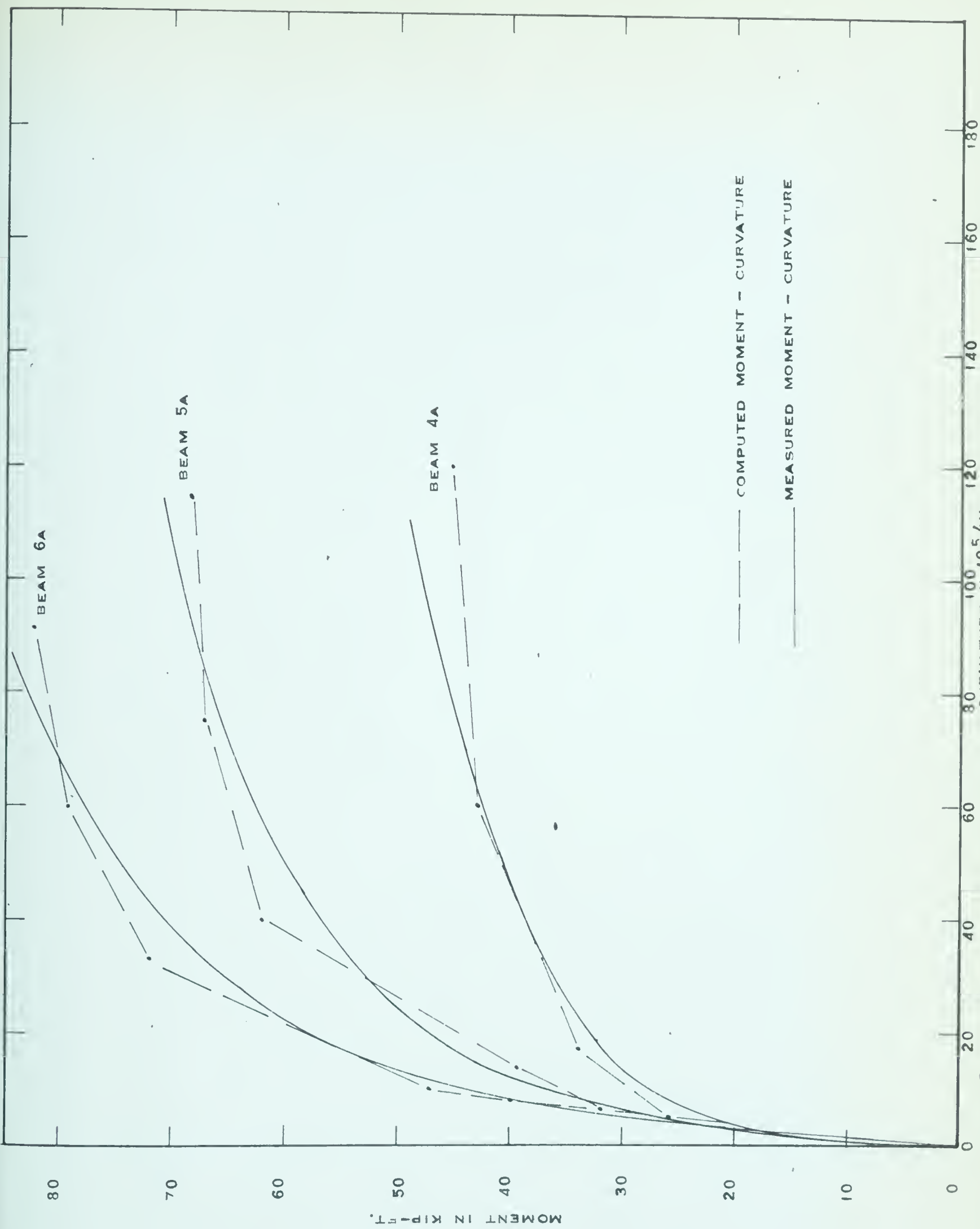
FIGURE 5.3 MEASURED AND COMPUTED MOMENT – CURVATURE RELATIONSHIPS
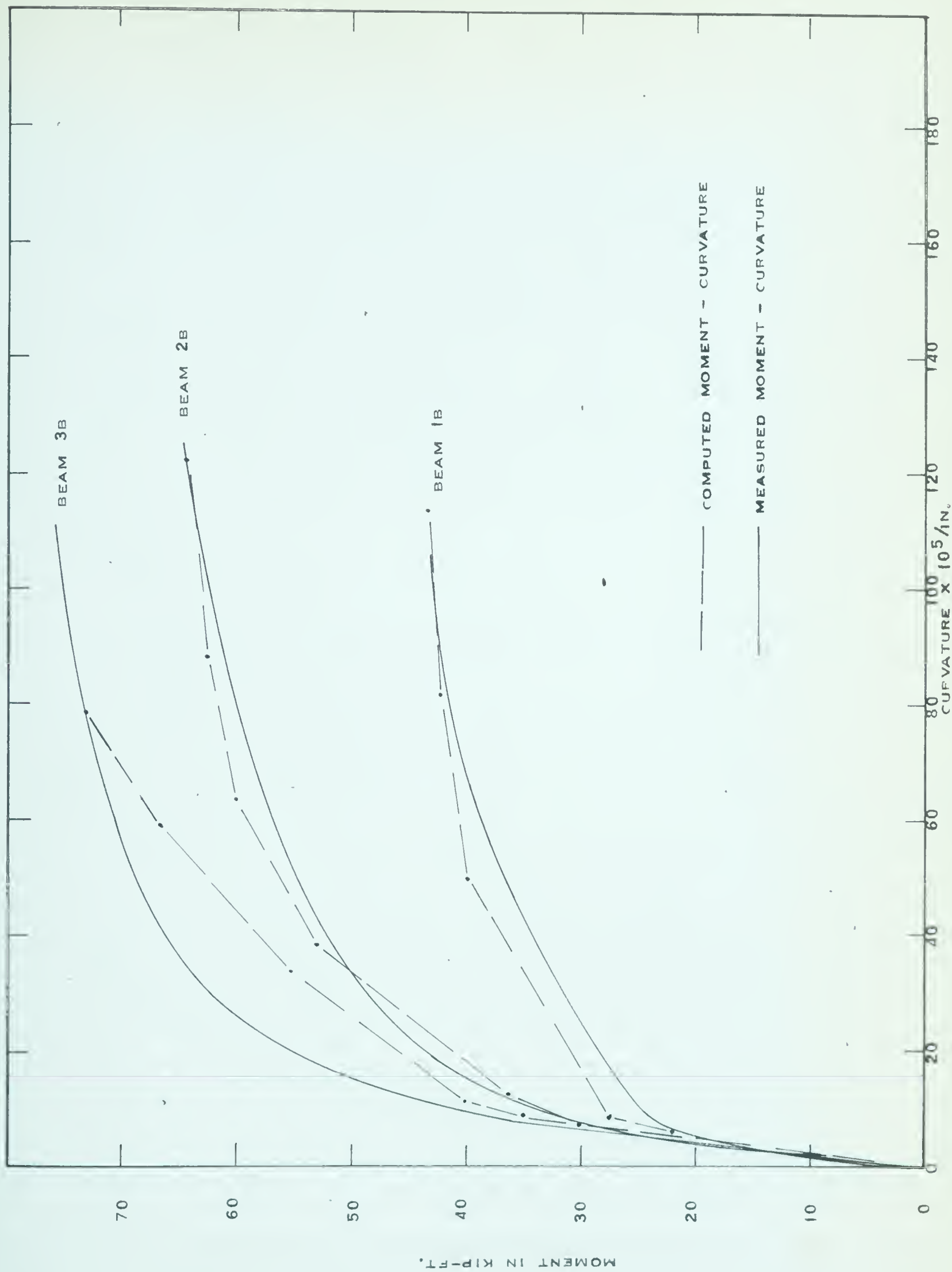
FIGURE 5.4 MEASURED AND COMPUTED MOMENT – CURVATURE RELATIONSHIPS
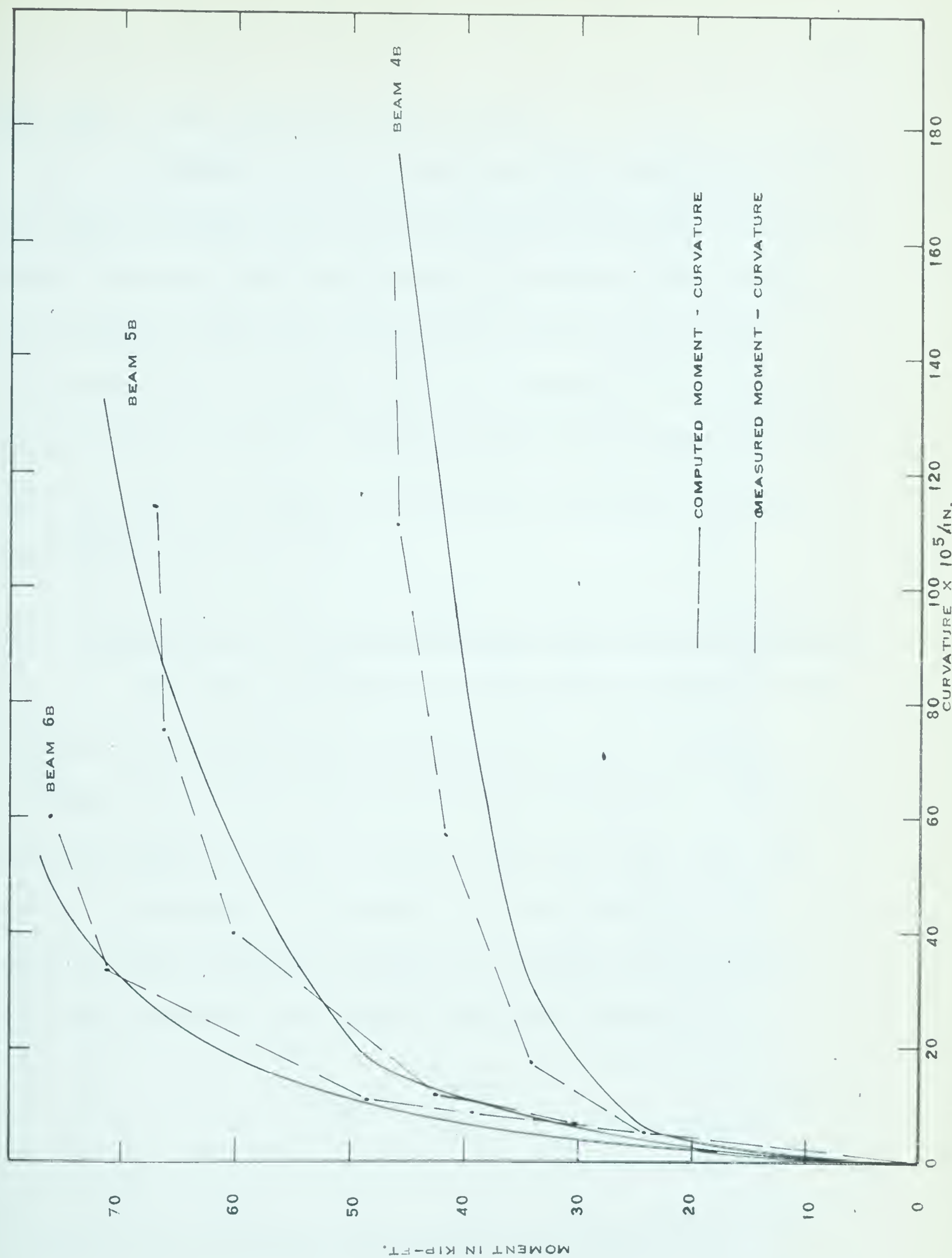
FIGURE 5.5 MEASURED AND COMPUTED MOMENT – CURVATURE RELATIONSHIPS

the same as the distribution of moment.

FIGURES 5.6 to 5.9 show distributions of curvature for each increment of load from initial cracking to failure. Before cracking the distribution of curvature was linear. As cracking progressed the rate of change in curvature increased until a maximum value was reached at the section where failure occurred. Distributions of curvature at the last recorded increment of load before failure are shown in FIGURES 5.10 and 5.11 .

## 5.3    Derivation of Theoretical Moment-Curvature Relationship

The two coordinates of the moment-curvature relationship corresponding to conditions at first flexural cracking and ultimate can be readily determined. The resisting moment at first flexural cracking, $M_{cr}$, was computed as described in Appendix B. The behavior of the beam at first flexural cracking was essentially elastic and the curvature was computed from the expression,

$$\phi_{cr} = \frac{M_{cr}}{E_c I} \quad *$$

---

* symbols and notation are tabulated in Appendix A
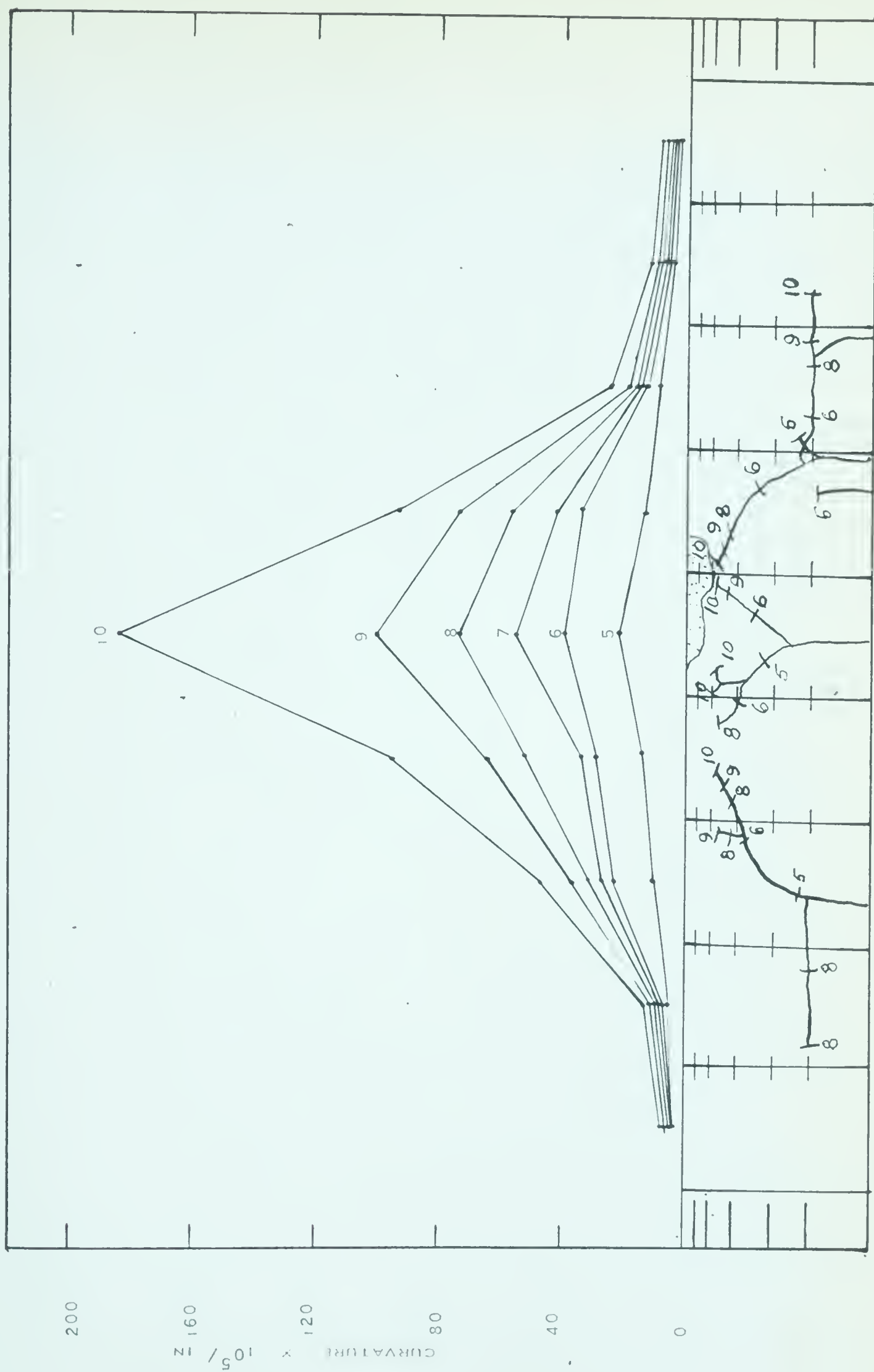
FIGURE 5 6 DISTRIBUTION OF CURVATURE ALONG THE BEAM AND CRACK PATTERN
BEAM IA

CURVATURE $\times$ $10^5/$ IN
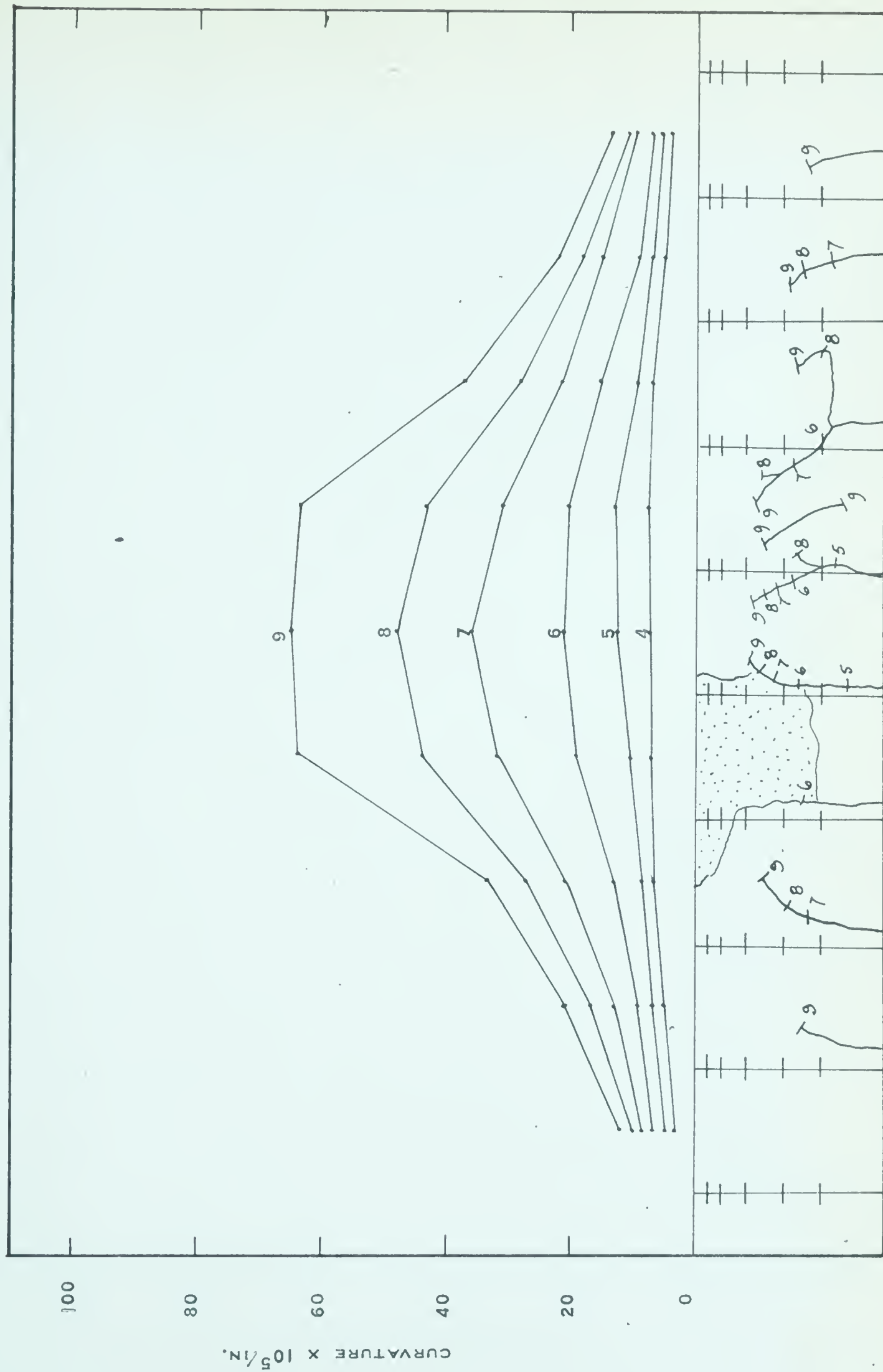
FIGURE 5.7 DISTRIBUTION OF CURVATURE ALONG THE BEAM AND CRACK PATTERN BEAM 3A
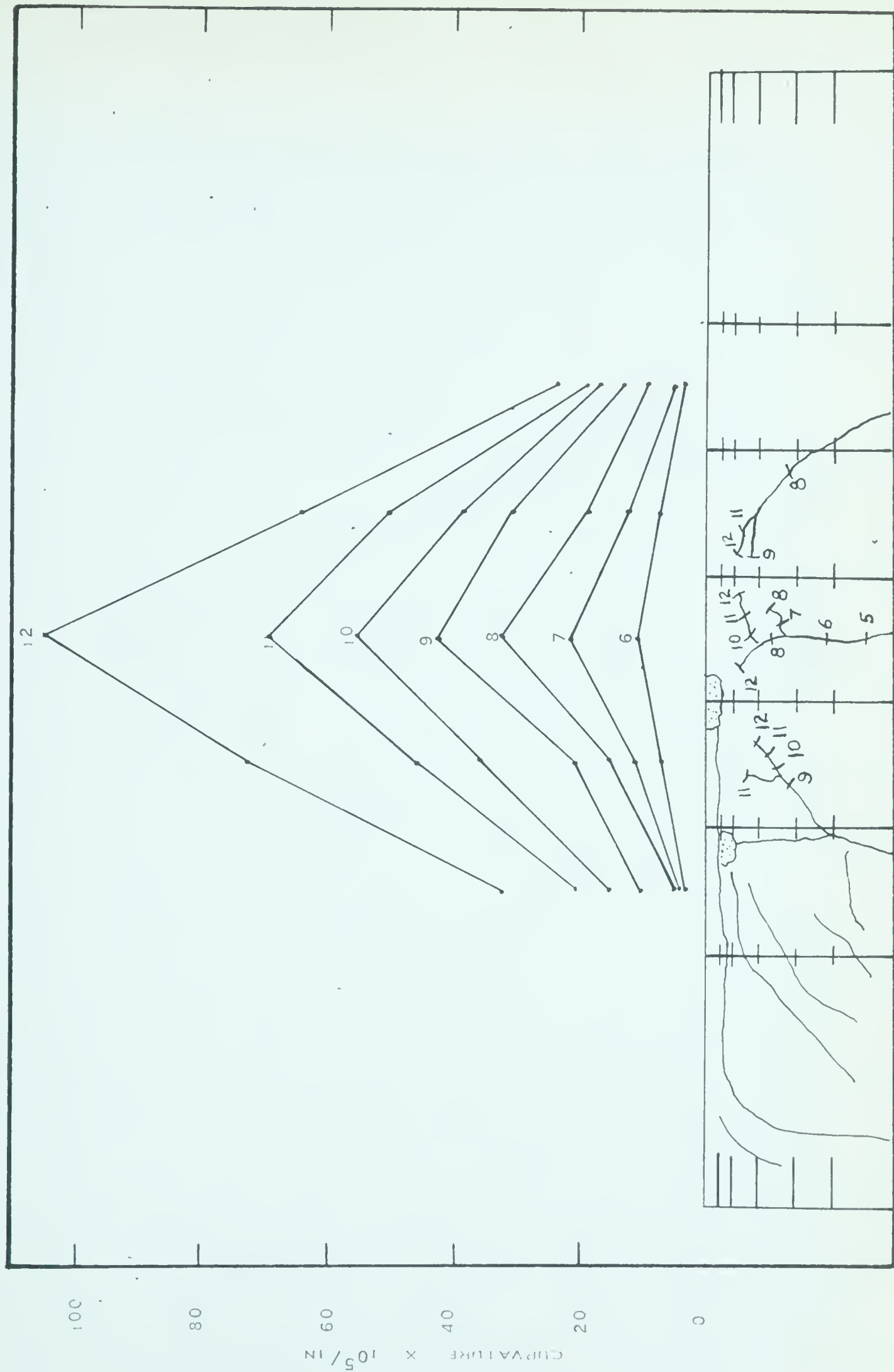
FIGURE 5.8 DISTRIBUTION OF CURVATURE ALONG THE BEAM AND CRACK PATTERN

BEAM 1B
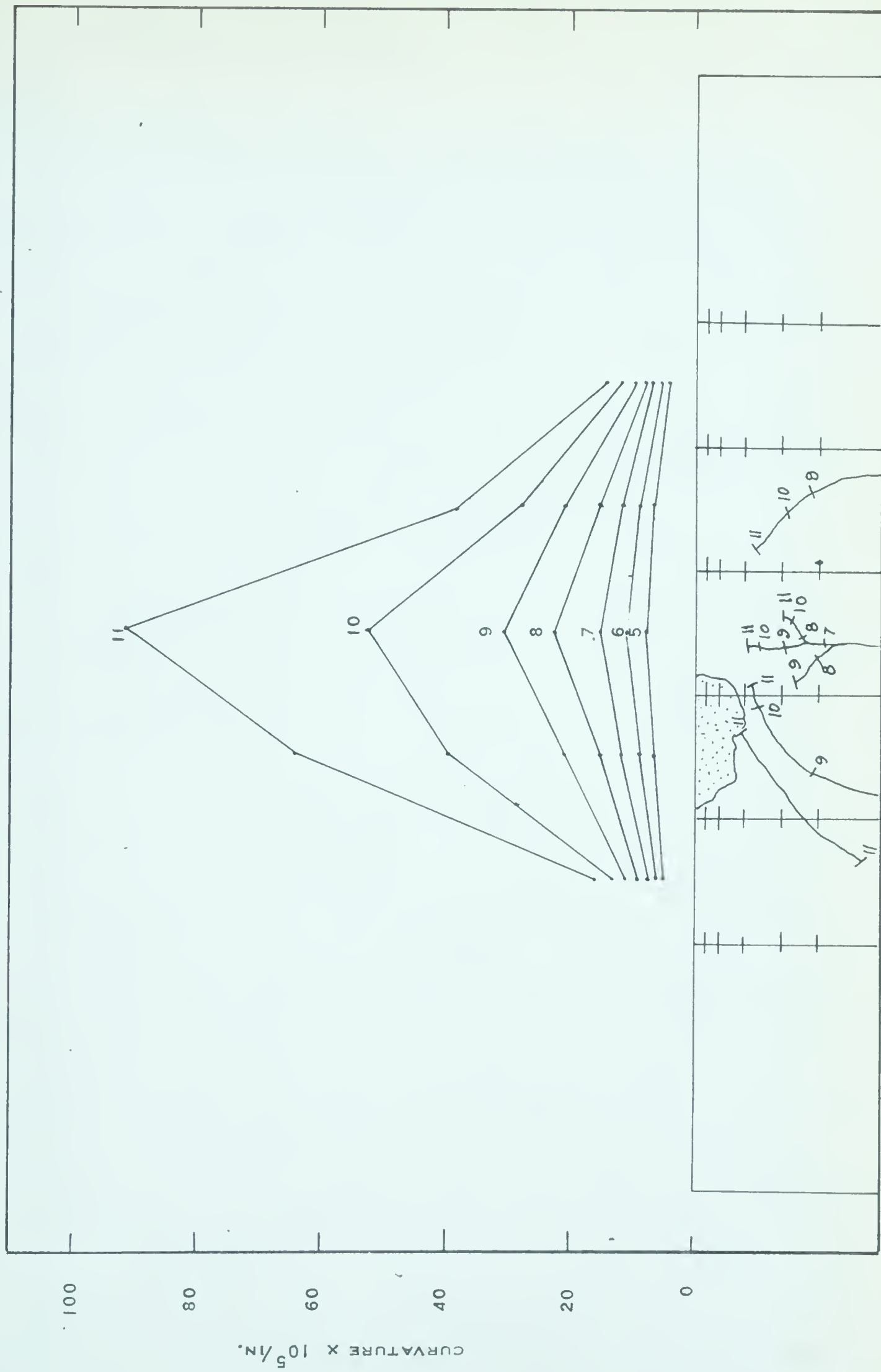
FIGURE 5.9 DISTRIBUTION OF CURVATURE ALONG THE BEAM AND CRACK PATTERN BEAM 3B
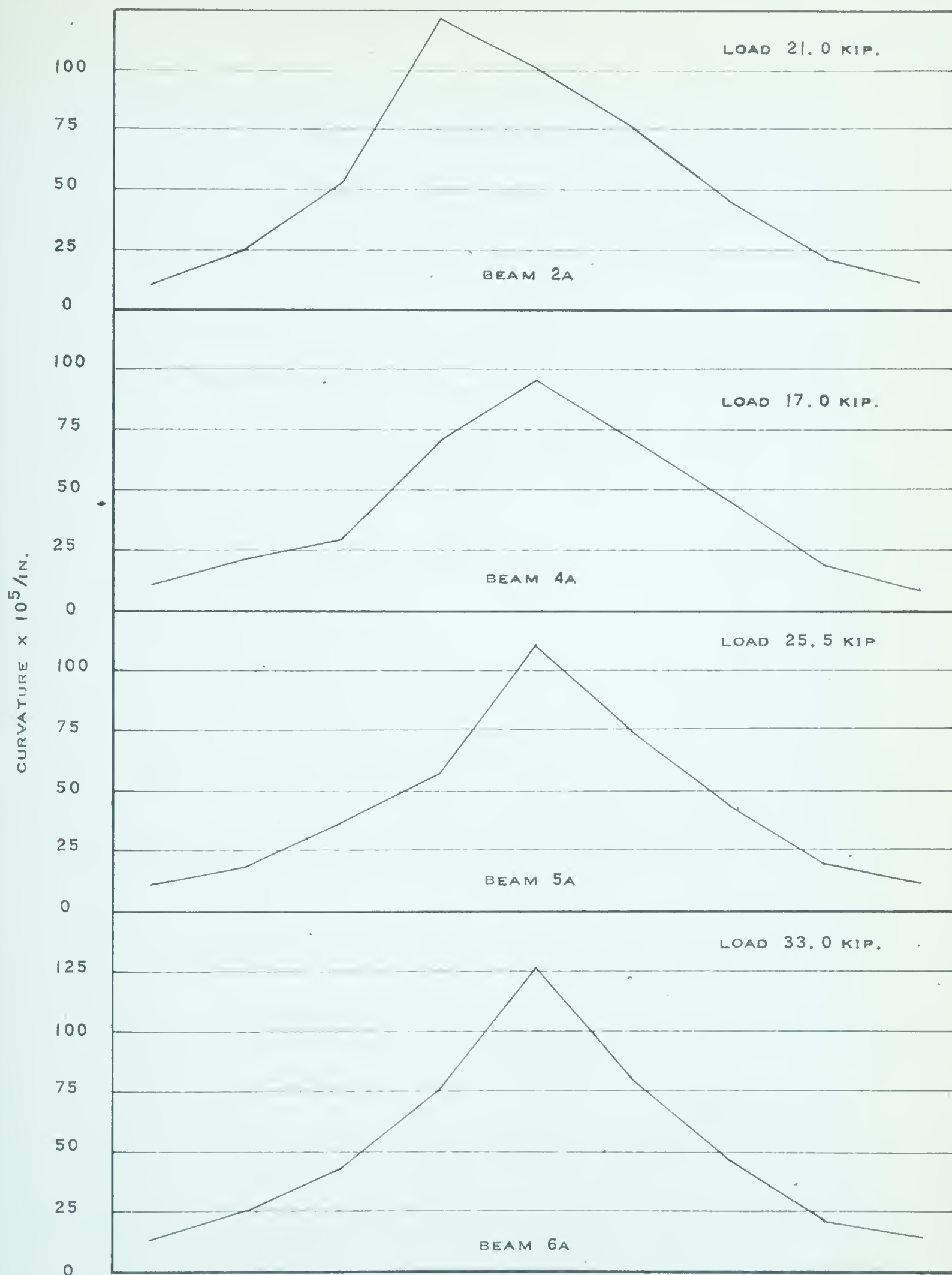
FIGURE 5.10 DISTRIBUTION OF CURVATURE ALONG THE BEAM
AT LAST RECORDED LOAD
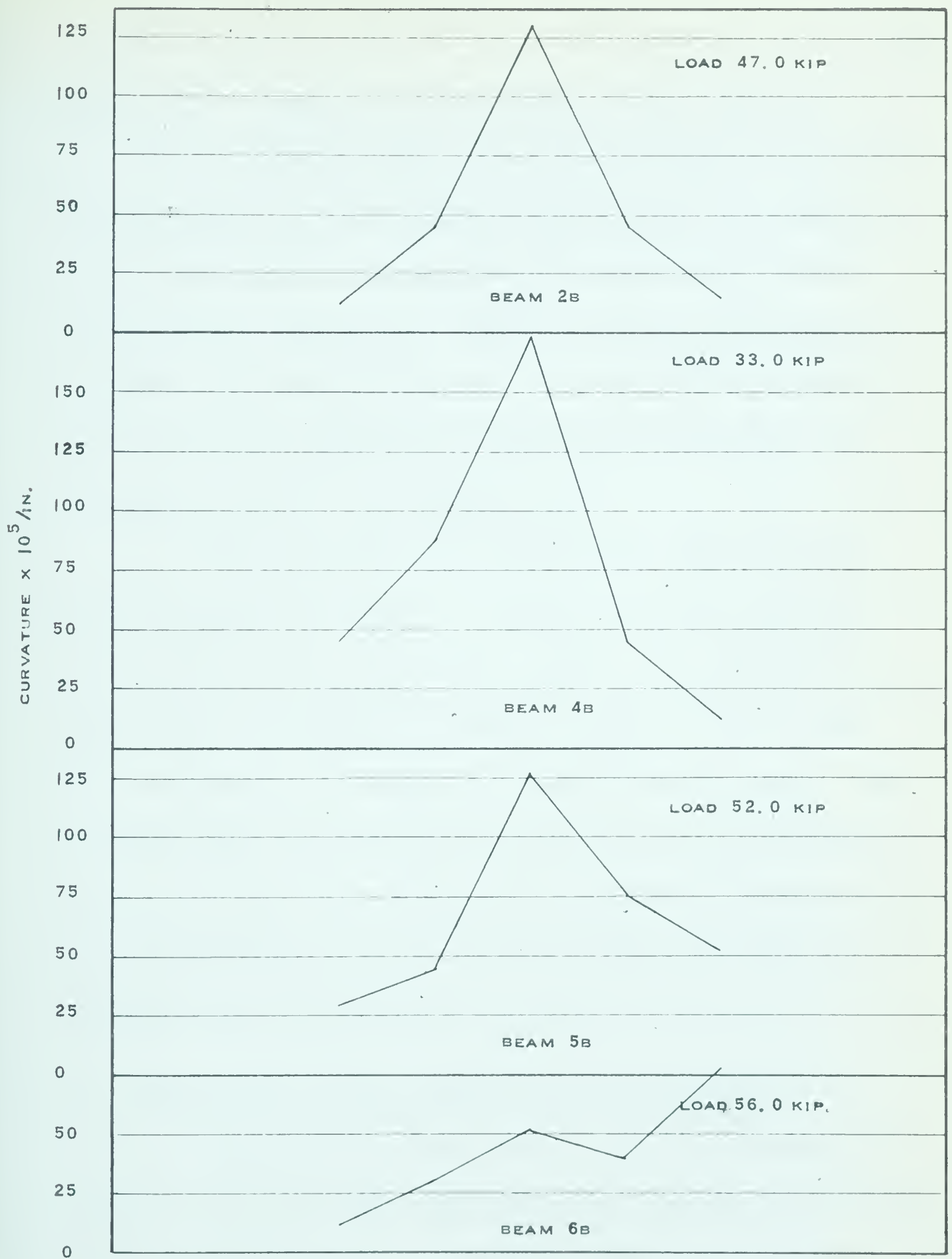
FIGURE 5.11 DISTRIBUTION OF CURVATURE ALONG THE BEAMS
AT LAST RECORDED LOAD

where, $E_c$ = modulus of elasticity of the concrete

I = gross moment of inertia of the cross-section.

The expression for evaluating ultimate moment $M_f$, depth of

neutral axis $k_u$ d, and increase of reinforcement strain

are derived in Appendix B. These quantities were used to

determine the theoretical moment and curvature at failure.

The theoretical curvature was obtained by dividing the

concrete strain by the quantity $k_u$ d.

The evaluation of intermediate points between

ultimate and first flexural cracking was more involved.

A knowledge of the relationship between the increase in

reinforcement strain and concrete strain in the extreme

fiber throughout all stages of loading was required. The

procedure used for determining this part of the average

moment-curvature relationship was outlined in reference (2).

The relationships obtained by this method are shown as

straight lines in FIGURES 5.1 to 5.5.

## 5.4   Derivation of Load-Deflection Relationships

Measured load-deflection curves for midspan, as

obtained from dial gage readings, were presented in Section

4.3 .  Load-deflection relationships were also computed

from the derived distributions of curvature. These computed values when compared to the measured deflections provided a means of checking the derived distributions of curvature.

To determine the deflection, the relationship between moment and curvature must be known at all sections along the span of the beam. If the distribution of curvature is known for any stage of loading, the deflection can be computed with ordinary methods of geometry. The conjugate beam method using an idealized average distribution of curvature, as discussed in Appendix B, was used to compute deflections at each increment of load. The distribution of curvature for the uncracked portion of the beam was assumed to be the same as the distribution of moment.

For the two-point loaded beams the average curvature was measured only in the constant moment region. Some cracking did occur outside this region, therefore, the distribution of curvature could not be assumed to be the same as the distribution of moment. The average curvature distribution, between the support and the load point, was obtained by distributing the curvature according to the moment-curvature relationships shown in FIGURE 5.2 . The
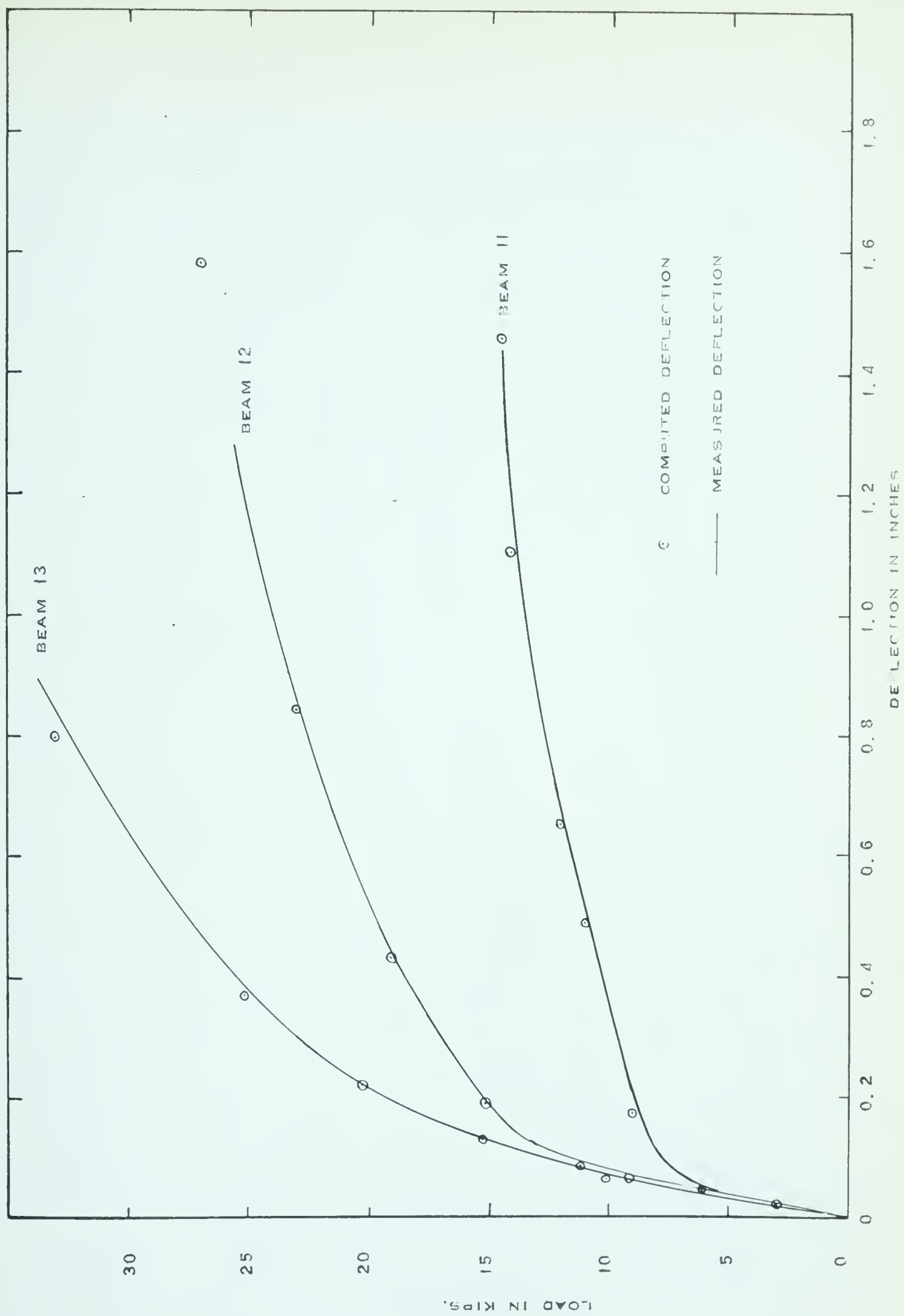
FIGURE 5.12 MEASURED AND COMPUTED LOAD – MIDSPAN DEFLECTION RELATIONSHIPS
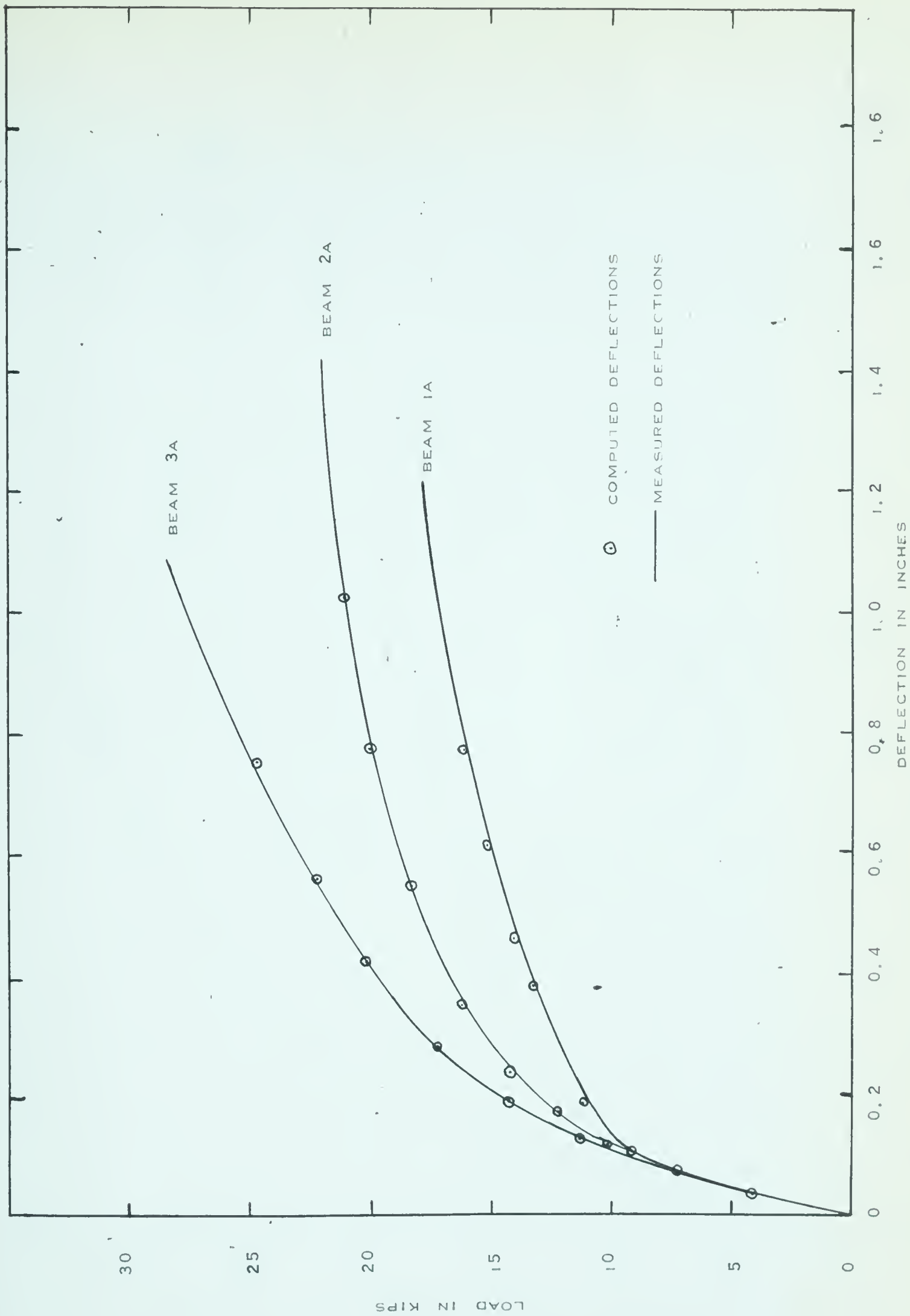
FIGURE 5.13 MEASURED AND COMPUTED LOAD – MIDSPAN DEFLECTION RELATIONSHIPS
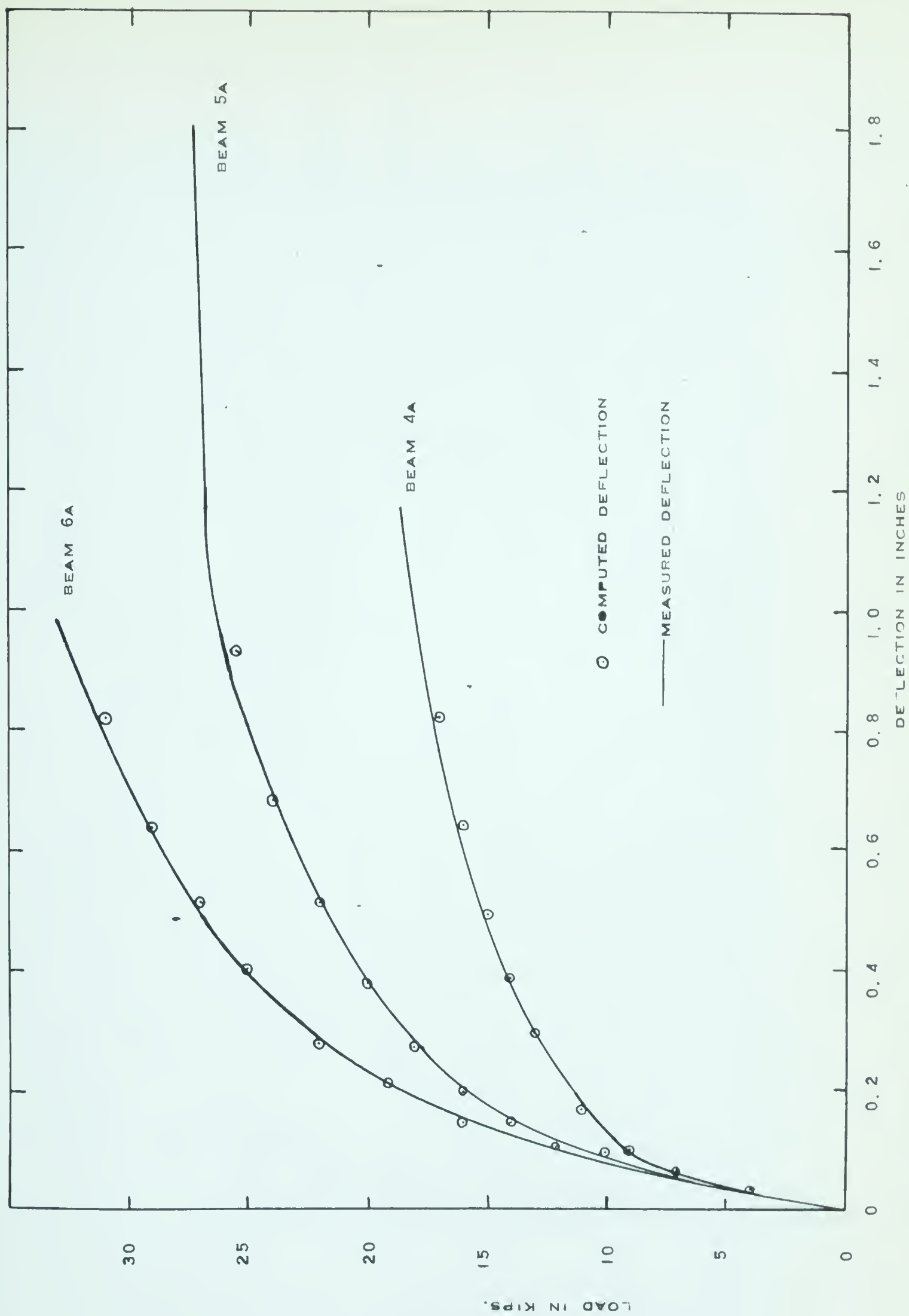
FIGURE 5.14 MEASURED AND COMPUTED LOAD - MIDSPAN DEFLECTION RELATIONSHIPS
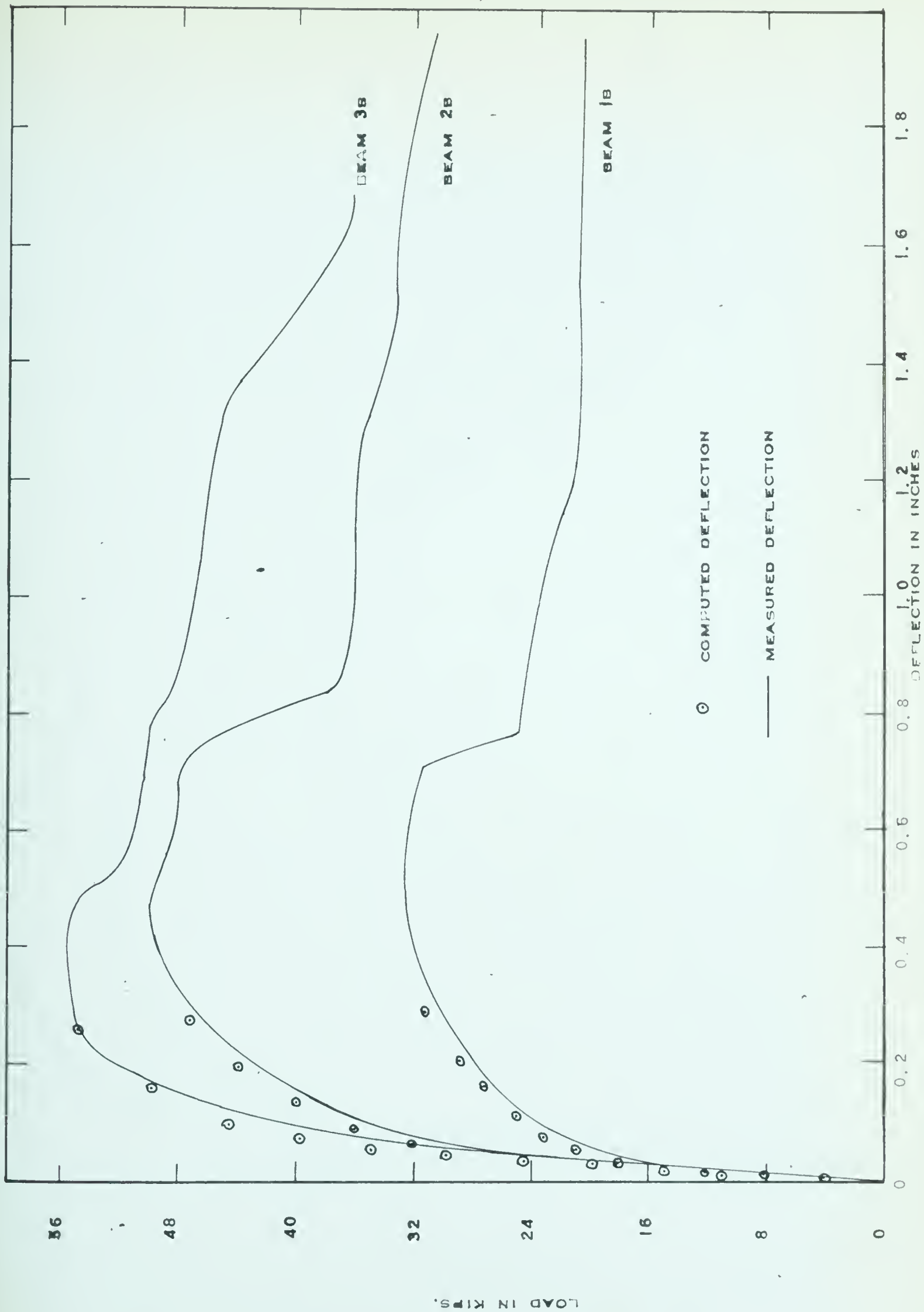
FIGURE 5.15 MEASURED AND COMPUTED LOAD - MIDSPAN DEFLECTION RELATIONSHIPS
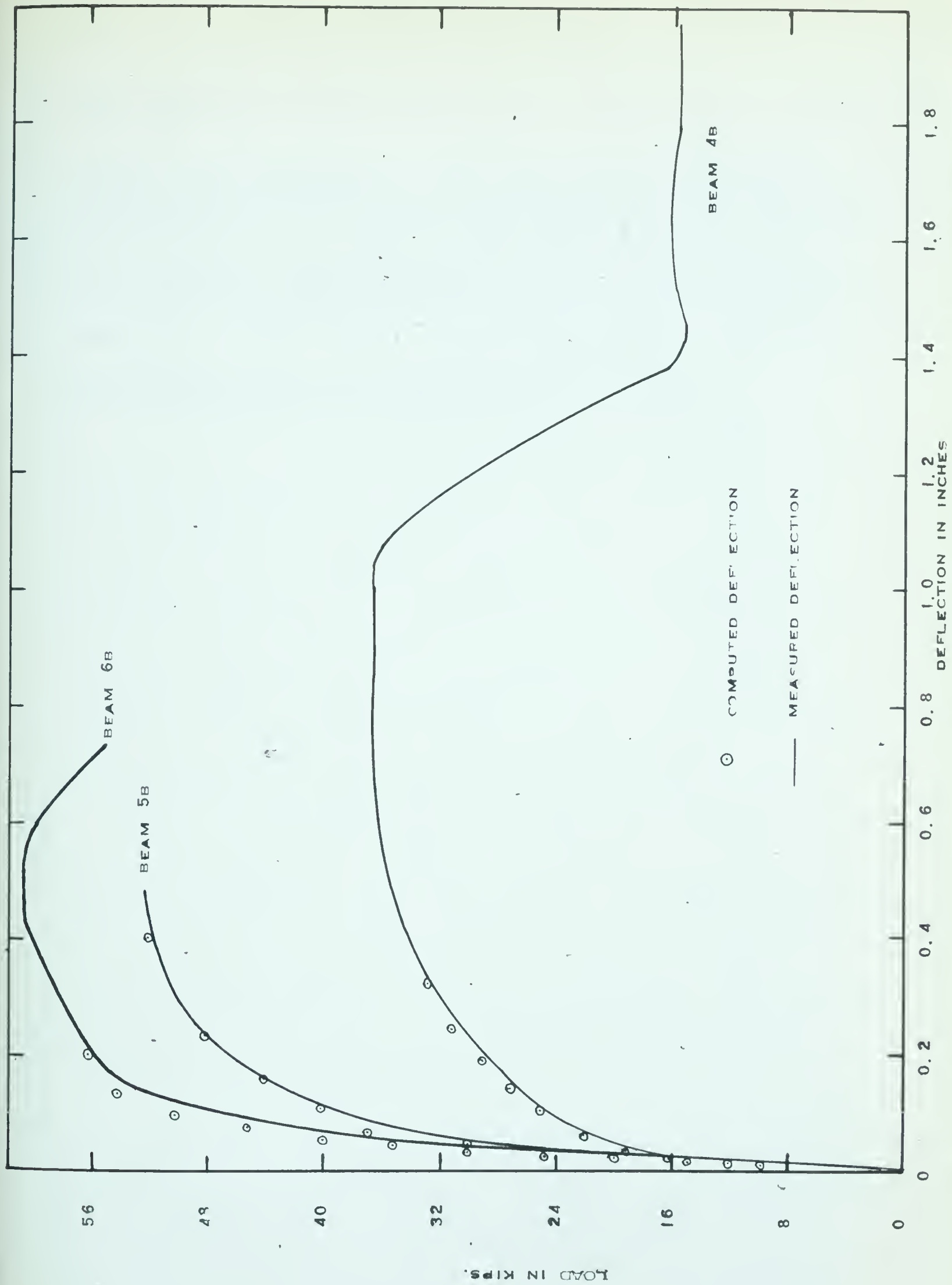
FIGURE 5.16 MEASURED AND COMPUTED LOAD - MIDSPAN DEFLECTION RELATIONSHIPS

distribution of curvature in the constant moment region was assumed to be uniform. The distribution of average curvature, determined in this manner, was used to compute the deflection at midspan for each increment of load. The deflections computed, in this manner, and corresponding loads are shown as plotted points in FIGURES 5.12 to 5.16 .

# CHAPTER VI

## DISCUSSION OF TEST RESULTS

### 6.1   Measured Moment-Curvature Relationships

The derivation of the moment-curvature relation-
ships is presented in Section 5.2 . The derived relation-
ships are shown in FIGURES 5.1 to 5.5 . Both the load de-
flection and the moment-curvature relationships depend
largely on the material properties that make up the cross-
section. This can be seen from the similarity of the
moment-curvature and load-deflection diagrams.

The moment-curvature diagrams exhibited three
stages of behavior similar to those discussed in Section
4.4 . The first stage of behavior corresponded to a linear
relationship between moment and curvature. First flexural
cracking marked the end of this stage. A rapid change in
the slope of the moment-curvature relationships occurred
throughout the second stage. This was caused by a diminish-
ing area of compressed concrete and an increasing stress in

96

the tension reinforcement. The third and final stage was initiated when the reinforcement stress approached the "inelastic" range. The moment-curvature relationship in this stage was flat and large deformations occurred for small increments of load.

The effects of varying the amount of reinforcement and the strength of the concrete, are illustrated in FIGURES 5.1 to 5.5 . The ratio of $p/f_c'$ relates the amount of reinforcement and the compressive strength of the concrete. This ratio describes the material properties of the cross-section. Because the level of effective prestress, $f_{se}$ is relatively constant, this ratio may be used as a criterion to compare the behavior of the beams.

Beams 1A and 5B had ratios of $p/f_c'$ that were nearly equal, $8.90 \times 10^{-7}/psi.$ and $8.95 \times 10^{-7}/psi.$ respectively. The ratio of $p/f_c'$ was the same even though Beam 1A was reinforced with 4 cables and $f_c' = 4310$ psi. while Beam 5B was reinforced with 6 cables and $f_c' = 6460$ psi. The deformation characteristics of these beams were generally the same, although Beam 5B had a considerably larger ultimate moment capacity. Failure of the tension reinforcement resulted for beams

having a ratio of $p/f'_c$ less than $8.50 \times 10^{-7}/psi$.

Although the level of effective prestress was not intended to be a variable, slight variation from beam to beam resulted. It is difficult to make comparisons since the variation was small. Some trends, however, are evident from the curves for Beams 3A and 3B and 4A and 4B. Increasing the level of prestress tended to reduce the second stage of behavior. Also the resisting moment at first flexural cracking is increased with increased effective prestress.

Changes in the moment-curvature relationships as the amount of tension reinforcement is increased, for a constant concrete strength and span length, are illustrated in FIGURES 5.1 to 5.5. The change of curvature for an increment of applied moment was reduced by increasing the amount of tension reinforcement. Doubling the percentage of reinforcement in the beams with high strength concrete, increased the moment required to produce a given curvature by a factor of 1.8 - 2.0. For the beams with low strength concrete, the corresponding factor was 1.6 - 1.8. Increasing the percentage of reinforcement was more effective for increasing the stiffness in beams with high concrete strength

than in beams with low concrete strength.

The effect on the moment-curvature relationship, of changing the concrete strength may be seen by comparing FIGURE 5.2 with 5.3 and FIGURE 5.4 with 5.5 . For the under-reinforced beams, with low values of $p/f_c'$, changes in the concrete strength had little effect. For beams which had sufficient reinforcement to insure compression failures the variation in concrete strength is more significant. Increasing the concrete strength increased the moment required to produce a given deformation.

The moment-curvature relationships were not affected significantly by the type of loading, since they are dependent only on the magnitude of the applied moment and the material properties of the section. This can be seen from a comparison of the moment-curvature relationships shown in FIGURES 5.1 and 5.2 .

Span length of the beams with a low percentage of reinforcement had little effect on the moment-curvature relationships. Short beams with high percentages of reinforcement required slightly larger moments to produce a given curvature than similar beams with a long span. The

increased stiffness of the short beams was probably due to closer spacing of the shear reinforcement. TABLE 3.5 shows the details of the shear reinforcement. For the beams with high percentages of reinforcement compression failures resulted. Closely spaced stirrups in these short beams provided considerable restraint and confinement for the concrete in the compression zone. The resultant deformation for these beams was reduced for a given increment of applied moment.

## 6.2 Comparison of Theoretical and Measured Moment-Curvature Relationships

Measured and theoretical moment-curvature relationships are shown in FIGURES 5.1 to 5.5 . Generally, the correlation between the curves obtained by the two methods was quite good, except for Beams 2A and 3B. Differences between the measured and theoretical relationship may be attributed to two factors which affect both methods. These are: (i) errors in determination of strength and (ii) determination of the curvature.

For the measured moment-curvature relationships the moment at a particular section was known. The curvatures, however, can vary considerably, depending on the location of cracks relative to the gage lines. The relationships

shown represent the "average" curvatures for an 8-in. portion of the beam at midspan. The location and magnitude of cracks within, or adjacent to this portion of the beam will have an effect on the curvature obtained from this gage line. With a well developed crack located in this portion of the beam large curvatures will be obtained for a particular applied moment. This was the case for Beam 2A. On the other hand, for Beam 3B, during the early stages of loading, the major deformation occurred at the gage lines adjacent to the midspan location and the measured midspan-curvature was small. However, in later stages of loading, the midspan deformations increased and the curvature obtained compared well with the theoretical curvature at this section.

Over the first stage of behavior the theoretical moment-curvature relationship is similar to the measured curve. The predicted cracking moment, however, is larger than the observed value, for beams with a low percentage of reinforcement. Over the second stage of behavior the slope of the theoretical curve is greater than the measured re-lationships, while over the third stage the slope is less than the measured. The theoretical ultimate strengths were

also found to be 5 to 10% lower than the measured values. These differences could be due, in part, to the use of the idealized stress-strain relationship, which gives a higher apparent concrete strength in the later stages of loading. Similar differences between the theoretical and measured moment-curvature relationships were observed, in reference (1).

## 6.3    Measured Distribution of Curvature

The distribution of curvature along the length of the beam was obtained for the single-point loaded beams only.   Before flexural cracking occurred the distribution of curvature corresponded to the distribution of moment across the span.  First flexural cracking in the region of maximum moment, caused a concentration of curvature at this point.  Consequently the distribution of curvature became non-linear.  Maximum curvatures, at the failure load, occurred at or near the midspan section.  The shape of the curvature distribution curve closely approximated the moment-curvature relationships obtained for the section at mid-span.  Variations of a local nature, however, were evident in the slope of the distribution curves.

It was not possible to obtain the distributions of curvature at the instant of failure. Distributions of curvature were obtained for the increment of loading just prior to failure and these are shown in FIGURES 5.6 to 5.11. These figures show that the maximum curvature occurred at the midspan section and the distribution of curvature generally was symmetrical with respect to midspan.

The moment-curvature relationships shown in FIGURES 5.1 to 5.5 were derived from strains measured at midspan. The load bearing plate at this location had a confining effect on the concrete. As a result the con-crete was subjected to a biaxial stress condition and required a larger moment to produce a given deformation. If the curvatures were distributed along the span according to the relationships in FIGURES 5.2 to 5.5, a lower bound for the curvature along the span would be obtained. For a given moment the curvature, at a section not influenced by the bearing plate, would be larger than that obtained at midspan.

The distributions of curvature were influenced by the same variables as the moment-curvature relationships. These were discussed in Section 6.1 .

6.4    Measured Load-Deflection Relationships

    The measured load-deflection relationships are shown in FIGURES 4.11 to 4.15, and the three stages of behavior exhibited by these curves are discussed in Section 4.4 . Examination of these relationships indicates that the difference in the shape of the curves for any group of beams, after cracking, is due to changes in the major variables such as the amount of reinforcement, the concrete strength and the span length.

    The effects of changing the amount of reinforcement are shown in FIGURES 5.12 to 5.16 . It can be seen that doubling the amount of reinforcement in these beams increased the load required to produce a given deflection by a factor of about 1.8 . The effect of changing the concrete strength on the load-deflection relationships may be seen by comparing FIGURE 5.13 with 5.14 and FIGURE 5.15 with 5.16 . For the beams with low $p/f_c'$ ratios, changes in the concrete strength had little effect. In beams with higher $p/f_c'$ ratios, increasing the concrete strength increased the stiffness significantly. Higher concrete strength increased the load required to produce a given deflection.

The effect of decreasing the span length, on the load-deflection relationships, of single-point loaded beams, is seen by comparing FIGURE 5.13 with 5.15 and FIGURE 5.14 with 5.16 . Reducing the span length by one-half increased the failure loads 1.75 to 2.25 times. The deflection at failure of the long beams, however, was 2.8 to 2.5 times larger than the corresponding deflections for the short beams. The flexibility and ability of the beam to deform was re-duced by decreasing the span length.

Unlike the moment-curvature relationships the load-deflection relationships were affected by the load condition applied to the beam. The single-point loaded beams deflected more for a given applied load. The difference in applied load, to produce a given deflection corresponded to the difference in the length of the shear spans. The single-point loaded beams had a shear span which was 1.83 times larger than the shear span of the two-point loaded beams. The load required to produce a given deflection, for the two-point loaded beams, was also about 1.83 times that for a similar single-point loaded beam.

## 6.5 Comparison of Computed and Measured Load-Deflection Relationships

Comparisons between the load-deflection relation-ships obtained from measurement and from the method outlined in Appendix B are shown in FIGURES 5.12 to 5.16. The correlation between the computed and measured deflections for the long beams was quite good. The computed deflections for the short beams, however, were considerably lower than the measured values.

The computed deflections were derived from distributions of curvature, which were obtained from measurements of strains over the side of the beams. These strains, measured in a longitudinal direction, were largely deformations due to flexural stress. Additional deformation was produced by the shearing force in the form of mutual sliding of adjacent cross-sections along each other. Shearing stresses caused previously plane sections to become curved and deformation of the member resulted.

The expression, derived in reference (12), for deflections at midspan, of a single-point loaded beam due to shearing forces is:

$$\delta_s = \frac{\propto PL}{4\ AG}$$

where,      P  =  magnitude of applied concentrated load

            L  =  span length

            A  =  area of the cross-section

            G  =  modulus of rigidity in shear

            $\propto$ =  shape factor = 3/2 for a rectangle.

This expression applies to an elastic member, but may be applied to the case of an uncracked concrete section with a fair degree of accuracy. After cracking occurs and failure is approached, the area of the cross-section A, and the modulus of rigidity G, cannot be determined accurately.

In the short beams, which had a shear-span-to-depth ratio of 3.3, the deflections due to shearing forces became a significant part of the total measured deflection. Using the above expression in the stages of loading before cracking, the deflections at midspan due to shear were found to be 15 to 20% of the measured values. This expression would have to be modified, for changes in the cross-section properties, before it could be applied to the stages of loading from cracking to failure.

The differences between measured and computed deflections, for the short beams, were found to be 5 to 30%

of the measured deflections throughout all stages of loading.
This difference was due to the effects of shear deformation,
unbonding of the cables and errors in the distribution of
curvature. In order to predict accurate deflections from
the derived distributions of curvature for the short beams,
a correction to account for these effects must be applied.
For the long beams, with a shear-span-to-depth ratio of
6.6, the difference between measured and computed deflections
were less than 10% of the measured deflections. For these
beams the deflections due to shear are not very significant
and a correction would not be required.

# CHAPTER VII

## SUMMARY, CONCLUSIONS AND RECOMMENDATIONS

### 7.1   Summary

Three series of pretensioned prestressed concrete beams with a 6 x 12-in. cross-section and a 10-in. effective depth were tested.  The first series consisted of three beams with a 11-ft. span length tested with a two-point load symmetrical about the center line.  The second and third series consisted of six beams each and were tested with a single-point load at the center line.  The span lengths for these were 11-ft. and 5.5-ft. respectively.  The variables in each series were: percentage of reinforcement, concrete strength and slight unintentional variation in the level of prestress.

The measurements taken were: strains over the depth of the beam, strains in the extreme compression fiber and deflections along the bottom of the beams.  From these measurements load-deflection relationships, moment-curvature

relationships, distributions of curvature and distributions of strain in the extreme compression fiber were obtained. In addition, moment-curvature relationships using the procedure in (2) and load-deflection relationships using the measured distributions of curvature were derived.

## 7.2   Conclusions

From a study of the test results and the behavior of test specimens the following conclusions have been drawn:

1.   For a constant level of effective prestress, increasing the percentage of tension reinforcement reduced the deformation of the beams for a given increment of applied moment.

2.   Increasing the percentage of reinforcement in beams with high concrete strength was more effective for increasing the stiffness than in beams with a low concrete strenth.

3.   For under-reinforced beams changes in the concrete strength had little effect on the deformation characteristics.

4.   For over-reinforced beams increasing the concrete strength increased the moment required to produce an increment of deformation.

5.   The moment-curvature relationship for a particular

section was not significantly affected by the type of loading.

6. Closely spaced lateral reinforcement decreased the deformation for an increment of applied moment.

7. Failure of the tension reinforcement occurred in beams having a ratio of $p/f_c'$ less than $8.50 \times 10^{-7}$/psi.

8. Theoretical ultimate strengths were found to be 5 to 10% lower than the measured values.

9. The distribution of curvature across the span could be approximated with the midspan moment-curvature relationship.

10. For the single-point loaded beams decreasing the span length to one-half decreased the deflection by a factor of 0.35 - 0.40 .

11. Single-point loaded beams deflected more for an increment of applied load than did similar two-point loaded beams.

12. Deflections computed from measured distributions of curvature, compared well with measured deflections, for beams with a shear-span-to-depth ratio of 6.6 .

13. Deflections computed from measured distributions of curvature for beams with shear-span-to-depth ratio of 3.3 must be corrected for the effects of deflection due to

shearing force.

## 7.3 Recommendations

The study of deformation characteristics of pre-stressed concrete beams, to this point, is by no means complete. It is recommended that the next step in this series of investigations be a thorough analytical study of the test data obtained from this investigation and in (1). The objects of this analytical study may to:

1. Derive an idealized stress-strain curve for concrete that would improve the theoretical moment-curvature relationship.

2. Derive idealized moment-curvature relationships that could be used to predict deflections with a fair degree of accuracy.

In addition tests may be conducted to determine:

1. The effect of closely spaced stirrups or spiral reinforcement, in the compression zone, on the deformation capacity of a section.

2. The deformation characteristics of two-span continuous members tested with concentrated loads.

# LIST OF REFERENCES

1.  Raffa, G., "Deformation Characteristics of Pretensioned Concrete Beams in Flexure", M.Sc. Thesis, University of Alberta, October 1964.

2.  Warwaruk, J., Sozen, M.A., Siess, C.P., "Strength and Behavior in Flexure of Prestressed Concrete Beams", University of Illinois Experimental Station Bulletin No. 464, August 1962.

3.  MacGregor, J.G., Sozen, M.A., and Siess, C.P. "Strength and Behavior of Prestressed Concrete Beams with Web Reinforcement", Civil Engineering Studies, Structural Research Series No. 201, University of Illinois, Urbana, Illinois, August 1960.

4.  Billet, D.F. and Appleton, J.H., "Flexural Strength of Prestressed Concrete Beams", Proceedings, American Concrete Institute, Vol. 50, 1954, p. 837.

5.  Janney, J.R., Hognestad, E., and McHenry, D., "Ultimate Strength of Prestressed and Conventionally Reinforced Concrete Beams", Proceedings, American Concrete Institute, Vol. 52, 1955-56, p. 601.

6.  Burns, N.H., "Moment-Curvature Relationship for Partially Prestressed Concrete Beams", Journal of Prestressed Concrete Institute, February 1964, Vol. 9, No. 1.

7.  Macchi, G., "Moment Redistribution Beyond Elastic Limit and at Failure in Prestressed Concrete Beams", Journal of Prestressed Concrete Institute, Vol. 2, September 1957, No. 2.

8. Ernst, G.C., "Plastic Hinging at the Intersection of
      Beams and Columns," Proceedings, American Concrete
      Institute, Vol. 53, 1956-57, p. 1119.

9. Yamashiro, R., and Siess, C.P., "Moment-Rotation
      Characteristics of Reinforced Concrete Members
      Subjected to Bending, Shear, and Axial Load,"
      Civil Engineering Studies, Structural Research
      Series No. 260, University of Illinois, Urbana,
      Illinois, December 1962.

10. Neville, A.M., "Properties of Concrete", Pitman and Sons,
      1963.

11. American Concrete Institute, "Building Code Require-
      ments for Reinforced Concrete, (ACI 318-63)",
      June 1963.

12. Timoshenko, S., "Strength of Material", Part I,
      D. Van Nostrand Co., 1955.

# Appendix A

## NOTATION AND THEORY

# NOTATION

## Cross-sectional Constants and Dimensions

$A_s$ = total area of prestressed reinforcement

b = width of rectangular beam

d = effective depth of prestressed reinforcement

I = gross moment of inertia of concrete cross section about the centroidal axis

$y_t$ = distance from centroidal axis to extreme fiber in compression

e = distance from centroidal axis to the total tensile force in the prestressed reinforcement

## Loads, Moments and Forces

C = total compressive force in the concrete

T = total tensile force in the prestressed reinforcement

P = total prestressing force

$M_{cr}$ = resisting moment at flexural cracking

$M_f$ = resisting moment at failure

## Stresses

$f_c'$ = compressive strength of concrete determined from 6 x 12-in. control cylinders

$f_{cu}$ = effective strength of concrete in the compression zone of a beam

$f_r$ = modulus of rupture determined from $3\frac{1}{2}$ x $4\frac{1}{2}$ x 16-in. control beams loaded at third points of an 12-in. span

$f_{se}$ = effective prestress

$f_{su}$ = stress in prestressed reinforcement at failure

$E_c$ = modulus of elasticity of concrete

## Strains

$\varepsilon_c$ = concrete strain

$\varepsilon_{ce}$ = strain at level of the reinforcement due to effective prestress

$\varepsilon_{sa}$ = increase in strain in the prestressed reinforcement between prestress and failure neglecting the effects of $\varepsilon_{ce}$

$\varepsilon_{sa}'$ = increase in strain in the prestressed reinforcement between prestress and failure

$\varepsilon_{se}$ = effective prestrain due to effective prestress

$\varepsilon_{su}$ = strain in the prestressed reinforcement at failure

$\varepsilon_u$ = useful limit of strain in the compressed concrete

## Dimensionless Factors

$k$ = ratio of the neutral axis depth to the effective depth

$k_u$ = ratio of the neutral axis depth at failure to the effective depth

$k_2$ = ratio of the depth of the compressive force to depth of the neutral axis

$p$ = $A_S/bd$ = reinforcement ratio

$F$ = strain compatibility factor

## A.1 Elastic Beam Theory

Consider an element of a beam subjected to pure bending, free from vertical shearing force as shown in FIGURE A.1 .
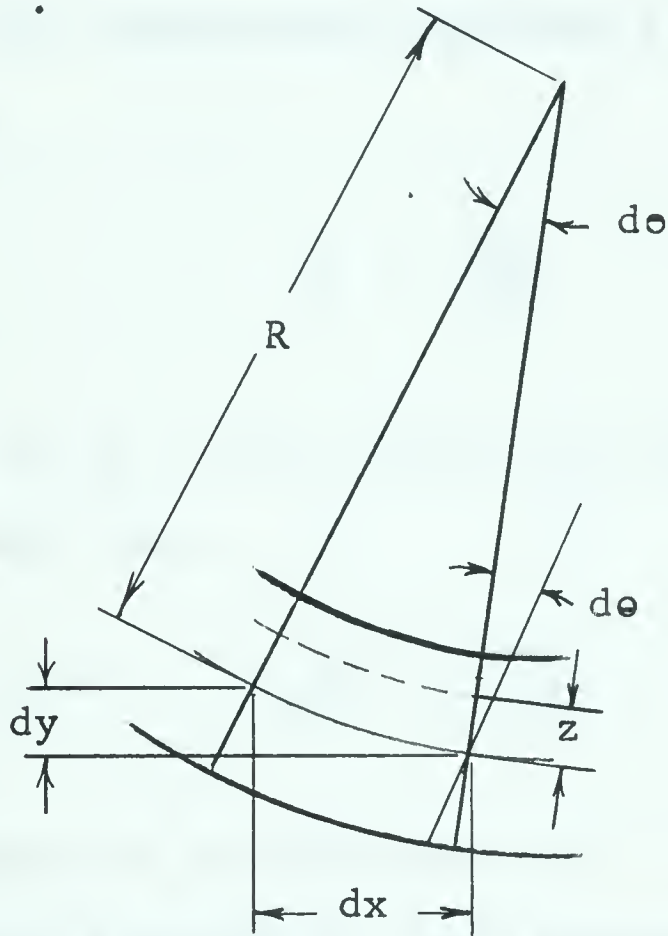
FIGURE A.1     GEOMETRY OF LOADED BEAM

If the deflection, y, is small compared to the length of the beam then;

$$Rd\theta \ = \ dx, \ or \ \frac{1}{R} \ = \ \frac{d\theta}{dx} \qquad (A.1)$$

$\frac{1}{R}$ is defined as the curvature.

Also since deformations are small;

$$\Theta = \frac{dy}{dx} \text{ , making } \frac{d\Theta}{dx} = \frac{d^2y}{dx^2} \tag{A.2}$$

By substituting EQUATION A.2 into EQUATION A.1 we obtain;

$$\frac{1}{R} = \frac{d^2y}{dx^2} \tag{A.3}$$

Similarly if $\varepsilon_x$ is the strain at a distance z, from the neutral axis then;

$$zd\Theta = -\varepsilon_x dx \text{ or } \frac{d\Theta}{dx} = -\frac{\varepsilon_x}{z} \tag{A.4}$$

where tension is assumed positive.

Substituting EQUATION A.4 into EQUATION A.1 the curvature may be expressed as;

$$\frac{1}{R} = -\frac{\varepsilon_x}{z} = \frac{d^2y}{dx^2} \tag{A.5}$$

in terms of strains.

From Hooke's Law; $\sigma_x = E\varepsilon_x$ where $\sigma_x$ is the stress at a distance z, from the neutral axis and E is the modulus

of elasticity.  The moment at the section is given by;

$$M = \int_{-b/2}^{+b/2} \sigma \times b \, z \, d \, z \qquad (A.6)$$

where b, is the width of the beam.

Combining EQUATIONS A.5 and A.6 the following relationship

is obtained;

$$\frac{M}{EI} = -\frac{d^2y}{dx^2} \qquad (A.7)$$

where, I is the moment of inertia of the cross-section

about the centroidal axis.

## A.2    Flexural Strength of Beams

Conditions of stress and strain at failure for

prestressed concrete beams, reinforced in tension only,

are shown in FIGURE A.2
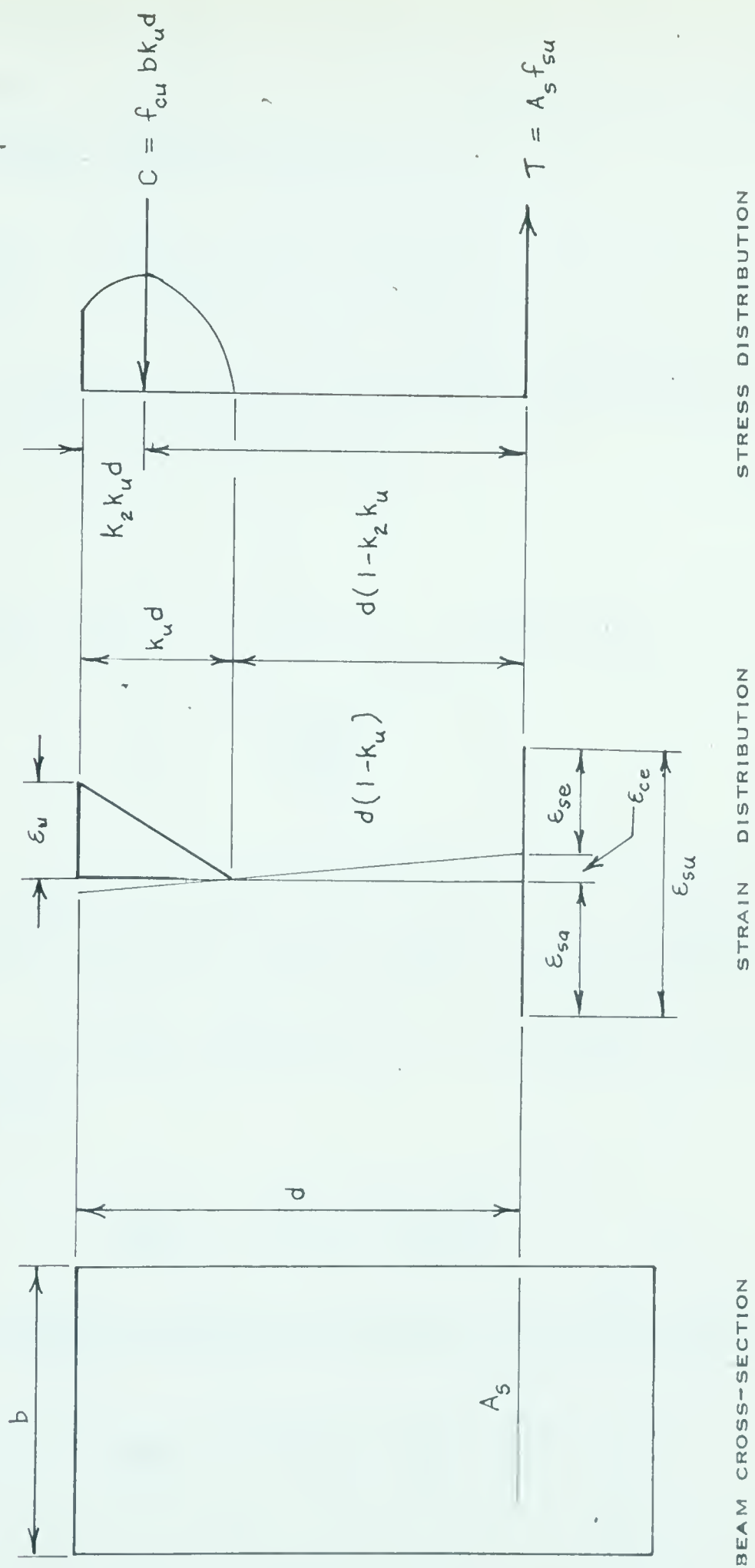
FIGURE A.2 CONDITIONS OF STRESS AND STRAIN AT FAILURE

An expression of ultimate moment may be written with reference to FIGURE A.2 by taking moments about the centroid of the compressive force, C.

$$M_f = A_s f_{su} d(1 - k_2 k_u) \tag{A.8}$$

Summation of forces in the longitudinal direction gives an expression for the ratio, $k_u$.

$$C = T$$

or $$f'_{cu} b k_u d = A_s f_{su} = p bd f_{su}$$

from which $$k_u = \frac{p f_{su}}{f_{cu}} \tag{A.9}$$

Using the strain distribution in FIGURE A.2, a relationship between the increase in reinforcement strain, $\varepsilon'_{sa}$, and the useful limit of concrete strain, $\varepsilon_u$, can be written.

$$\varepsilon'_{sa} = F\varepsilon_u \left(\frac{1 - k_u}{k_u}\right) \tag{A.10}$$

The reinforcement strain at failure, $\varepsilon_{su}$, becomes;

$$\varepsilon_{su} = \varepsilon_{se} + \varepsilon_{ce} + \varepsilon'_{sa} \tag{A.11}$$

Combining EQUATIONS A.10 and A.11 gives;

$$\varepsilon_{su} = \varepsilon_{se} + \varepsilon_{ce} + F\varepsilon_u \left(\frac{1 - k_u}{k_u}\right) \tag{A.12}$$

The average curvature at failure is obtained from;

$$\text{Average } \phi = \frac{F\varepsilon_u}{k_u d} = \frac{\varepsilon_{sa}}{d - k_u d} \tag{A.13}$$

# Appendix B

# METHODS OF CALCULATION

B.1    Flexural Strength

   B.1.1    Ultimate Moment

      A trial and error solution was used to determine
the theoretical ultimate moment of each beam tested.  Step
by step procedures for obtaining the ultimate moment for
beams reinforced in tension only and beams with supplementary
reinforcement are outlined in reference (2).

      The procedure used was as follows:

   1.    Assume a value for $k_u$

   2.    Determine $F\varepsilon_u$

   3.    Determine $\varepsilon_{su}$

   4.    Determine $f_{su}$ (from reinforcement stress-
                    strain curve)

   5.    Using $f_{su}$ and EQUATION A.9 compute $k_u$

   6.    Compare computed $k_u$ with assumed value

   7.    If values of $k_u$ not equal repeat steps (1) to (6)

   8.    If values of $k_u$ are equal compute $M_f$ using
         EQUATION A.1

      The expression for $F\varepsilon_u$ used in this analysis

was:

$$F\varepsilon_u = \frac{1 + 2k_u}{600} \leq 0.004$$

This expression was derived empirically from tests (2), performed on bonded beams. To determine the value of $k_u$ from EQUATION A.9 the effective strength of the concrete $f_{cu}$ is required. The value of $f_{cu}$ derived from tests (2) of beams bonded at midspan was found to be:

$$f_{cu} = 1.4f_c'$$

The calculated values of theoretical ultimate moment compared to actual test values are summarized in TABLE B.1 .

### B.1.2    Cracking Moment

The theoretical resisting moment at flexural cracking was computed using an "elastic" analysis with the modulus of rupture as the limiting stress. The modulus of rupture was determined from $3\frac{1}{2}$ x $4\frac{1}{2}$ x 14-in. control specimens loaded at the third points of a 12-in. span. The size of the control specimen used influenced the value obtained for the modulus of rupture, (10). Small control specimens tended to give high values for the modulus of rupture.

The relationship between the compressive strength

## TABLE B.1

### CRACKING AND ULTIMATE MOMENTS

| Beam No. | Observed $M_u$ KIP-FT | Theoretical $M_u$ KIP-FT | Observed $M_{cr}$ KIP-FT | Theoretical $M_{cr}$ KIP-FT | Mode of Failure |
|---|---|---|---|---|---|
| 11 | 22.5 | 23.0 | 13.5 | 15.8 | Tension |
| 12 | 42.2 | 41.4 | 21.0 | 22.3 | Compression |
| 13 | 57.5 | 53.6 | 30.0 | 28.5 | Compression |
| 1A | 48.5 | 45.3 | 27.5 | 22.6 | Compression |
| 2A | 60.5 | 62.6 | 30.2 | 28.7 | Compression |
| 3A | 67.0 | 75.4 | 41.0 | 33.4 | Compression |
| 4A | 50.9 | 47.5 | 26.2 | 26.4 | Tension |
| 5A | 74.8 | 68.6 | 34.4 | 32.2 | Compression |
| 6A | 96.3 | 89.0 | 44.0 | 39.6 | Compression |
| 1B | 44.8 | 44.5 | 20.6 | 22.3 | Bond |
| 2B | 68.7 | 65.0 | 35.7 | 30.6 | Compression |
| 3B | 75.6 | 75.4 | 44.0 | 35.4 | Compression |
| 4B | 50.5 | 47.0 | 21.6 | 24.9 | Compression |
| 5B | 71.5 | 68.6 | 36.3 | 30.7 | Bond |
| 6B | 83.6 | 87.0 | 44.5 | 39.1 | Bond |

and the modulus of rupture data did not warrant use of the

results of individual control specimens, an expression which

relates the modulus of rupture to the compressive strength

was used. This expression is given in reference (2) and

(3) as follows:

$$f_r = \frac{3,000}{3 + \frac{12,000}{f'_c}}$$

This expression was derived from tests of 6 x 6 x 20-in.

control specimens loaded at the third points of an 18-in.

span. As shown in FIGURE 1.B, this relationship represents

a lower bound for the test data obtained from the 3½ x 4½ x

14-in. control specimens. Since the above expression was ob-

tained from control specimens of a larger size than the 3½ x

4½ x 14-in. control specimens, the modulus of rupture would

be more representative for the test beams.

The relationship for the moment at which

flexural cracking occurred, in terms of the modulus of

rupture $f_r$, and stress conditions at flexural cracking is,

$$M_{cr} = \frac{I}{y_b} (f_r + \frac{P}{A} + \frac{Pe}{I/y_b})$$

where $y_b$, is the distance from the centroidal axis to the

extreme fiber in tension.

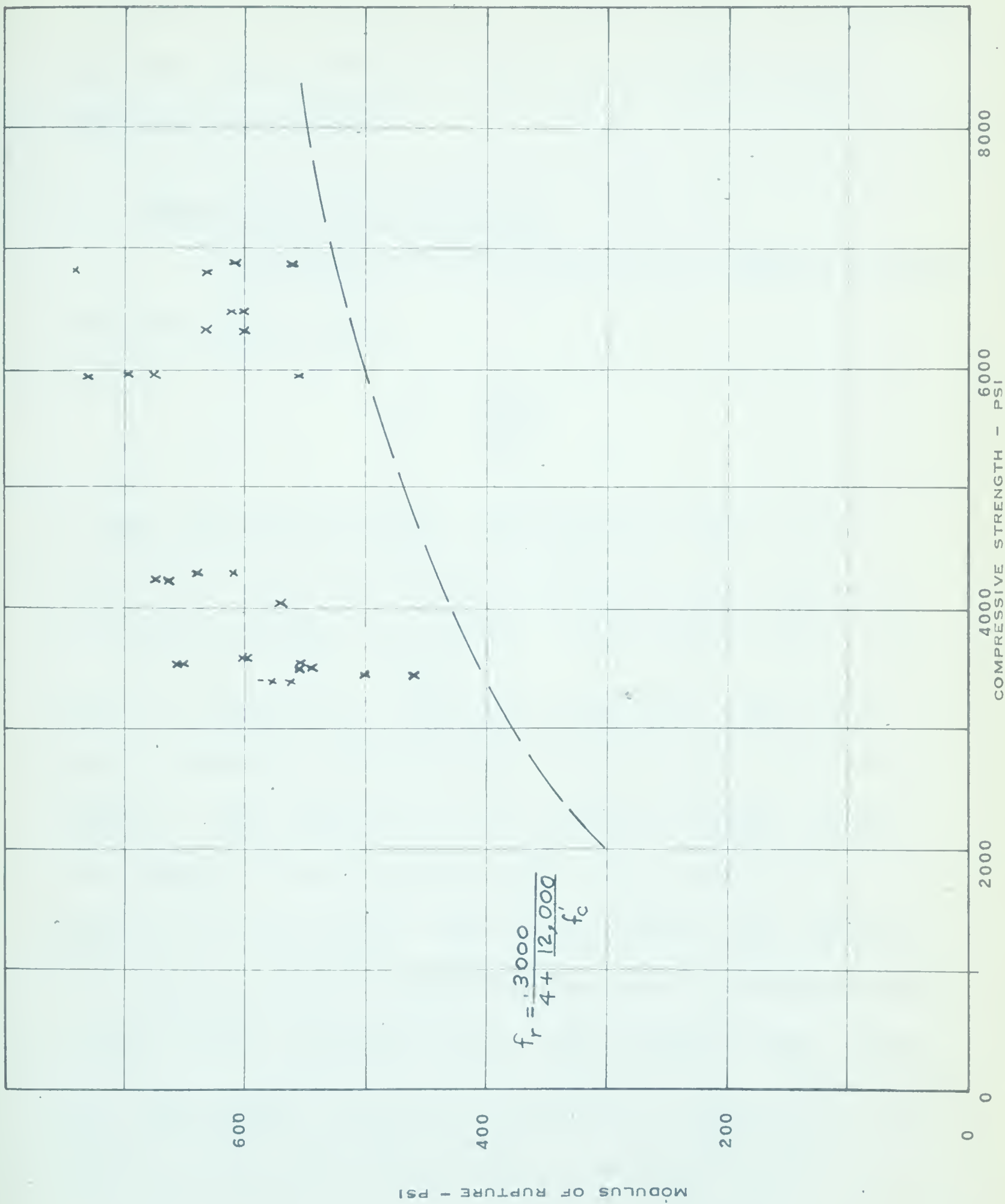FIGURE B.I RELATIONSHIP BETWEEN STRENGTH AND MODULUS OF RUPTURE

$$f_r = \frac{3000}{4 + \frac{12,000}{f'_c}}$$

COMPRESSIVE STRENGTH – PSI

MODULUS OF RUPTURE – PSI

The theoretical resisting moments at flexural cracking, as determined by the above relationship are summarized in TABLE B.1

B.2    Computation of Deflections

In APPENDIX A the curvature of an elastic prismatic beams was found to be

$$\frac{1}{R} = \frac{d^2y}{dx^2}$$

If the curvature is known, the numerical value of the deflection, y may be determined from the above expression by means of double integration.  The conjugate beam method which is a process of numerical integration may also be used to determine the deflection from a known curvature diagram.  The ordinates of the curvature diagram become the loading of the conjugate beam.  The slope and the deflection of the actual beam at any section are given by the shearing force and bending moment at the corresponding section of the conjugate beam.  The conjugate beam, loaded with the average curvatures as derived in Section 5.2, was used to compute the deflections.  The distribution of

curvature was idealized as shown in FIGURE B.2 (a) and
was reduced to equivalent concentrated angles acting at
each of the gage lines as shown in FIGURE B.2 (b) .

100

74.4

19.5

7.0  10.7
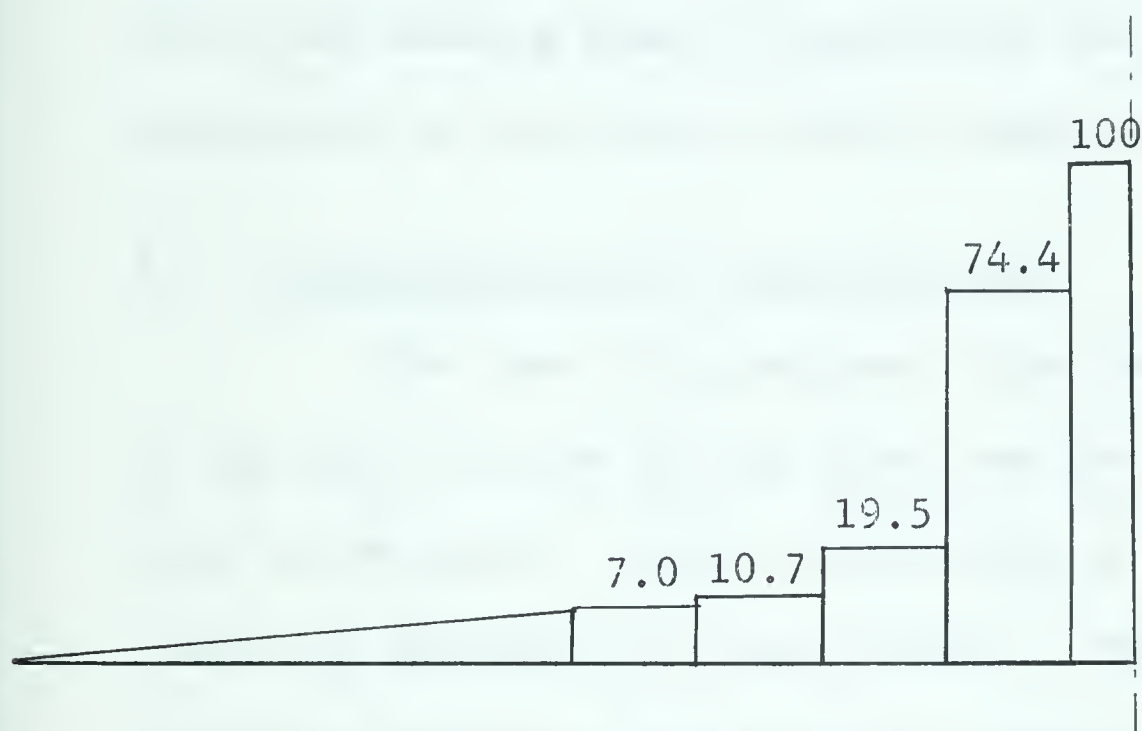
(a)  Distribution of Curvature - (rad./in. x 10$^5$)

698

376

121

98

71

35
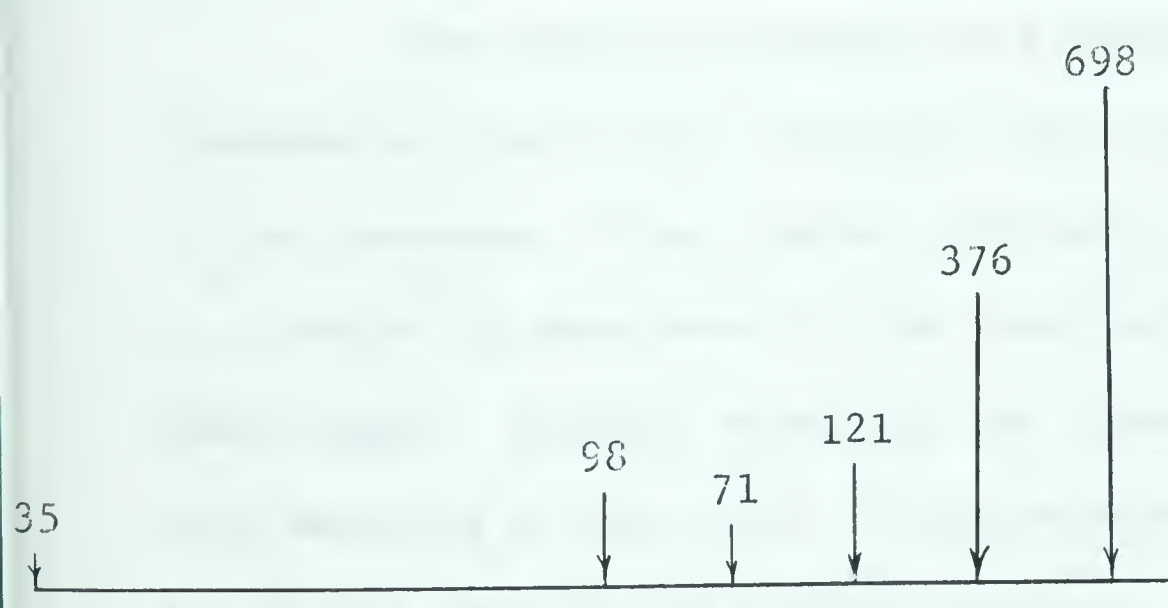
(b)  Equivalent Concentrated Angles - (rad. x 10$^5$)

FIGURE B.2  CONJUGATE BEAM LOADING -
BEAM 1A AT 16.0 KIPS

A numerical procedure was then used to determine the shearing force and bending moment in the conjugate beam at each gage line for all increments of load. The shear force and bending moment represented the slope and deflection in the actual beam at these sections.

B.3   Determination of Prestress Loss

The loss of prestress, from the time of casting to the time of test of the beam, was due to stress relaxation in the steel, elastic shortening of the concrete and creep and shrinkage of the concrete. The initial prestress, effective prestress and measured losses for the test beams are summarized in TABLE B.2 .

The initial prestress was measured with the dynamometers and strain indicator just prior to the casting of the concrete. The elastic shortening of the beam due to transfer of prestress to the concrete was measured with Demec gages. Strains caused by the transfer of prestress were measured at the level of the reinforcement and on the top of the beam at the midspan position. From these strains the stress distribution across the section and the loss of prestress due to elastic shortening was determined. Strain

## TABLE B.2

## LOSS OF PRESTRESS IN THE REINFORCEMENT

| Beam No. | Average Initial Prestress (Ksi) | Average Elastic Shortening | | Average Time Losses | | Effective Prestress |
|---|---|---|---|---|---|---|
| | | (in/in) | (Ksi) | (in/in) | (Ksi) | Ksi |
| 11 | 153.5 | .00014 | 3.7 | .00041 | 11.0 | 138.8 |
| 12 | 162.0 | .00045 | 12.2 | .00039 | 10.5 | 139.3 |
| 13 | 171.5 | .00058 | 15.6 | .00069 | 18.7 | 137.2 |
| 1A | 166.0 | .00039 | 10.5 | .00065 | 17.5 | 138.0 |
| 2A | 171.2 | .00059 | 15.9 | .00066 | 17.8 | 137.5 |
| 3A | 177.0 | .00093 | 20.4 | .00098 | 26.4 | 130.2 |
| 4A | 169.0 | .00038 | 10.4 | .00048 | 12.8 | 145.8 |
| 5A | 173.0 | .00048 | 13.1 | .00067 | 18.1 | 141.8 |
| 6A | 180.5 | .00071 | 19.2 | .00065 | 17.5 | 143.8 |
| 1B | 170.0 | .00047 | 12.7 | .00061 | 16.4 | 140.9 |
| 2B | 175.0 | .00057 | 15.4 | .00088 | 23.8 | 135.8 |
| 3B | 181.5 | .00077 | 20.7 | .00088 | 23.8 | 137.0 |
| 4B | 170.0 | .00047 | 11.1 | .00058 | 15.7 | 143.2 |
| 5B | 175.0 | .00043 | 11.7 | .00075 | 20.4 | 142.9 |
| 6B | 181.5 | .00058 | 15.7 | .00081 | 21.8 | 144.0 |

measurements were taken again at these gage lines just prior to testing. From these measurements, the total losses due to shrinkage and creep of the concrete during curing and relaxation of steel stresses were determined.